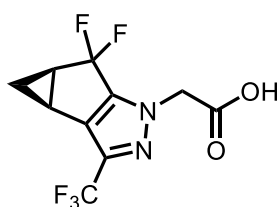


Medicines for All Institute

Summary of Process Development Work on Asymmetric Synthesis of the Frag C of Lenacapavir



Report Prepared by:

Dr. Limei Jin
Dr. Justina M. Burns
Dr. John M. Saathoff
Dr. Daryl Guthrie
Dr. Rajkumar Lalji Sahani
Dr. Aline Nunes de Souza
Dr. Nagaraju Sakkani
Sam R. Hochstetler

Contact: m4all@vcu.edu

July 2024



Virginia Commonwealth University
College of Engineering
Department of Chemical and Life
Science Engineering
Biotech 8, 737 N. 5th St
Richmond, VA 23219
www.medicines4all.vcu.edu



Executive Summary

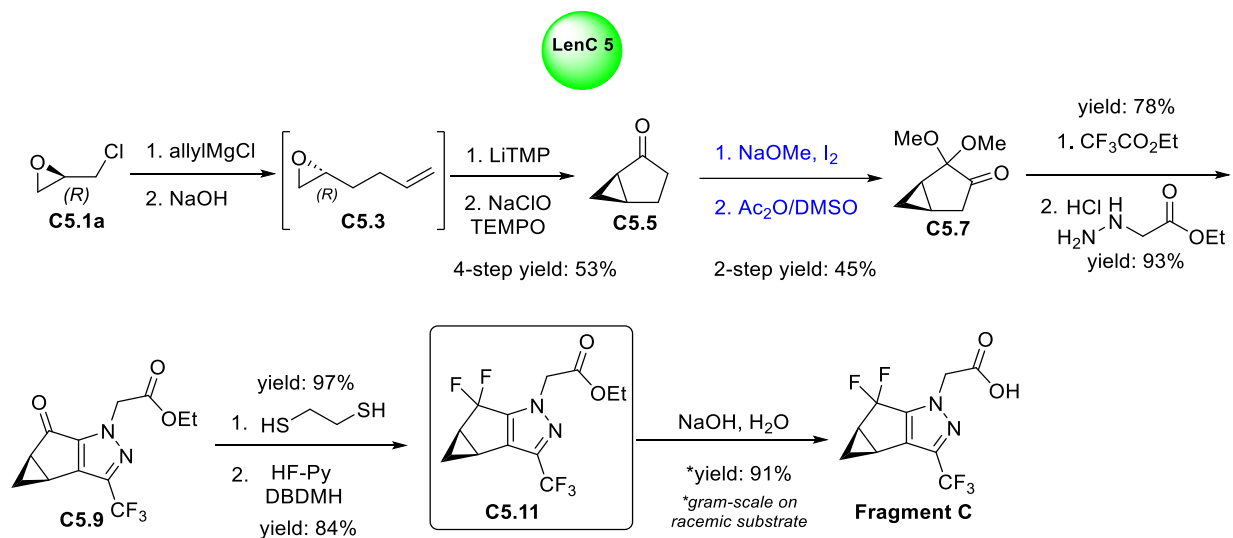
This process development report (PDR) describes the results of synthetic route scouting and scale-up optimization efforts at Medicines for All Institute (M4ALL) to discover new, cost-effective synthetic strategies to make a key intermediate and cost-driver in the synthesis of lenacapavir: 2-((3bS,4aR)-5,5-difluoro-3-(trifluoromethyl)-3b,4,4a,5-tetrahydro-1H-cyclopropa[3,4]cyclopenta[1,2-c]pyrazol-1-yl)acetic acid (**Frag C**). Lenacapavir is a first-in-class drug that targets the HIV capsid protein, developed by Gilead Sciences Inc., and approved by the FDA in 2022. Gilead's baseline route (medicinal chemistry route) comprises a racemic preparation of 2-(5,5-difluoro-3-(trifluoromethyl)-3b,4,4a,5-tetrahydro-1H-cyclopropa[3,4]cyclopenta[1,2-c]pyrazol-1-yl)acetic acid followed by chiral supercritical fluid chromatography (SFC) separation to provide the desired enantiomer **Frag C**.^a Expensive starting materials and reagents, space-time-yield inefficiencies intrinsic to the racemic preparation, and chiral SFC purification contribute to high costs for **Frag C**. Herein, we report an enantioselective 11-step synthesis (LenC 5) of **Frag C** commencing from (*R*)-(-)-epichlorohydrin.^b Key steps include a 4-step telescoped bicyclic ketone synthesis, I₂-promoted hydroxylation, Albright-Goldman oxidation, and HF·Py-mediated oxidative fluorination. Process development of the LenC 5 was done up through the penultimate step (**C5.11**).^c This process affords **C5.11** (precursor to **Frag C**) as a single enantiomer in 10-15% overall yield and has been demonstrated at up to a 100-gram scale. Techno-economic (TE) cost

^a Since the time of report preparation, Gilead Sciences Inc., published an article delineating an asymmetric synthesis of **Frag C**, employing strategies and methodologies bearing similarities to those disclosed herein. M4ALL's raw material cost assessments were made prior to the release of this publication and do not take into account potential cost reduction derived from this updated synthesis from Gilead (Kadunce, N. et. al. Synthetic Development and Scale-Up of a Complex Pyrazole Fragment of Lenacapavir. *Org. Process Res. Dev.* 2024, 28, 3368–3381. <https://pubs.acs.org/doi/10.1021/acs.oprd.4c00235>)

^b Two additional synthetic approaches to **Frag C** are summarized in the Appendix of this document, LenC 2 and LenC 3. They were not advanced for optimization, in view of the superior performance of LenC 5. Please see the appendices for further details.

^c **C5.11** is the ethyl ester form of **Frag C**. A simple hydrolysis transformation of **C5.11** would afford the **Frag C**. Due to the limited timeline of the project, we will complete the scale-up of the hydrolysis step in future studies.

analysis suggests that, compared to the baseline route starting from cycloprop-3-en-1-ol, the LenC 5 route could offer an overall raw material cost (RMC) reduction of 63-77%.



Medicines for All – Contributors to the Research and Report

Contributor	Title / Role
Dr. Ryan Littich	Head of R&D ^d
Dr. Limei Jin	Sr Scientist (Project Lead)
Dr. John M. Saathoff	Research Scientist
Dr. Daryl Guthrie	Research Scientist
Dr. Rajkumar Lalji Sahani	Research Scientist
Dr. Aline Nunes de Souza	Postdoctoral Researcher
Dr. Nagaraju Sakkani	Postdoctoral Researcher
Dr. Daniel W. Cook	Senior Analytical chemist
Sam Hochstetler	Analytical chemist
Dr. Justina M. Burns	Associate Director of Analytical Chemistry
Dr. Michel Nuckols	Sr. Scientist ^d

^d PDR review, revisions, additions

Janie Wierzbicki	Project Manager
------------------	-----------------

*With research support provided by WuXi Apptec (China)

Contents

Executive Summary	2
1 Introduction	6
1.1 Background of Frag C in lenacapavir synthesis.....	6
1.2 Introduction of LenC 5	8
2 Results & Discussion.....	10
2.1 Milestone 1: Synthesis of chiral epoxide C5.3	10
2.1.1 Optimization of C5.3 synthesis.....	10
2.1.2 Scale-up of C5.3 synthesis.....	21
2.2 Milestone 2: Synthesis of bicyclic chiral ketone C5.5	22
2.2.1 Familiarization of C5.5 synthesis	22
2.2.2 Four-step telescoped synthesis of C5.5 from C5.1a	22
2.3 Milestone 3: Synthesis of chiral pyrazole C5.9	25
2.3.1 Optimization of C5.9 synthesis.....	25
2.3.2 Scale-up of C5.9 synthesis.....	35
2.4 Milestone 4: Synthesis of Frag C	39
2.4.1 Optimization of the Frag C synthesis	39
2.4.2 Scale-up of the Frag C synthesis.....	45
3 Experimental Sections	47
3.1 Analytical Report for Lenacapavir Frag C	47
3.1.1 Pharmacopoeia Methods.....	48
3.1.2 Method Development.....	48
3.1.3 Impurities	55
3.1.4 Forced Degradation Studies.....	55
3.1.5 Methods.....	56
3.2 Detailed Experimental Procedures	57
3.2.1 General Methods.....	57

3.2.2	Experimental Procedure.....	57
3.3	NMR & GCMS Spectra	74
4	Appendix	98
4.1	Route scouting of LenC 2.....	98
4.2	Route scouting of LenC 3.....	100
4.3	Standard operating procedure (SOP) for HF-pyridine chemistry	103
4.4	X-ray crystal structure and data.....	111
4.4.1	X-ray crystal structure of C5.9	111
4.4.2	X-ray crystal structure data for C5.9	111
4.4.3	X-ray crystal structure of C5.11	117
4.4.4	X-ray crystal structure data for C5.11	117
4.5	Acquisition methods, retention times, chromatograms, and MS spectra	124
4.5.1	LenC-1 (GC-MS).....	124
4.5.2	LenC-2 (GC-MS).....	128
4.5.3	LenC-3 (Chiral, GC-FID)	131
4.5.4	LenC-4 (Chiral, GC-MS).....	132
4.5.5	LenC-5 (Chiral, GC-FID)	133
4.5.6	LenC-6 (Chiral, SFC-DAD).....	134
4.5.7	LenC-7 (Chiral, SFC-DAD).....	136
4.5.8	LenC-8 (Chiral, SFC-DAD).....	139
4.6	Acronyms	140
5	Acknowledgements	143
6	References	143

1 Introduction

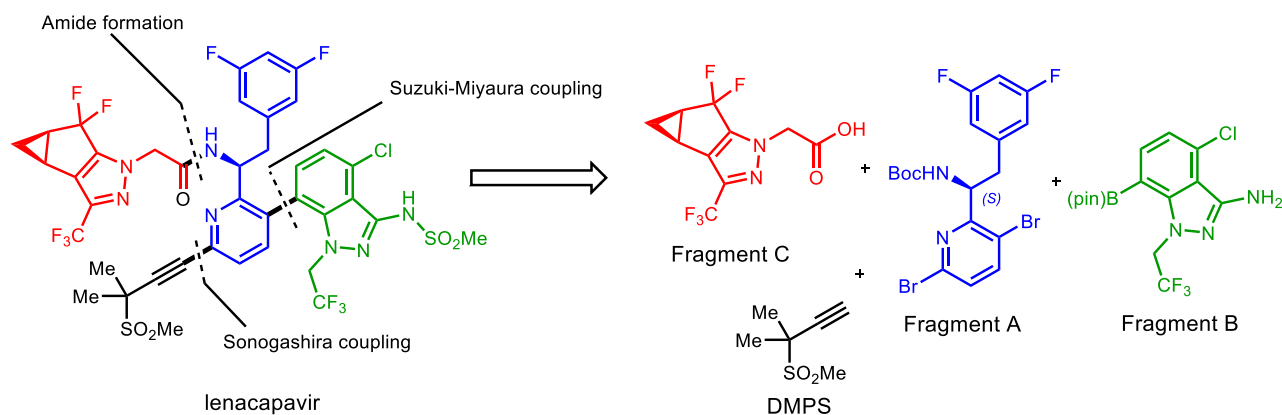
Human immunodeficiency virus (HIV), the virus that causes AIDS (acquired immunodeficiency syndrome), is one of the world's most serious health and development challenges. Approximately 39 million people are currently living with HIV, and tens of millions of people have died of AIDS-related causes since the beginning of the epidemic.¹ In 2020, there were approximately 20 million people on antiretroviral therapy (ART), a number which was expected to reach 24 million by 2024. Approved HIV treatment regimens currently fall into seven drug classes, based on their distinct mechanism of action. Today, approximately 22 million individuals are on a dolutegravir-based regimen: the “gold-standard” treatment comprises the combination of two nucleoside reverse transcriptase inhibitors (NRTIs), tenofovir disoproxil and lamivudine, and the integrase strand transfer inhibitor dolutegravir.²

Lenacapavir (Sunlenca[®]) is a high-potency HIV treatment in development by Gilead Sciences. The drug is a first-in-class HIV-1 capsid protein inhibitor that displays picomolar activity, extended pharmacokinetics, and little to no cross-resistance with clinically used antiretroviral agents.^{3,4} Lenacapavir achieves its revolutionary anti-HIV-1 activity by blocking the viral replication of the HIV-1 virus, which is closely related to many processes of the viral lifecycle: uptake, assembly, and release.⁵ Because of this classification, the FDA has designated lenacapavir as a breakthrough drug. The novel therapy earned approval from both the European Commission and the FDA in 2022 as a treatment for multidrug-resistant HIV (MDR HIV) infections.⁶⁻⁸ In 2023, in the United States, the cost for HIV-indicated injections and tablets (wholesale; not for PrEP) was \$42,450 per patient per year.⁹⁻¹¹ To ensure patients' access to lenacapavir-for-PrEP globally, significantly lower annual costs must be realized.¹⁰

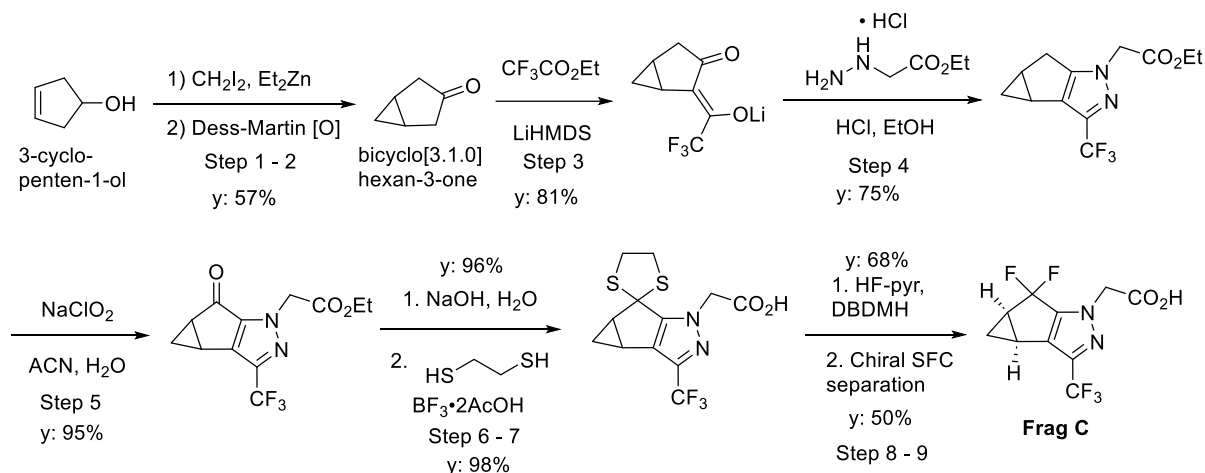
1.1 Background of **Frag C** in lenacapavir synthesis

Structurally speaking, lenacapavir is an extremely complex active pharmaceutical ingredient (API), with three chiral sp³-hybridized carbon centers and 10 fluorine atoms in four different functional environments. Lenacapavir consists of three advanced intermediates - Fragment A, Fragment B, and Fragment C (**Frag C**) - as shown in Figure 1.1.1.

Figure 1.1.1 Retrosynthetic disconnections in lenacapavir



Gilead has published several patents related to the initial synthesis and optimization of this molecule with several approaches to each fragment being demonstrated.¹²⁻¹⁵ As depicted in Scheme 1.1.1, the synthesis of **Frag C** utilizes expensive starting materials and reagents and rely on costly chiral separation techniques that are not amenable to scaleup.^{5,16}



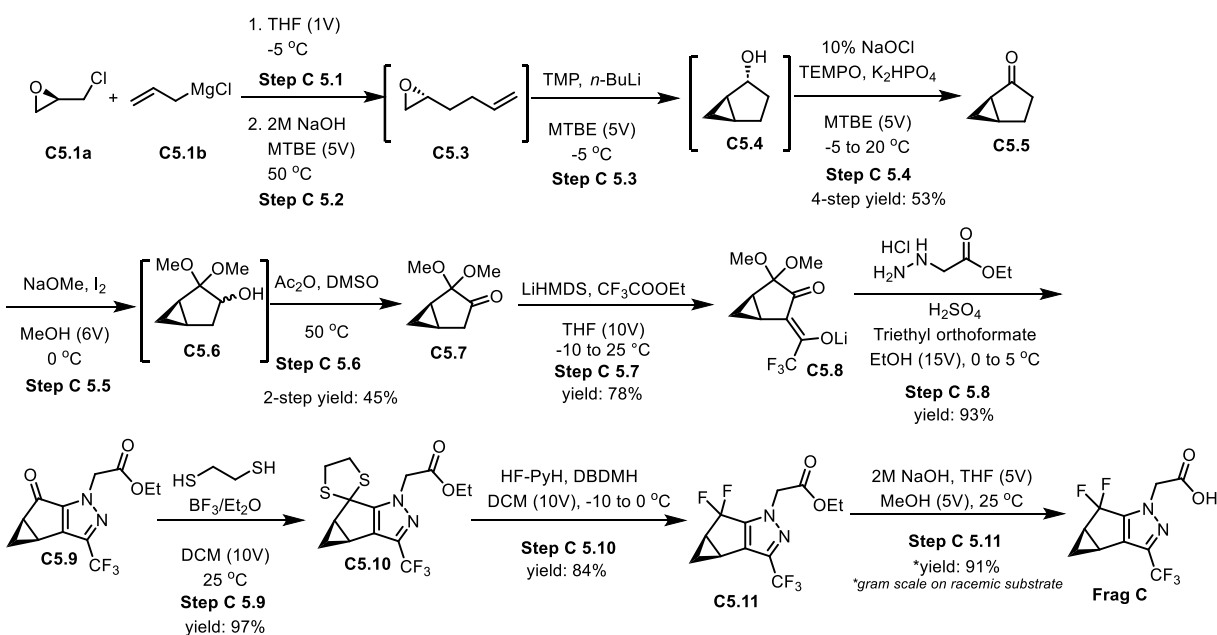
Scheme 1.11.1 Gilad chiral SFC approach to synthesis of **Frag C**.

With support from the Bill and Melinda Gates Foundation (BMGF), M4ALL has been tasked with lowering the overall cost of this complex molecule. **Frag C** is the most complex and chemically step-intensive of the three advanced intermediates that converge to form lenacapavir.^{5,16,17} M4ALL techno-economic analysis indicates that **Frag C** is the most significant

contributor to lenacapavir's overall RMC of its three constituent fragments. In their recent publication, Gilead separate out the alkynyl fragment to list four but no need to change here. Thus, improvements to the synthesis of **Frag C** can materially reduce the overall cost of this breakthrough drug.

1.2 Introduction of LenC 5

M4ALL enacted an enantioselective 11-step approach to drive down **Frag C** raw material costs. This new process was developed through four key project milestones: an asymmetric epoxide synthesis (Milestone 1), bicyclic ketone synthesis (Milestone 2), pyrazole synthesis (Milestone 3), and fluorination (Milestone 4). M4ALL's synthesis starts from the reaction of (*R*)-(-)-epichlorohydrin (**C5.1a**) and allyl magnesium chloride (**C5.1b**). Enantioselective ring-opening of epichlorohydrin and ring-closure of the incipient chlorohydrin afforded epoxide *R*-(+)-1,2-epoxyhex-5-ene (**C5.3**) (Milestone 1).¹⁸⁻²⁰ Hodgson cyclopropanation then NaOCl-TEMPO oxidation provided (1*R*,5*S*)-bicyclo[3.1.0]hexan-2-one (**C5.5**) (Milestone 2). I₂-mediated α -hydroxylation of **C5.5** followed by oxidation yielded the acetal-protected ketone (**C5.7**). After Claisen condensation and Knorr cyclization, **C5.9** is obtained (Milestone 3). **C5.9** was then converted to the thioacetal intermediate **C5.10** and the subsequent fluorination of **C5.10** with HF-Py (Milestone 4) furnished **Frag C** as an enantiopure compound.



Scheme 1.2.1 M4ALL asymmetric synthesis of **Frag C**.

As mentioned in the Executive Summary, some strategies in this report are mirrored by Gilead's recent prepublication disclosure to BMGF. Conversely, some elements of the herein-reported synthesis share similarities to previous reports.

- Synthesis of chiral epoxide (**C5.3**) from (*R*)-(-)-epichlorohydrin (**C5.1a**) is reported.^{21–24} Its synthesis was demonstrated on a gram scale and column purification was invoked; the procedure was not appropriate for scale-up, as defined.
- Process development from **C5.3** to **C5.5** has been reported by Merck,^{25–27} thus allowing our expedited focus on other challenging milestones - Milestones 3 and 4.
- Synthesis of racemic **Frag C** (with SFC chiral separation from cyclopent-3-en-1-ol) has been reported;¹⁶ SFC has limited scale and availability across innovator and contract manufacturing environments and is associated with high operating costs.
- Phenyliodine(III) diacetate (PIDA) was used as a stoichiometric oxidant in the α -hydroxylation of racemic **C5.5**. PIDA's high cost represents an opportunity for improvement.

- Swern oxidation was used to generate racemic **C5.7**, under cryogenic conditions. The need of cryogenic condition and the intrinsic safety issues of Swern oxidation impede the scale-up.
- HF-pyridine-mediated fluorination provided racemic **Frag C**. Fluorination was reported on small scale^e (~1 g) and lacked sufficient procedural details (i.e., purifications, purity profiles, and safety assessment of fluorination) to judge fitness for scale-up and tech transfer.

All the aforementioned issues and unknowns presented challenges to our LenC 5 route design. These could only be resolved through independent process research and development. To this end, M4ALL developed an asymmetric process to prepare **Frag C** from readily available (*R*)-(-)-epichlorohydrin. We highlight an efficient 4-step telescoped bicyclic ketone synthesis, I₂-promoted hydroxylation, and Albright-Goldman oxidation to access **C5.7**. We, furthermore, provide detailed process development assessments of the Claisen condensation, Knorr pyrazole synthesis and HF/Py-promoted fluorination. Together, these insights provide informative and valuable data for the large-scale synthesis of **Frag C**.

2 Results & Discussion

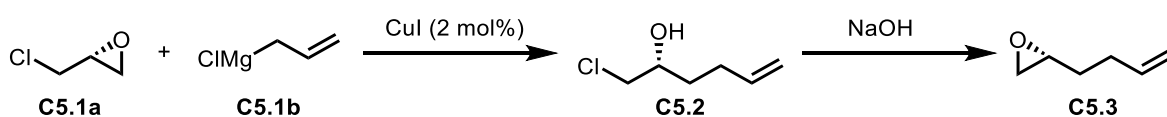
2.1 Milestone 1: Synthesis of chiral epoxide **C5.3**

2.1.1 Optimization of **C5.3** synthesis

Work toward Milestone 1 began with an evaluation of the literature method (Scheme 2.1.1) to make epoxide **C5.3**: Treatment of (*R*)-epichlorohydrin **C5.1a** (1.0 eq) with allylmagnesium chloride **C5.1b** (1.2 eq; allylMgCl), in the presence of catalytic CuI (2 mol%), gave **C5.2** (60% isolated yield) after column purification.^{21–24} Epoxide **C5.3** was obtained in a quantitative yield by reaction of intermediate **C5.2** with NaOH. Low yields in the ring opening step and chromatographic purification are impediments to scale-up. To troubleshoot the former, M4ALL

^e The same is true of Knorr pyrazole and other reaction steps: small scale preparations with limited procedural details were reported.

investigated the impurity profile of the crude reaction mixture by GCMS. Major impurities included $\leq 20\%$ TIC A% 1,5-hexadiene (**1**), $\leq 4\%$ TIC A% dichlorohydrin (**2**) and $\leq 2\%$ TIC A% 1,8-nonadien-5-ol (**3**). To achieve a scalable epichlorohydrin process, we aimed to minimize the formation of side products **1**, **2**, and **3** (thus improving the yield of the compound **C5.3**) and to eliminate column purification (thereby minimizing processing costs and enabling scalability). We thus divided the synthesis into two steps: 1) ring opening of **C5.1a** and 2) ring closure of **C5.2** to optimize each step, individually, before enacting a telescoped process.



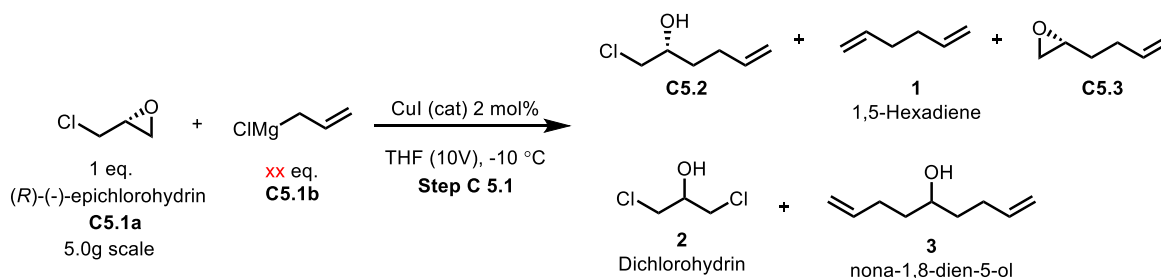
Scheme 2.1.1 A reported method to synthesize **C5.3** from (*R*)-epichlorohydrin **C5.1**.

2.1.1.1 Ring opening of *R*-epichlorohydrin **C5.1a**

2.1.1.1.1 Varying equivalents of **C5.1b**

To determine the optimal amount of allylmagnesium chloride (**C5.1b**) in the epichlorohydrin ring-opening reaction, the incremental addition of **C5.1b** was investigated (Table 2.1.1). Initially, 0.6 eq of **C5.1b** was charged over an hour with a peristaltic pump, then a sample was withdrawn to monitor the reaction progress. Another 0.4 eq of **C5.1b** was then charged over another hour, followed by two portions of 0.1 eq of **C5.1b** over 10 minutes each. Reaction with 0.6 eq of allylMgCl showed 26.3% GCMS TIC A% epichlorohydrin remaining (Table 2.1.1, Entry 1) as well as 1,5-hexadiene (**1**) as a significant impurity (15.4% GCMS TIC A%) within 1 hour. The amount of the **1** increased to 20.1% GCMS TIC A% with further addition of **C5.1b** (Entries 1-4). Other impurities observed during the reaction included epoxide **C5.3** (arising from ring closure of **C5.2**), dichlorohydrin (**2**), generated by nucleophilic ring opening of starting material **C5.1a**, and 1,8-nonadien-5-ol (**3**). Hypothesizing that trace oxygen promoted homocoupling of the Grignard reagent to form **1**,²⁸ ring-opening reactions with a nitrogen purge - with and without copper catalyst - were investigated (vide infra).

Table 2.1.1 Incremental addition of **C5.1b** to convert **C5.1a** to **C5.2**



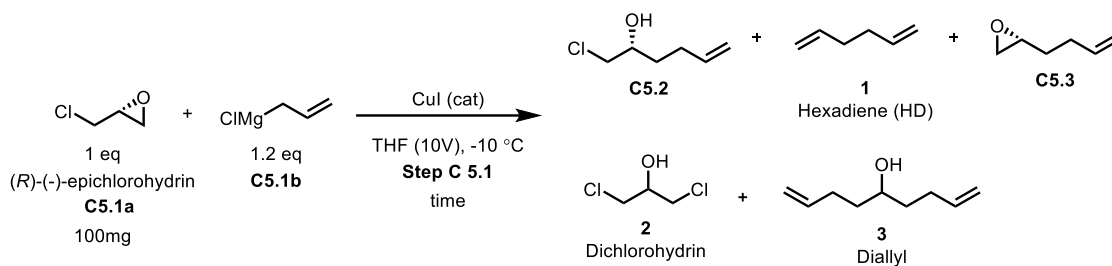
Entry ¹	C5.1b (eq)	TIC A%, GCMS ²					
		1	C5.1a	C5.3	2	3	C5.2
1	0.6	15.4	26.3	2.5	0.0	ND	48.4
2	1.0	18.9	8.1	2.4	0.7	0.6	60.1
3	1.1	19.6	5.0	2.2	0.7	0.7	62.4
4	1.2	20.1	2.8	2.2	0.7	0.9	63.5

¹C5.1a, CuI, and THF were mixed and cooled to -10 °C, followed by adding C5.1b (2M in THF) in four portions: 0.6 eq in an hour, 0.4 eq in the second portion, followed by two equal dosages of 0.1 eq each; ²GCMS data was recorded after each addition was finished. ND: not detected.

2.1.1.1.2 Investigating the role of catalyst

Optimal conditions identified in Table 2.1.1 (1.2 eq C5.1b) were applied to the ring opening of C5.1a, under nitrogen purge (Table 2.1.2, Entry 1). Carefully removing oxygen by purging the reaction mixture with nitrogen showed no improvement when compared to the reaction performed under air (Table 2.1.2, Entry 2). Formation of **1** was suppressed when catalytic CuI was omitted from the reaction. *Without* cuprous iodide, treatment of C5.1a with 1.2 eq of C5.1b afforded compound C5.2 in up to 81% TIC A% (GCMS) with only 1.1% TIC A% (GCMS) of **1** (Table 2.1.2, Entry 3). Furthermore, byproducts **2** and **3** were not detected. Based on this result, reaction conditions were optimized without CuI by investigating addition order, the equivalents of C5.1b, and reaction temperature.

Table 2.1.2 Conversion of C5.1a to C5.2 w/ or w/o CuI under nitrogen (or air)



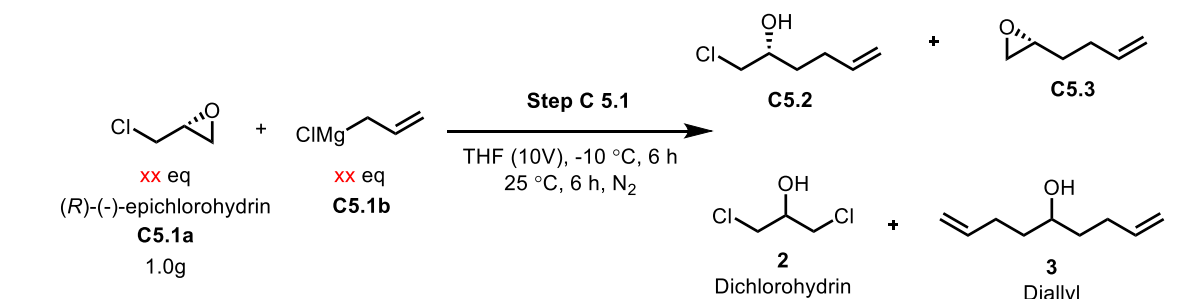
Entry ¹	CuI (mol%)	Atmosphere	Time (min)	TIC A%, GCMS ²					Remark
				1	C5.1a	2	C5.2	3	
1	2.0	N ₂ (dry)	30	21.5	1.0	3.5	60.3	1.2	Baseline
2	2.0	Air	5	18.5	6.1	0.0	59.3	1.6	Impurity 1 is CuI dependent
3	none	N ₂ (dry)	5	1.1	0.0	0.0	81.0	7.3	New Baseline

¹Reactions were conducted on 100 mg scale. **C5.1a**, CuI (Entries 1 and 2), THF were cooled to -10 °C, and **C5.1b** was added over 5-30 minutes; ²Reactions were stopped right after the addition and GCMS was recorded.

2.1.1.1.3 Equivalent screening of **C5.1a** and **C5.1b** without CuI

Reactions were performed which varied the relative stoichiometry of **C5.1a** and **C5.1b** between 1.0 and 1.2, without CuI. When the **C5.1a** reagent was used in excess (Table 2.1.3, Entries 1-3), higher amounts of dichlorohydrin **2** impurity were observed (6%-20.6% TIC A%, GCMS). Also, equal equivalents of **C5.1a** and **C5.1b** resulted in increased **C5.3** formation (Table 2.1.3, Entry 4). Experiments with excess **C5.1b**, observed prevalence of impurities was high (Table 2.1.3, Entries 5-6). 1.05 eq of **C5.1a** in combination with 1.0 eq of **C5.1b** (Table 2.1.3, Entry 3) was selected as the optimal baseline for further evaluation and optimization.

Table 2.1.3 Equivalents screen of **C5.1a** and **C5.1b** without CuI as a catalyst



xx eq
(*R*)-(-)-epichlorohydrin
C5.1a
1.0g

xx eq
C5.1b

Step C 5.1

THF (10V), -10 °C, 6 h
25 °C, 6 h, N₂

C5.2
C5.3

2
Dichlorohydrin
3
Diallyl

TIC A%, GCMS				Remark

Entry ⁱ	C5.1a (eq)	C5.1b (eq)	C5.1a	C5.3	2	C5.2	3	
1	1.2	1.0	3.3	11.6	20.6	50.6	ND	C5.1a remaining
2	1.1	1.0	6.2	10.2	15.0	48.6	ND	C5.1a remaining
3	1.05	1.0	1.2	12.7	6.4	61.1	ND	Baseline
4	1.0	1.0	3.6	22.2	11.3	51.2	ND	Highest C5.3 A%
5	1.0	1.05	5.2	11.6	22.4	42.7	1.6	Highest 2 A%
6	1.0	1.2	2.0	15.3	9.6	54.0	1.2	---

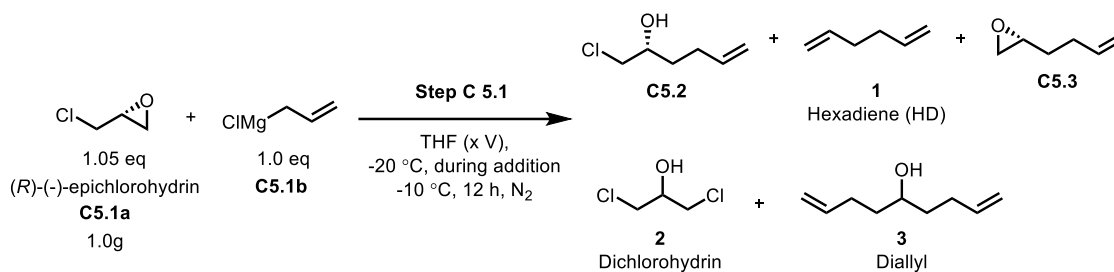
ⁱ**C5.1b** was charged dropwise to a 10V THF solution of **C5.1a** while maintaining the internal temperature below -10.0 °C. Once the addition of **C5.1b** was complete, the reaction mixture was maintained at -10.0 °C for 6 hours before warming to room temperature for another 6 hours.

2.1.1.1.4 Solvent volume screening (intensification)

Solvent volume was screened to maximize product formation and reactor volume efficiency on scale. 2M **C5.1b** in THF was used as a reagent in these transformations.^f As such, we examined a reaction in which no additional tetrahydrofuran volumes were used. Reverse addition of **C5.1a** (over 1 hour 24 minutes), maintaining the internal temperature below -10 °C, resulted in complete conversion but significant quantities of the byproduct **2** (13.6% TIC A%, GCMS) (Table 2.1.4, Entry 1). Adding **C5.1b** to a cooled 1V THF solution of **C5.1a** decreased impurity **2** formation to 2.1% TIC A%, GCMS (Table 2.1.4, Entry 2). Other solvent variations in regular and reverse addition fashion were investigated. Ultimately, the regular addition of **C5.1a** with 1V THF yielded the best results (Table 2.1.4, Entries 3-5 vs Entry 2). However, motivated by its prospective manufacturing simplicity, the authors further investigated the no-THF-added reaction protocol (with reverse addition) on a slightly larger scale (Section 2.1.1.1.5).

Table 2.1.4 Investigation of the effect of solvent volume on **C5.2** synthesis

^f The preformed solution of 2 M allylmagnesium chloride in THF (1.90 – 2.20M) was purchased from Aldrich and used as received.



Entry	THF (V)	Addition time	TIC A%, GCMS ³					Remark
			C5.1a	C5.3	2	C5.2	3	
1 ¹	0 (Neat)	1 h 24 min	0.0	0.7	13.6	81.2	0.9	Cleaner reaction, except for 2
2 ²	1	2 h 7 min	0.0	1.5	2.1	87.9	3.8	Baseline
3 ²	5	38 min	2.9	6.3	23.4	52.7	ND	Highest formation of 2
4 ²	10	45 min	1.0	2.5	4.4	65.7	ND	---
5 ¹	10	16 min	1.5	0.9	23.1	67.4	ND	Fastest addition of C5.1b

¹Reverse addition: **C5.1a** was added to a cooled solution of **C5.1b** at -20 °C for specified addition time and the reaction mixture was stirred for 12 hours at -10 °C; ²Regular addition: **C5.1b** was charged to a THF solution of **C5.1a** over specified time and then the reaction mixture was stirred for 12 hours at -10 °C; ³GCMS data was recorded after 12 hours.

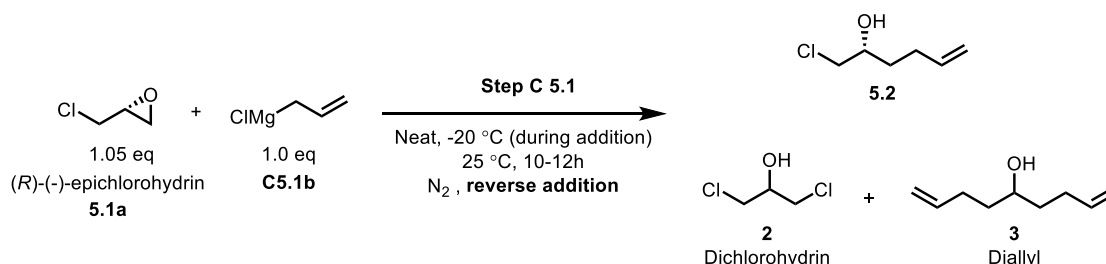
2.1.1.1.5 No-THF-added allylMgCl addition on larger scale

Two variables were examined in the no-THF-added reaction paradigm – scalability and temperature – with reverse addition used throughout. Scalability was evaluated in five reactions of varying scale (i.e., 10-50 g).^g The reaction with the lowest internal temperature upon complete addition of epichlorohydrin (0.2 °C) showed the most favorable impurity profile for **2** and **3** (Table 2.1.5, Entry 2). Reactions with internal temperature exceeding 10 °C resulted in the highest amount of **2** and **3**, suggesting a thermal acceleration of competitive nucleophilic ring opening of epichlorohydrin with chloride ion *and* homologation with allylMgCl to generate impurities **2** and **3**, respectively (Table 2.1.5, Entries 1 and 3-5, Figure 2.1.1). Furthermore, concentrations of **2** and **3** increased if the reaction duration was extended at room temperature (Table 2.1.6, Entries 1-5, Figure 2.1.2). From these observations, three byproduct minimization strategies were envisioned:

^g Target temperatures were achieved by adjusting **C5.1a** addition rates into chilled **C5.1b**.

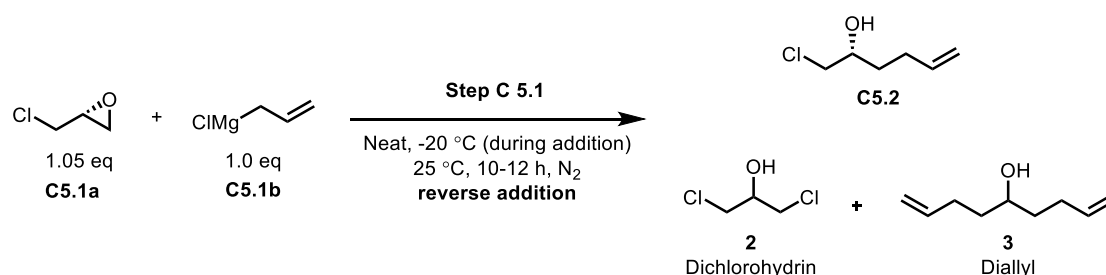
1) using equimolar amounts of **C5.1a** and **C5.1b** to avoid **2** formation (i.e., with excess epichlorohydrin); 2) operating at -10 °C to keep the internal temperature below 0 °C during **C5.1a** addition and quenching immediately, upon reaction completion; 3) regular addition to avoid excess allylMgCl (responsible for diallyl **3** impurity formation).

Table 2.1.5 Impurity profile after complete reverse addition of **C5.1a** to **C5.1b**



Entry	Scale (g)	Internal temp (°C)	Addition time	GCMS TIC A%			Remark
				2	C5.2	3	
1	10.0	10.0	27 min	12.1	78.5	5.4	Fastest addn. Highest 2 A%.
2	10.0	-0.2	2 h 36 min	4.0	88.2	2.9	Slowest addn. Lowest 2+3 A%
3	25.0	20.0	42 min	7.4	78.0	13.2	Highest temp. High 3 A%
4	25.0	16.8	60 min	2.9	79.9	14.7	Highest 3 A%
5	50.0	11.2	1 h 26 min	4.7	82.1	10.9	Significantly higher impurities

Table 2.1.6 Impurity profile of same reactions from Table 2.1.5 after 6-12 hours



Entry	Scale (g)	Internal temp (°C)	Reaction time (h)	GCMS TIC A% ¹			Remark
				2	C5.2	3	
1	10.0	-	6	16.2	74.8	8.0	Significant increase in both dichlorohydrin and diallyl impurities
2	10.0	-	12	13.1	81.9	4.2	
3	25.0	-	12	9.8	72.8	16.2	
4	25.0	-	12	6.2	66.7	25.8	
5	50.0	-	12	1.1	77.1	15.9	

							during warm up of the reaction to 25 °C
--	--	--	--	--	--	--	---

¹A% was taken of the crude material via GCMS after aqueous work-up.

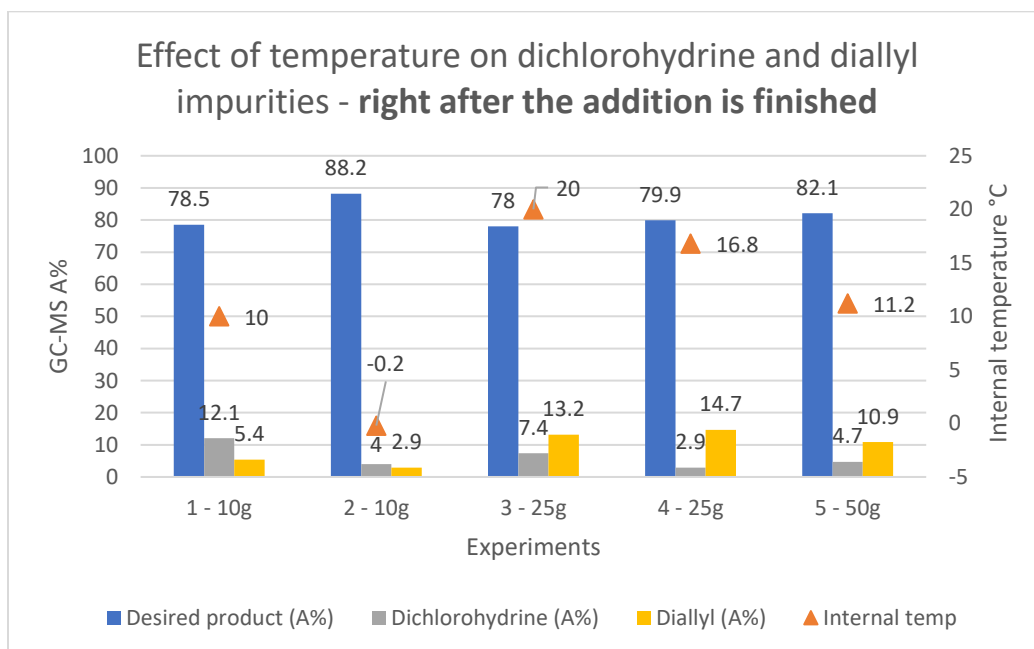


Figure 2.1.1 Impurity profile of the reverse addition reaction right after the addition of **C5.1a** is finished.

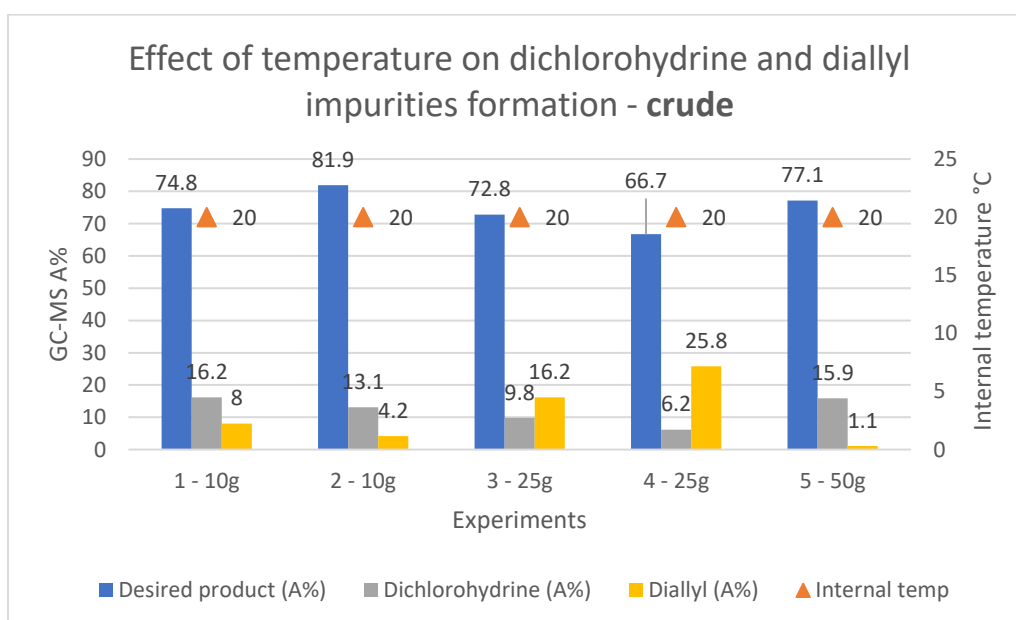
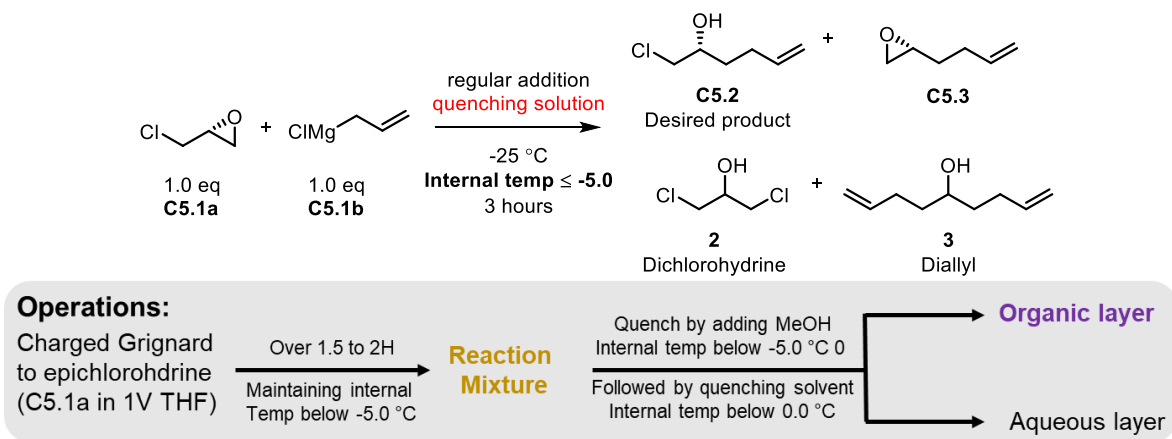


Figure 2.1.2 Impurity profile of the crude of the same reactions mentioned in Table 2.1.5 after work-up

2.1.1.1.6 Optimization of quench/workup in C5.2 synthesis

MeOH quench is critical before the workup.²¹ Clear aqueous and organic phase separation was achieved via MeOH quench followed by neutralization with 2M HCl. Without a preliminary MeOH quench, direct acid neutralization of the reaction mixture generated an intractable gel-like mass within the reactor. A similar impurity profile was obtained when acidifying the reaction mixture with aq. H₂SO₄ (1M) or saturated aq. NH₄Cl (Table 2.1.7, Entries 2 and 3). In all cases, the aqueous layer contained C5.2 less than 5% TIC A% by GCMS after MTBE extraction (5V × 1). Attempts to purify chlorohydrin C5.2 by distillation – i.e., to purge impurities 2 and 3 – failed; the three compounds feature comparable boiling points.^h

Table 2.1.7 Effect of different quenching solutions on impurity profile of ring-opening reaction of C5.1a to C5.2



Entry	Scale (g)	Quenching solution	Reaction stage	TIC A%, GCMS ¹			
				C5.3	2	C5.2	3
1	10.0	2.0 eq HCl	Rxn. Mix.	1.1	2.3	91.4	0.4
			Org. Layer	0.0	2.2	94.3	0.4
2	25.0	2.0 eq 2M NH ₄ Cl	Rxn. Mix.	-	-	-	-
			Org. Layer	0.0	2.1	86.6	0.0
3	25.0	1.0 eq	Rxn. Mix.	0.6	2.4	86.4	0.5

^hBoiling point of C5.2: 212±28 °C/760 Torr (Scifinder); 3: 212-216 °C/760 Torr; 2: 174 °C/760 Torr

		1M H ₂ SO ₄	Org. Layer	3.9	2.1	81.7	0.4
--	--	-----------------------------------	---------------	-----	-----	------	-----

¹Hexenone (2.1-10.3 A%) was detected during the GCMS measurement for these samples and crude ¹HNMR of the sample showed no hexenone peaks.

Thus, optimized reaction conditions for **C5.2** formation are:

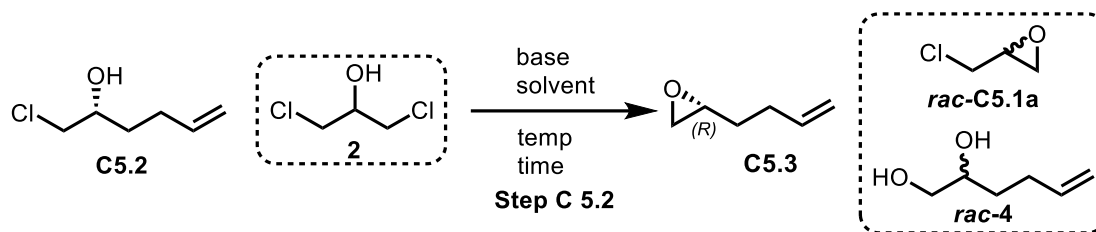
- Regular addition, in an equimolar reaction between **C5.1b** and **C5.1a** at 0 ± 5 °C, in 1V THF, gave **C5.2** in 94% TIC A%, GCMS.
- Minimal impurity **3** was observed (0.4% TIC A% (GCMS)). Impurity **2** was 2.2% TIC A%, GCMS. Impurity **1** was not detected under this condition (Table 2.1.7, Entry 1).
- Robust repeatability was observed; comparable results were obtained on a 25 g scale.

2.1.1.2 Intramolecular Williamson ether synthesis of **C5.2** to give (*R*)-**C5.3**

Administration of solid NaOH, for the intramolecular Williamson ether synthesis, is not easily managed on a manufacturing scale.ⁱ Different bases, solvents, and temperatures were screened to develop a more practical process. As summarized in Table 2.1.8, a milder base, K₂CO₃, under incumbent conditions, yielded 44% TIC A%, GCMS of **C5.3** (Table 2.1.8, Entry 2). In polar protic ethylene glycol, the K₂CO₃ reaction proceeded more efficiently. Treating **C5.2** with K₂CO₃ in ethylene glycol afforded the epoxide in 88% TIC A% (GCMS), but was accompanied by about 10% TIC A% (GCMS) of an ethylene glycol-epoxide adduct (Table 2.1.8, Entry 3). The hindered organic base DIPEA gave no product in ethylene glycol or diglyme at 60°C (Table 2.1.8, Entries 4 and 5). NaOH was thus revisited.

Table 2.1.8 Screening of different bases, solvents, and reaction temperatures to drive ring closure of **C5.2**

ⁱ Additionally, utilizing NaOH at 60 °C may cause etching of glass-lined reactors.



Entry ¹	Conditions	C5.3 (A%) ²	<i>ee</i> (%)	<i>rac</i> - C5.1a (A%)
1	NaOH (2 eq, pellets), neat, RT–60 °C, 2 h	94	99.9	1.5
2	K ₂ CO ₃ (2 eq), neat, 60 °C, 2 h	44 ³	--	--
3	K ₂ CO ₃ (1 eq), ethylene glycol, 60 °C, 4 h	88 ^{3,4}	--	--
4	DIPEA (1 eq), ethylene glycol, 60 °C, 4 h	0 ³	--	--
5	DIPEA (1 eq), diglyme, 60 °C, 4 h	0 ³	--	--
6	2M NaOH (2 eq), water, RT, 12 h	72.8 ⁵		
7	2M NaOH (1.2 eq), MTBE (2V), RT, 12 h	95	99.9	2
8	2M NaOH (1.2 eq), MTBE (2V), 50 °C, 2 h	98 ⁶	99.9	2

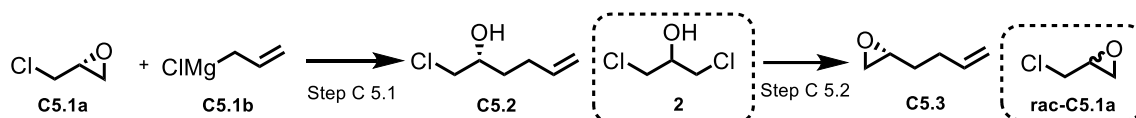
¹All reactions were performed with **C5.2** (1 g, 1 eq) and base under the conditions as indicated in table, *rac*-**C5.1** was observed in all conditions; ²A% was calculated based on GCMS by total ion chromatogram (TIC); ³Estimated by ¹H NMR; ⁴Ring-opening with ethylene glycol was the major side-reaction; ⁵20.6% TIC A%, GCMS of **C5.2** was unreacted; ⁶About 1.5% TIC A%, GCMS of **C5.2** remained.

Aqueous NaOH (2M) showed promising preliminary results in the intramolecular etherification of **C5.2**. Chlorohydrin **C5.2**, on treatment with 2.0 eq of aq. NaOH (2M) at room temperature for 12 h, provided epoxide **C5.3** in 73% TIC A% (GCMS) yield and ca. 21% TIC A% (GCMS) residual starting chlorohydrin (Table 2.1.8, Entry 6). When the solvent was switched to MTBE (2V), 1.2 eq of NaOH (2M) enabled >95% conversion within 12 h at room temperature (Table 2.1.8, Entry 7). The impurity hex-5-ene-1,2-diol (*rac*-**4**) was not detected under these conditions, suggesting **C5.3** was inert to residual NaOH under the reaction conditions. Increasing the reaction temperature to 50 °C for 2 h - holding reaction stoichiometry, solvent, and concentration constant – generated **C5.3** in >98 % TIC A%, GCMS (Table 2.1.8, Entry 8). Successful epoxide formation in MTBE thus opened the possibility of using the MTBE medium from the preceding Grignard addition directly in the epoxide-forming step. To that end, treatment of the MTBE solution of the crude product **C5.2** (from Step C 5.1) with 1.2 eq of NaOH (2M) at 50 °C for 2 h achieved full conversion to **C5.3**. The in-solution yield was up to 90 %, and the purity was up to 96% TIC A% (GCMS) after water wash. All epoxide **C5.3** obtained through this process was the (*R*)-enantiomer (>99.9 % *ee*), as confirmed by a chiral GC analysis.

2.1.2 Scale-up of **C5.3** synthesis

Using the optimized 2-step epichlorohydrin route for the production of **C5.3**, a hundred-gram scale-up (150-200 g) was demonstrated in a 5L ChemRxnHub reactor (Table 2.1.9). This process generated the epoxide with an overall in-solution yield of 72-90 %, a chemical purity of 91-96 A%, and an *ee* of up to 99.9 %. After distillation, **C5.3** was obtained in assay corrected yields of 52-64 % and 98-99 A% purity (Table 2.1.9).

Table 2.1.9 Two-step process for the synthesis of **C5.3** from **C5.1a**



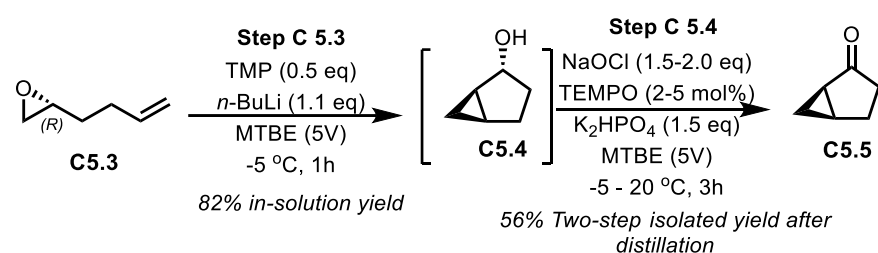
Step C 5.1: Ring opening of epichlorohydrin to form C5.2					
Entry ¹	Scale (g)	Compound C5.2 (A%) ²		Impurity 2 (A%) ²	
1	148	93 %		2.5 %	
2	150	80 %		3.8 %	
3	100	92 %		3.6 %	
Step C 5.2: Ring closure of C5.2 to yield the epoxide C5.3					
Entry	Scale (g)	In-solution yield of C5.3 ³	In-solution purity ²		Yield of C5.3 after distillation ⁴ gram, A% purity, wt% purity, assay corrected yield based on wt%, <i>ee</i> ⁵
			C5.3	<i>rac-C5.1a</i>	
4 ⁶	--	90 %	96 %	1.0 %	97 g, 99 A%, 86 wt%, 53 %, 99.9 %
5 ⁷	--	--	96 %	1.6%	91 g, 98 A%, 85 wt%, 52 %, 99.9 %
6 ⁸	--	79 %	92 %	1.1 %	68 g, 99 A%, 91 wt%, 58 %, 99.9 %

¹See our recent publication²⁹ for experimental details; ²A% was obtained by GCMS-TIC with exclusion of solvents; ³In-solution yields were calculated based on GCMS (wt%) with comparison to a known standard; ⁴0.4 A% of **3** was also detected; ⁵The area purity was obtained by GCMS (TIC A%), wt% was obtained by GCMS (wt%) with comparison to a known standard, the mass/yield was corrected data, and *ee* was obtained by chiral column GC; ⁶The distillation of compound **C5.3** was performed under 70-80 Torr at 80 °C; ⁷Atmospheric distillation at 170 °C with N₂ flow; ⁸Atmospheric distillation at 170 °C without N₂ flow.

2.2 Milestone 2: Synthesis of bicyclic chiral ketone **C5.5**

2.2.1 Familiarization of **C5.5** synthesis

Hodgson cyclopropanation of epoxide **C5.3** to make **C5.5** has been reported on kilogram scale.²⁷ Following this protocol, the obtained chiral epoxide **C5.3** was then advanced to the synthesis of bicyclic ketone **C5.5** via Hodgson cyclopropanation and the subsequent oxidation (Scheme 2.2.1).

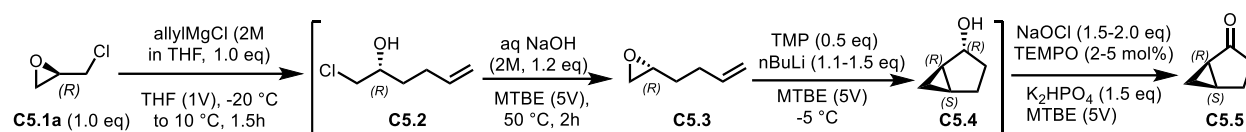


Scheme 2.2.2 Two-step synthesis of **C5.5** from **C5.3**

As depicted in Scheme 2.2.3, treatment of **C5.3** with n -BuLi and TMP enabled the formation of **C5.4** in 83% in-solution yield. The oxidation of the crude **C5.4** with aq NaOCl (10-15 w/w available chlorine assay) in the presence of a catalytic amount of TEMPO proceeded smoothly to deliver the bicyclic ketone **C5.5**. The pure ketone **C5.5** was obtained after distillation and the isolated yield of this two-step process was 56%. The overall isolated yield of **C5.5** from **C5.1a** (4 steps in total) was low, only 31-33% mainly due to a significant amount of product loss in each distillation. Considering the high in-solution yield and purity in each step, our effort was then focused on the telescoping process development of the synthesis of **C5.5**, aiming to improve the overall isolated yield of **C5.5** with a minimal number of distillations of the intermediates.

2.2.2 Four-step telescoped synthesis of **C5.5** from **C5.1a**

As discussed above, we successfully developed the process to make **C5.5** from **C5.1a** with two distinct distillations.²⁹ To achieve a more practical and streamlined synthesis of **C5.5**, a 4-step telescoped process to make **C5.5** was developed (Scheme 2.2.1).



Scheme 2.2.2 Telescoped synthesis of (*1R,5S*)-bicyclo[3.1.0]hexan-2-one (**C5.5**)

The aforementioned two-step process to synthesize **C5.3** from **C5.1a** and **C5.1b** afforded an excellent purity profile of the crude epoxide **C5.3**, providing possible telescoping options for the subsequent Hodgson cyclopropanation. A hundred-gram scale reaction of **C5.1a** with **C5.1b** gave a solution of **C5.2** in MTBE with a quantitative in-solution yield. The solution of **C5.2** was then treated with NaOH (2M), affording an MTBE solution of **C5.3** (770 g total solution mass) with a 98.8% TIC A% by GCMS after an aqueous workup. The water content of this crude solution before drying was 1.5% by a Karl Fischer (KF) titration measurement, indicating the total water mass for the reaction mixture was approximately 7.3 g (Table 2.2.). As the subsequent Hodgson reaction is moisture sensitive,²⁵ the reaction mixture of **C5.3** was dried before implementing the Hodgson conditions to produce **C5.4**. An azeotropic distillation method was developed to dry the reaction mixture of **C5.3**.³⁰ It is known that MTBE forms an azeotropic mixture with water (b.p. 53 °C) and the water content of this binary azeotrope was 4 wt%.³⁰ Thus, the crude solution of **C5.3** was heated at 70 °C under atmospheric pressure with a Dean-Stark trap for 12 h (until no more water to come off) with a resulting water loss of 10 g (0.15% by KF). Notably, the mass loss of **C5.3** was 4% in this azeotropic distillation process and the two-step overall assay yield was 87% after drying of the reaction mixture (Table 2.2.). As a result, this drying approach was used to dry the crude of **C5.3** in our telescoping process development to synthesize (*1R,5S*)-bicyclo[3.1.0]hexan-2-one (**C5.5**).

Table 2.2.1 Drying the crude reaction solution of **C5.3** by azeotropic distillation with Dean-Stark trap at 70 °C

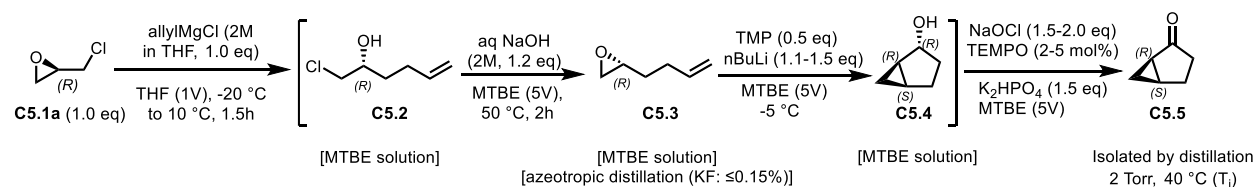
C5.3 in MTBE	Before azeotropic distillation¹	After azeotropic distillation
Total mass of solution (g)	770	731
KF (%) of solution	1.45	0.15
Mass of water content (g)	11	1
C5.3 in solution wt%²	18	18

C5.3 mass by wt% (g)	137	131
C5.3 TIC A% (GCMS)	98.8 ³	98.4 ⁴

¹After treating with aq NaOH, the telescoped reaction mixture from **C5.1a** (148 g) was washed by water, and brine before azeotropic distillation; ²wt% was obtained by GCMS with comparison to a known standard; ³MTBE and THF solvent peaks were excluded, containing epichlorohydrin 1.2% TIC A% by GCMS; ⁴MTBE and THF solvent peaks were excluded, containing epichlorohydrin 1.6% TIC A% by GCMS; the higher percentage of epichlorohydrin after azeotropic distillation might be probably due to small amount of loss of **C5.3** during the distillation. Be aware that the solvent peaks were excluded, this is why the A% and the wt% do not match.

After the azeotropic distillation, the solution of **C5.3** (0.15% water by KF) was subject to the next Hodgson reaction.³¹ Under the reported protocol,²⁷ the treatment of the **C5.3** solution with 1.1 eq of *n*-BuLi in the presence of 0.5 eq of TMP at 0 °C afforded **C5.4** in 70-74 % in-solution yield with a purity of 85-91% TIC A% by GCMS (Table 2.2.2). After an aqueous workup, the resulting mixture of **C5.4** in MTBE was concentrated to 5 volumes and then subjected to oxidation with NaOCl/TEMPO. **C5.5** was produced with an in-solution assay yield of 90-98%. After an aqueous workup, the resulting organic layer was concentrated at 40 °C under vacuum (110 Torr) to remove MTBE. The concentrated mixture was distilled under 1-2 Torr to afford **C5.5** with a purity of 92-98 A% (GCMS-TIC) and enantiomeric excess of >99.9 % (chiral SFC). As summarized in Table 2.2., this 4-step telescoped protocol featured a high overall isolated yield (48-56 % vs 31-33 % in the stepwise protocol), minimal number of distillations, only one distillation of **C5.5** in the 4-step telescoped protocol), and good reproducibility and scalability (demonstration on hundred-gram scale, Table 2.2., Entries 1-3).

Table 2.2.2 Telescoped synthesis of (*1R,5S*)-bicyclo[3.1.0]hexan-2-one (**C5.5**)



Entry	C5.1a (g)	Assayed yield (purity TIC A% by GCMS) ¹				C5.5 (after distillation) ²		
		C5.2 ³	C5.3 ⁴	C5.4 ⁵	C5.5 ⁶	Amount (g)	Purity ⁷ (TIC A% by GCMS)	4-step yield ⁸
1	148	88 (95)	98 (99)	70 (91)	98 (97)	76	97 % ⁹	48 %
2	148	99 (95)	87 (99)	72 (89)	94 (93)	92	92 % ¹⁰	56 %

3	137	94 (93)	96 (98)	74 (85)	90 (98)	88	98 % ¹¹	53 %
---	-----	---------	---------	---------	---------	----	--------------------	------

¹The assayed yield was obtained by GC-MS and TIC A% purity was measured by GCMS; ²Distillation condition: MTBE was removed under 110 Torr at 40 °C and **C5.5** was distilled out under 2 Torr at 40 °C; ³The resulting reaction mixture of **C5.1a** and allylMgCl was quenched by MeOH, acidified with 2M HCl and extracted with MTBE (740 mL). The solution of **C5.2** in MTBE was washed by 2M HCl and water then used for the next step; ⁴The resulting solution of **C5.3** in MTBE (KF = 1.5%) was heated at 70 °C to remove water by azeotropic distillation to achieve a KF of 0.15% for the next step; ⁵The resulting solution of **C5.4** in MTBE (~2.2 L) was concentrated to ~800 mL under 150 Torr at 40 °C for next step; ⁶The resulting solution of **C5.5** in MTBE (~1.8 L) was concentrated under 110 Torr at 40 °C to remove most of MTBE for further distillation to afford **5.5**; ⁷TIC A% was measured by GCMS; ⁸Corrected isolated yield; ⁹Containing unknown peaks (<1% TIC A% by GCMS each); ¹⁰Containing TEMPO (4% TIC A% by GCMS), **C5.4** (2% TIC A% GCMS) and several unknown peaks (<1% TIC A% by GCMS each); ¹¹Containing **C5.4** (1.7% TIC A% by GCMS).

2.3 Milestone 3: Synthesis of chiral pyrazole **C5.9**

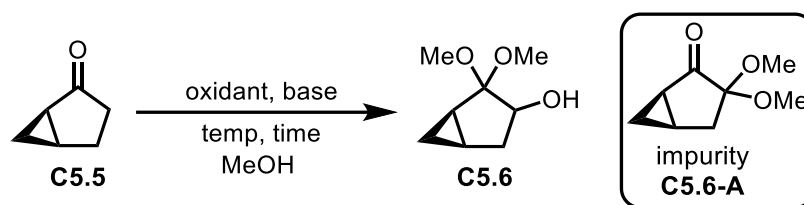
2.3.1 Optimization of **C5.9** synthesis

2.3.1.1 Hydroxylation of **C5.5**

With chiral compound **C5.5** in hand, the initial oxidation of **C5.5** with (diacetoxyiodo)benzene (PIDA) was performed according to the literature.¹² Under standard conditions, the reaction of **C5.5** and 1.5 eq of PIDA in the presence of KOH afforded **C5.6** in 71 TIC A% by GCMS (Table 2.3.1, Entry 1). Due to iodobenzene byproduct formation, column chromatography was required for purification. Additionally, the high cost and low market volume of PIDA made this PIDA-promoted hydroxylation undesirable for scale up. To ensure a more practical and affordable process to access **C5.6**, we aimed to: 1) utilize an inexpensive oxidant in this hydroxylation and 2) eliminate the need for column purification. A variety of readily available oxidants in the hydroxylation of **C5.5** (Table 2.3.1, Entries 2-5) were evaluated. However, no hydroxylation occurred when employing TCCA/TEMPO,³² I₂/DMSO, or NBS/DMSO³³ as the oxidative systems (Table 2.3.1, Entries 2-3). The OXONE[®] afforded 15% TIC A% by GCMS of α -hydroxylated product,³⁴ but attempts to further improve the yield via an increase in equivalents of OXONE[®], longer reaction time, and enhancement of reaction temperature resulted in no improvement of the yield (Table 2.3.1, Entry 4). Interestingly, I₂ was found to afford **C5.6** in a good yield (61% GCMS TIC A%) with KOH as a base (Table 2.3.1, Entry 5).³⁵ The I₂ was superior to PIDA due to its abundant availability, and more importantly, the absence of iodobenzene formation which removes the need for column chromatography. Optimization of the I₂-based oxidation found that using NaOMe as a base resulted in a cleaner reaction profile which may be

attributed to NaOMe's better solubility and stronger basicity. Treatment of **C5.5** and NaOMe with a solution of I₂ in MeOH at 0-25 °C afforded **C5.6** in 80% TIC A% by GCMS (Table 2.3.1, Entry 6). Notably, a slow addition of I₂ solution in MeOH was imperative to achieve a high yield. Lowering the reaction temperature to -9 to 0 °C further improved the GCMS TIC A% of **C5.6** to 86% (Table 2.3.1, Entry 7). Optimized conditions for this oxidation were demonstrated on a 30 g scale, providing **C5.6** in 87% TIC A% by GCMS for crude **C5.6** and 73% isolated yield after distillation (Table 2.3.1, Entry 8). It is worth mentioning that 5%-7% TIC A% by GCMS of proposed impurity **C5.6-A** was constantly formed in this I₂-promoted oxidation. The proposed compound **C5.6-A** showed a similar ¹H NMR pattern and the same mass spectrum as ketone **C5.7**, suggesting it may be a regioisomer of **C5.7**. Nevertheless, as a total of 37V of solvents were required for this hydroxylation, an investigation was performed to lower the solvent volume and achieve a more practical and scalable process of the I₂-promoted hydroxylation (vide infra).

Table 2.3.1 Hydroxylation of **C5.5** to **C5.6**



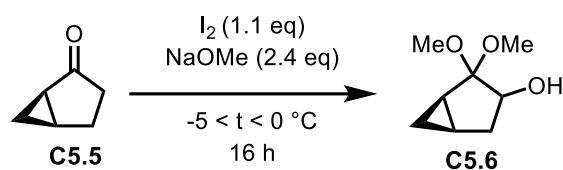
Entry ¹	Variations of the baseline condition	Assay Yield (TIC A%, GCMS)
1	Baseline condition ² : PhI(OAc) ₂ (1.5 eq), KOH (3.5 eq), MeOH (13V), 0-6 °C, 2 h	71 ³
2	TCCA (1.05 eq) / TEMPO (0.01 eq), DCM (16V), 0-25 °C, 16 h	9.8
3	I ₂ (0.2 eq) or NBS (0.2 eq), DMSO, 60 °C, 24 h	ND
4	OXONE® (monopersulfate, 2.7 eq), TFAA (7 eq), PhI (0.2 eq), H ₂ O (42V)/CH ₃ CN (125V), 40-90 °C, 22 h	15 ⁴
5 ⁵	I ₂ (1.2 eq), KOH (2.4 eq), MeOH (37V), 0-25 °C, 14 h	61
6	I ₂ (1.2 eq), NaOMe (2.4 eq), MeOH (37V), 0-25 °C, 14 h	80
7	I ₂ (1.2 eq), NaOMe (2.4 eq), MeOH (37V), -9°C-0 °C, 12 h	86
8	I ₂ (1.2 eq), NaOMe (2.4 eq), MeOH (37V), -9°C-0 °C, 12 h	87 ⁶

¹In these condition screens, racemic **C5.5** was used; ²Typical procedure with PIDA unless otherwise stated: KOH (3.5 eq) dissolved in MeOH (13V) at 55 °C, cooled to 0-6 °C, **C5.5** (1 g) was added slowly, stirred at 0-6 °C for 45 min, PIDA (1.5 eq) was added slowly at 0-6 °C and stirred at the same temperature until completion (2 h), purified by column chromatography (SiO₂, Hexanes/EtOAc, 8/2, v/v); ³Isolated yield: 61% after column chromatography; ⁴15% GCMS TIC A% of α-hydroxylated product was formed, 85% GCMS TIC A% of **C5.5** remained, increase of

equivalents of OXONE[®], longer reaction time or enhancement of reaction temperature resulted in no improvement; ⁵Typical procedure with I₂ unless otherwise stated: NaOMe (2.4 eq) in MeOH (19V) was cooled to 0-6 °C, **C5.5** (1 g) was added slowly, 10 min later, I₂ (1.2 eq) in MeOH (18V) was added slowly at 0-6 °C, the mixture was stirred until completion (~12-14 h). The reaction mixture was concentrated to remove MeOH under reduced pressure at rt. The residue was extracted with DCM, and washed with sat. Na₂SO₃. All DCM layers were concentrated and distilled at 60-70 °C under vacuum (10 Torr) to afford **C5.6**, 5%-7% GCMS TIC A% **C5.6-A** (tentative) was consistently formed; ⁶30 g of **C5.5**, isolated yield: 73% after distillation.

I₂-promoted hydroxylation of **C5.5** afforded **C5.6** in excellent yield when charging **C5.5**, NaOMe/MeOH, and I₂/MeOH in order (Table 2.3.2, Entry 1). The drawback to this approach is the need for a large volume of solvent, primarily from diluting NaOMe (19V) and dissolving I₂ (18V). To ensure a practical and viable hydroxylation process, the reduction of solvent volumes in the hydroxylation of **C5.5** is necessary. The initial effort utilized NaOMe (25 wt%, 6V) without diluting the mixture (Table 2.3.2, Entry 2). Using the aforementioned charging order, the reaction of **C5.5**, NaOMe/MeOH (6V), and I₂/MeOH (18V) lowered the solvent volume to 24V. However, **C5.6** was formed with a lower purity profile (69% GCMS TIC A%). The addition of I₂/MeOH to a mixture of **C5.5**/NaOMe/MeOH was exothermic and the slow addition of the I₂/MeOH (18V) solution is critical to afford a clean profile of **C5.6** (Table 2.3.2, Entry 1). We hypothesized slow addition of **C5.5** to the mixture of I₂/NaOMe/MeOH could also mitigate the exothermic heat generation, thus allowing a reduction in MeOH volume. This hypothesis proved correct (Table 2.3.2, Entries 3-5). We found I₂ solubility in NaOMe (25 wt%) was markedly increased when compared with MeOH alone, such that a solution readily forms even at reaction temperatures (-5 °C to 0 °C). In a one-pot fashion, charging NaOMe (6V) followed by the addition of solid I₂, the resulting solution reacted with **C5.5** to deliver **C5.6** in 87% GCMS TIC A% (Table 2.3.2, Entry 5). It should be noted that the reaction with the charging order of **C5.5**, I₂, and NaOMe resulted in a low purity profile of **C5.6** (Table 2.3.2, Entries 6-7). Ultimately, the reaction of NaOMe (6V), I₂ solid, and **C5.5** in order afforded **C5.6** with an excellent purity profile, such that crude **C5.6** could be used without further purification (vide infra). This hydroxylation process dramatically reduced the total solvent volume to 6V and removed the need for column chromatography, which is suitable for scale-up.

Table 2.3.2 Investigation of reagent order of addition to reduce solvent volumes



Entry ¹	Charging order			Total solvent (V)	C5.6 (A%) (GCMS TIC) ²
	1 st	2 nd	3 rd		
1	C5.5 (neat)	NaOMe / MeOH (19V)	I ₂ / MeOH (18V)	37	87
2	C5.5 (neat)	NaOMe (6V)	I ₂ / MeOH (18V)	24	69
3	I ₂ / MeOH (18V)	NaOMe (6V)	C5.5 (neat)	24	75
4	I ₂ / MeOH (10V)	NaOMe (6V)	C5.5 (neat)	16	79
5	NaOMe (6V)	I ₂ (s)	C5.5 (neat)	6	87
6	I ₂ / MeOH (10V)	C5.5 (neat)	NaOMe (6V)	16	50
7	I ₂ (s)	C5.5 / MeOH (6V)	NaOMe (6V)	12	40

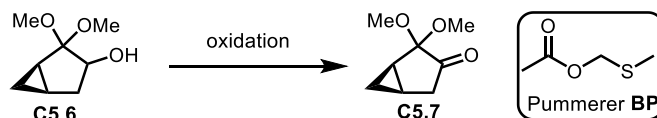
¹Typical procedure: NaOMe (2.4 eq) in MeOH, C5.5 (1 g), I₂ (1.1 eq), MeOH at -5 to 0 °C according to the addition order and conditions as shown in the table; ²TIC A% of IPC was measured by GCMS.

2.3.1.2 Oxidation of C5.6

With a practical method for the preparation of C5.6 in hand, our focus was then shifted to the oxidation of C5.6 to furnish the desired ketone C5.7. The Swern oxidation of C5.6 accomplished the formation of C5.7 quite smoothly (Table 2.3.3, Entry 1).³⁶ However, a cryogenic condition was needed to achieve a good yield of C5.7, and messy reaction mixture profiles were obtained with higher temperatures (Table 2.3.3, Entries 1-3). As an alternative to the cryogenic Swern oxidation conditions, TFAA can replace oxalyl chloride allowing for a higher reaction temperature.³⁷ The oxidation of C5.6 with TFAA/DMSO in the presence of TEA at -20 °C yielded C5.7 in 67% GCMS TIC A% (Table 2.3.3, Entry 4). Unfortunately, optimization of this oxidation by varied conditions (i.e., increase of equivalent of TFAA, reaction time, and temperature) resulted in no improvement and rather low yields and poor purity profiles of C5.7 obtained in the reaction mixtures. Oxidation of C5.6 under Dess-Martin conditions³⁸ effectively produced C5.7 in 87%

GCMS TIC A% (Table 2.3.3, Entry 5). Ley-Griffith oxidation (morpholine N-oxide (NMO)/tetrapropylammonium perruthenate (TPAP)) was also effective in the oxidation of **C5.6** to **C5.7** (Table 2.3.3, Entry 6).³⁹ However, neither Dess-Martin nor Ley-Griffith oxidation is process-friendly due to the safety concerns and the high cost associated with the reagent and catalyst. Finally, Albright-Goldman oxidation was identified as a possible scalable condition to yield **C5.7** (Table 2.3.3, Entries 7-13).⁴⁰ Under a standard Albright-Goldman oxidation, the reaction of **C5.6** with DMSO (7 eq) and Ac₂O (11 eq) at 50 °C afforded **C5.7** in 79% GCMS TIC A% yield (Table 2.3.3, Entry 7). It was found that an excess of Ac₂O and DMSO was required to achieve a >80% GCMS TIC A% of **C5.7**. Attempts to decrease the amount of Ac₂O and DMSO with solvents resulted in low conversion (30%-60% GCMS TIC A%) (Table 2.3.3, Entries 8-10). It is worth mentioning that the formation of the Pummerer rearrangement byproduct (**BP**) was inevitable under this Albright-Goldman condition, and the amount of the Pummerer rearrangement byproduct depended on the reaction time. As shown in Entry 7 (Table 2.3.3), a high level of the Pummerer rearrangement byproduct (**C5.7:BP** = 1:5) was observed. An increase in the equivalents of Ac₂O and DMSO dramatically shortened the reaction time, resulting in decreased byproduct formation.⁴¹ For example, a reaction of **C5.6** with DMSO (11 eq) and Ac₂O (14 eq) at 50 °C was complete within 7 h, delivering **C5.7** in 86% GCMS TIC A%, with a **C5.7:BP** ratio of 1:2 (Table 2.3.3, Entry 11). A mixture of DMSO (14 eq)/Ac₂O (14 eq) allowed for reaction completion within 4 h, and the ratio of **C5.7:BP** was 1:1 (Table 2.3.3, Entry 12). The ratio of **C5.7:BP** was increased to 2:1 when performing the oxidation with DMSO (19 eq) / Ac₂O (14 eq), in which the reaction was complete within 2 h (Table 2.3.3, Entry 13). After workup (basification with sat. NaHCO₃ and extraction with ethyl acetate), the resulting organic mixture was vacuum distilled to afford the pure **C5.7** in ~70% isolated yield. Considering that DMSO and Ac₂O are economical reagents and the feasibility of purging them out from the reaction mixture at the end, this Albright-Goldman oxidation (DMSO (19 eq) / Ac₂O (14 eq)) was used for the scale-up of **C5.7** (vide infra).

Table 2.3.3 Oxidation trials for the conversion of **C5.6** to **C5.7**



Entry ¹	Variations of the baseline condition	C5.7 (A%) (TIC A%, GCMS)
1	Baseline condition: (COCl) ₂ (1.2 eq), TEA (5 eq), DMSO (2.4 eq), DCM (15V), -60 °C, 1 h	92 ³
2	(COCl) ₂ (1.2 eq), TEA (5 eq), DMSO (2.4 eq), DCM (15V), -20 °C, 1 h	complex
3	(COCl) ₂ (1.2 eq), TEA (5 eq), DMSO (2.4 eq), DCM (15V), 0 °C, 1 h	complex
4	TFAA (1.2 eq), DMSO (1.1 eq), TEA (3.3 eq), DCM (10V), -20 to 15 °C, 1 h	67 ⁴
5	DMP (1.25 eq), 25 °C, DCM (5V), 1 h	87
6	NMO (2.7 eq), TPAP (0.09 eq), 25 °C, 24 h	61 ⁵
7	Ac ₂ O (11 eq), DMSO (7 eq), 50 °C, 14 h	79 (C5.7:BP =1:5) ⁶
8	Ac ₂ O (2 eq), DMSO (7 eq), 80 °C, 2 h	59 ⁴
9	Ac ₂ O (2 eq), DMSO (2 eq), 50 °C, 18 h, toluene	30 ⁴
10	Ac ₂ O (2 eq), DMSO (2 eq), 80 °C, 16 h, toluene	50 ⁴
11	Ac ₂ O (11 eq), DMSO (14 eq), 50 °C, 7 h	86 (C5.7:BP = 1:2) ⁶
12	Ac ₂ O (14 eq), DMSO (14 eq), 50 °C, 4 h	89 (C5.7:BP = 1:1) ⁶
13	Ac ₂ O (14 eq), DMSO (19 eq), 50 °C, 1.5-2 h	89 (C5.7:BP = 2:1) ⁶

¹Typical procedure: **C5.6** (purified, 0.5 g), oxidant, conditions as shown in the table; ²TIC A% of IPC was measured by GCMS; ³Isolated yield: 72%, after column purification; ⁴Major starting material **C5.6** remained; ⁵Isolated yield: 52%, after column purification; ⁶**BP**: methylthiomethyl acetate generated from the Pummerer rearrangement, the ratio was obtained by crude ¹H NMR.

The optimized Albright-Goldman oxidation affords **C5.7** in good isolated yield after aqueous workup and distillation. It should be noted that the basification process is necessary to terminate the undesired Pummerer rearrangement and this requires a large amount of sat. NaHCO₃ solution. It was found that 50V of sat. NaHCO₃ was needed to adjust the reaction mixture to pH = 7, resulting in a maximum operating volume of 70V, which would be problematic at scale. To accomplish a more practical workup process of the Albright-Goldman oxidation, stronger and more concentrated bases were examined, aimed at decreasing operating volumes. NaOH was first examined to replace the NaHCO₃ for basification. The basification proceeded smoothly with 5M NaOH and the total quenching volume was decreased to 14V. It was critical to control the temperature < 10 °C, otherwise some unknown impurities were generated during the quenching process. However, the NaOH-based quenching process is extremely exothermic and it will be challenging to control the low temperature at scale. Lowering the concentration of NaOH from 1M to 2M facilitated lower temperature control and mitigated the side reactions, but the total operating

volume increased to 65-130V. Switching to a 28 wt% NH_4OH , 10V of the basic solution allowed for the basification, unfortunately, imine impurities were observed by ^1H NMR. The possible side reaction between NH_4OH and the ketone functional group in **C5.7** may occur during the quenching process. Treating the reaction mixture with ice water (10V), followed by extraction with ethyl acetate allowed the partitioning of **C5.7** and Ac_2O into the organic phase, while leaving DMSO in the aqueous phase. There are two major advantages to using a water quench compared to a basic quench: 1) there is no exotherm in the water quench process, as Ac_2O hydrolysis is minimized, thus mitigating unexpected side reactions during the workup and 2) DMSO is miscible with water and allows separation from Ac_2O after ethyl acetate extraction, terminating the Pummerer rearrangement. The identification of cold water for the workup dramatically reduced the operating volume and the subsequent purification process was straightforward. For example, after quenching with ice water (10V), the reaction mixture was extracted with ethyl acetate ($10\text{V} \times 3$), and all of **C5.7**, **BP**, Ac_2O , and a small amount of DMSO and AcOH were detected in the organic layer. Further washing the organic layer with NaHCO_3 ($9\text{V} \times 3$) allowed for the removal of all DMSO and AcOH , and the resulting organic layer was subjected to distillation to afford **C5.7** in up to 56% yield (two steps, from **C5.5**), >95 A% purity and 100% *ee* (*vide infra*, see Table 2.3.4).

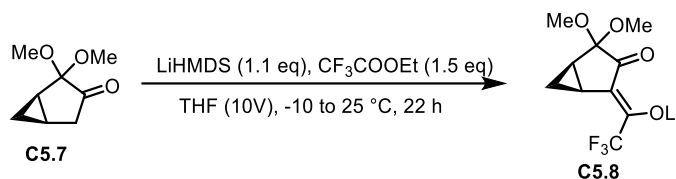
2.3.1.3 Acylation of **C5.7**

LiHMDS-mediated enolization has previously been reported on related structures to bicyclic ketone **C5.7**.^{5,16,42} To this end, the enolization of **C5.7** was conducted with LiHMDS and ethyl 2,2,2-trifluoroacetate on a small scale (300 mg) to verify this transformation. The initial experiment afforded **C5.8** in 48% assay yield (51 A% purity). A column purification (SiO_2) failed to improve the purity probably due to the instability of the **C5.8** moiety on the column.

Nonetheless, these conditions were repeated at various scales (Table 2.3.5). The reaction proved very efficient at producing **C5.8** with >80% isolated yield at a 1–20-gram scale. The compound **C5.8** was obtained as an off-white solid after *in vacuo* concentration (268 Torr, 40 °C) followed by trituration from *n*-hexane. Notably, a high purity of **C5.7** (>95 wt%) is required to ensure good repeatability for the synthesis of the **C5.8**. As illustrated in Entries 2 and 3 (Table 2.3.5), **C5.7** with 95 wt% purity produced **C5.8** with a purity of 81 wt% while **C5.7** with 91 wt% purity afforded

C5.8 with a purity of 73 wt%. This was further backed up by Entry 4, which used **C5.7** with a low purity (i.e., 94 wt%) and produced **C5.8** with a lower purity (i.e., 74 wt%) albeit slightly higher yield.

Table 2.3.5 Optimization summary for LiHMDS-mediated acylation of **C5.7**



Entry	Input (Purity) ¹	Output	Purity ¹	Yield ²
1	1.0 g (97.7%)	1.59 g	85.0% ³	83.0%
2 ⁴	2.1 g (95.0%)	3.7 g	81.4%	91.3%
3 ⁴	2.0 g (90.6%)	3.3 g	73.3%	80.8%
4	5.0 g (94.2%)	10.4 g	74.0% ³	95.0%
5 ⁴	10.0 g (95.0%)	18.5 g	83.4%	98.0%
6	10.0 g (97.7%)	17.2 g	85.7% ³	91.3%
7 ⁴	20.0 g (95.0%)	36.7 g	88.5%	97.5%
8	20.0 g (97.7%)	29.4 g	100.6% ³	91.6%

¹Purity measured by qNMR; ²Yield calculated via qNMR after trituration from *n*-hexane; ³Impurity is an isomer of **C5.8** that converts to **C5.9** in the next step, determined by variable temperature NMR; ⁴Reaction were done with racemic **C5.7**.

Unfortunately, other drawbacks were identified that are not amenable to scale-up, i.e., long reaction times, tedious workup and poor impurity profiles. We decided to fix the extended reaction time (22h), as unreacted starting material was seen in in-process analysis taken at 1, 3, and 6 hours.^j After the reaction was complete, the reaction mixture was concentrated inside the reactor to a wet solid (i.e., ~1V THF remaining) and then co-distilled with a higher boiling point solvent (i.e., heptane), it served as a practical process. This process yielded material that has increased purity and higher yield. Comparing Entries 6 and 8 we saw drastic differences in qNMR purity, 86 wt%, and 100 wt%, respectively. The variation in work-up is the likely culprit for this discrepancy, e.g.,

^j We hypothesize that reducing THF from 10V to 5V would reduce the cycle time from 22 hours. The optimization of reaction time will be pursued in our Y2 project.

Entry 6 was concentrated to dryness and then triturated with *n*-hexane. In contrast, Entry 8 was concentrated to a wet solid, co-distilled with heptane, and finally triturated with heptane.

This optimized work-up procedure adds true value in several ways: 1) it replaces *n*-hexane with heptane, a more scalable solvent, without yield loss, 2) it avoids complete distillation of reaction solvent (i.e., THF) to give a solid, which is unattainable in a batch reactor, 3) it limits compound loss in the mother liquor by co-distilling with heptane. To this end, we have demonstrated an optimized process that delivers **C5.8** as a white solid in >90% isolated yield and >99 wt% purity after vacuum drying at 40 °C for 12h. This optimized process was therefore performed at scale in a batch reactor to give **C5.8** (see section 2.3.2).

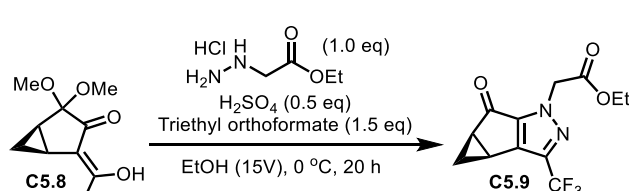
2.3.1.4 Pyrazole Synthesis

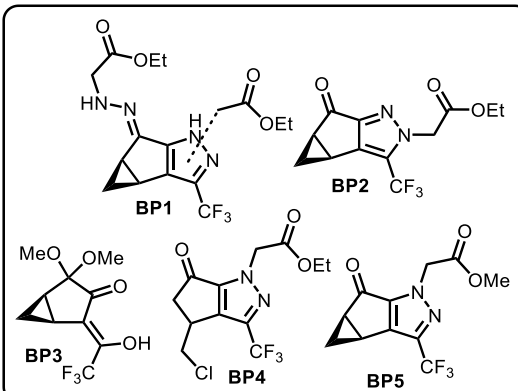
One of the most crucial steps in synthesizing **Frag C** is forming the heterocyclic pyrazole moiety. Previously, the pyrazole (**C5.9**) synthesis was accomplished via the Knorr pyrazole synthesis,^{5,16} an organic transformation that converts a hydrazine or its derivatives and a 1,3-dicarbonyl compound to a pyrazole using an acid catalyst (e.g., H₂SO₄). The mechanism begins with an acid-catalyzed imine formation, where in the case of hydrazine derivatives (used herein), the attack can happen on either carbonyl carbon and results in two possible regioisomer products.⁴³ Fortunately, the trifluoromethyl ketone moiety found on **C5.8** is more electrophilic than the bicyclic ketone, and thus favors the formation of **C5.9** over the other regioisomers.⁴⁴

The initial attempt of Knorr pyrazole synthesis from **C5.8** was conducted under slightly modified baseline conditions¹² (i.e., ethyl amino glycinate hydrochloride (EAG/HCl), H₂SO₄, triethyl orthoformate, EtOH, 0-25 °C (baseline ran at <5 °C), 16 hours). It was found that five major side-products could be produced during this transformation. However, under the baseline conditions (i.e., EAG/HCl, H₂SO₄, triethyl orthoformate, absolute EtOH, <5 °C, 20 hours) **C5.9** was produced in 94 A% with only 1.5 A% **BP4** (by GCMS-TIC) being observed during IPC measurement (**Error! Reference source not found.**, Entry 1). Comparison of denatured EtOH with alcohols (90/5/5, v/v/v, EtOH/*i*PrOH/MeOH) to absolute EtOH gave a similar reaction profile (**Error! Reference source not found.**, Entries 1 and 2). However, denatured EtOH with ketone and *i*-PrOH were both inadequate in this transformation (60 A% and 67 A% via GCMS-TIC,

respectively) (Table 2.3.5, Entries 3 and 4). Several other factors were also examined (i.e., reaction time, solvent volume, and triethyl orthoformate equivalents) in addition to solvent. The extended reaction time of the transformation is not affected by reducing the solvent volumes (15V to 5V). Moreover, a decrease in the volumes, as well as the equivalents of triethyl orthoformate, led to a decrease in the purity profile aid (i.e., 90 A% with 5V absolute EtOH (Table 2.3.5, Entry 5) and 91 A% with 1 eq triethyl orthoformate (Table 2.3.5, Entry 6)). In the end, the optimized reaction conditions (1 eq **C5.8**, 1 eq EAG/HCl, 0.5 eq H₂SO₄, 1.5 eq triethyl orthoformate, 15V denatured EtOH, <5 °C, 20 hours) were demonstrated at a 20-gram scale (**Error! Reference source not found.**, Entry 7), forming 14.0-grams of **C5.9** as a yellow solid after precipitation from water (water content = 0.37 % after drying), with excellent purity (i.e., 91.0 wt% via qNMR and 99.3 A% GCMS TIC). No further drying was required to proceed. Unfortunately, the isolated yield was quite low (i.e., 58.8%). The possible factors include: 1) this material sublimed when heated at >40 °C under reduced pressure (i.e., 0 Torr); 2) a significant amount of material stays in the aqueous layer. To obtain more **C5.9** from the aqueous layer, as demonstrated in Entry 3 (**Error! Reference source not found.**), the aqueous layer was extracted thrice with EtOAc (5V) and then the organic extractions were passed through a short pad of SiO₂ with 7% EtOAc in *n*-hexanes as an eluent to afford 2.82-grams of **C5.9** with good purity (95% via qNMR), increasing the overall yield of the reaction to 78%.

Table 2.3.6 Optimization summary for Knorr pyrazole synthesis of chiral **C5.9**





Entry ¹	Input (Purity) ²	Output	A% (GCMS-TIC) ³					Yield (%) ⁴	
			C5.9	BP1	BP2	BP3	BP4		BP5
1	1.0 g	1.0g	94	ND	ND	ND	1.5	ND	72

2 ⁵	(85.0 %)	1.0 g	93	ND	ND	ND	1.3	0.5	79
3 ⁶		0.96 g	60	ND	ND	ND	ND	ND	>99
4 ⁷		1.0 g	67	ND	ND	ND	14	ND	43
5 ⁸		1.0 g	90	ND	ND	ND	3.7	0.4	68
6 ⁹		1.1 g	91	ND	ND	ND	0.7	ND	75
7 ⁵	20.0 g (97.0 %)	14.0 g ¹⁰	99	ND	<1	ND	<1	ND	59 ¹¹
		2.82 g ¹²	95	ND	ND	ND	<1	<1	78 ¹³

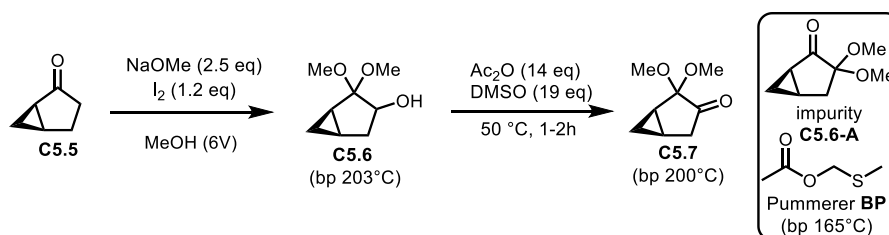
¹Conditions: **C5.8** (1 eq), EAG/HCl (1 eq), H₂SO₄ (0.5 eq), triethyl orthoformate (1.5 eq), abs EtOH (15V), <5 °C, 20 hours; ²Purity measured by qNMR; ³A% was obtained via GCMS TIC A%, ND = non detected; ⁴Crude yield calculated via qNMR after work-up; ⁵Denatured EtOH with alcohols (90/5/5, v/v/v, EtOH/*i*PrOH/MeOH) was used instead of abs EtOH; ⁶ EtOH denatured with ketone was used instead of abs EtOH; ⁷*i*-PrOH was used instead of abs EtOH; ⁸5V abs EtOH was used instead of 15V; ⁹1 eq triethyl orthoformate was used instead of 1.5 eq; ¹⁰Precipitated H₂O (30V); ¹¹Isolated yield measured by qNMR after precipitation; ¹²Filtrate was purified by a short column (SiO₂, 7% EtOAc in hexanes); ¹³Yield measured by qNMR after combination of precipitated and column-purified material.

2.3.2 Scale-up of **C5.9** synthesis

Using optimized conditions for **C5.7** production, a hundred-gram scale reaction was demonstrated in a 2L ChemRxnHub reactor (Table 2.3.7). This two-step process generated **C5.7** from **C5.5** in overall isolated yields of 45%-56% with one distillation. The chemical purity of **C5.7** was >95% TIC A% by GCMS and the enantiomeric excess was >99% (assuming the desired enantiomer based on the x-ray structure of **C5.11**). The major impurities were the Pummerer rearrangement byproduct **BP** (<1% TIC A%, GCMS) and the possible regioisomer **5.6-A** (~3%-4% TIC A%, GCMS). These impurities were purged via a low-temperature trituration with a high recovery of **C5.7** as shown in Entry 1 (Table 2.3.7). At the **C5.5** 100 g scale, the I₂-promoted hydroxylation afforded **C5.6** with 80% in-solution yield with the developed new addition order (i.e., NaOMe/MeOH (6V), followed by the addition of I₂ and then **C5.5**). The major impurity was the tentative regioisomer **5.6-A** (5%-7% TIC A%, GCMS). The crude reaction mixture was concentrated for the subsequent Albright-Goldman oxidation without further purification. Treatment of the crude **C5.6** with DMSO/Ac₂O at 50 °C afforded the **C5.7** with a 72% in-solution yield. Notably, the ratio of **C5.7:BP** was 2.4:1, which was slightly higher than the small-scale trials. After a standard aqueous workup (partitioning with cold water (10V)/ethyl acetate (10V × 3), followed by a sat. NaHCO₃ (9V × 3) wash), DMSO and AcOH were purged. After removing ethyl acetate, the resulting mixture (containing Ac₂O, the Pummerer **BP**, **C5.7**, and a small amount of **C5.6-A**) was subjected to vacuum distillation. Ac₂O and Pummerer **BP** were purged by

distillation under 7 Torr at 50 °C, and further distillation under 1-2 Torr at 60 °C afforded **C5.7** in 56% isolated yield with >95 A% (GCMS-TIC) (**BP** <1 A% and **5.6-A** <4 A%). The purity of **C5.7** was further improved to >98 A% by GCMS-TIC when the distilled **C5.7** was triturated with hexanes at -45 °C. The mass recovery yield of the trituration process was >90%. Gaining more distillation experience from the first batch, the proficient operation delivered higher isolated yields in the second and third batches (Table 2.3.7, Entries 2, 3).

Table 2.3.7 Hundred-gram-scale demonstration of synthesis of **C5.7**.



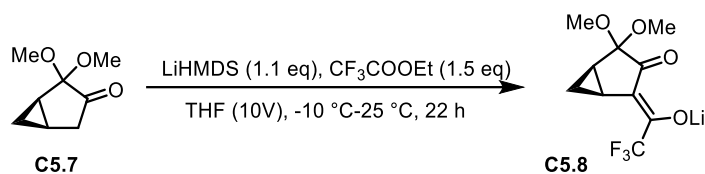
Entry	C5.5 (g)	Assayed yield (crude)		C5.7 (after distillation) ¹	
		C5.6	C5.7	Output (Yield)	Purity (A%) ³
1	100	80%	72%	77 g (45%) ⁴	94 (98) ⁵
2	100	74%	84%	91 g (56%)	95 (97) ⁵
3	90	79%	77%	77 g (51%)	95 (99) ⁵

¹Distilled at 50 °C under 7-35 Torr to remove EtOAc, Ac₂O, and Pummerer **BP**, and at 60 °C under 1-2 Torr to afford **C5.7**; ²Corrected two-step isolated yield; ³Purity was obtained by TIC A% GCMS, Pummerer **BP** <1% TIC A% by GCMS and possible isomer **C5.6-A** ~3%-4% TIC A% by GCMS; ⁴The product loss during distillation resulted in a low isolated yield of this batch; ⁵Purities in parenthesis were obtained after trituration with hexanes at -45 °C.

The aforementioned optimized process (see Section 2.3.1.3) for the synthesis of **C5.8** was conducted thrice on dimethyl acetal ketone **C5.7** (>97 % purity) at >50-gram scale producing ~277 g of **C5.8** in total (Table 2.3.8). This material formed 5%-12% of a major impurity (by NMR), which is significantly higher than what was formed during optimization (<5%). This impurity was determined to be a rotamer of **C5.8**, via variable temperature NMR, and thus is converted to **C5.9** in the next step. As seen in Table 2.3.8, Entry 1 suffers from a lower-than-average yield (i.e., 72.7%) compared to the other large-scale reactions. Material loss to the mother liquor after filtration was due to an excess of THF in the heptane solution during trituration (the co-distillation process using 10V heptane, see Section 2.3.1.3, was done once). The material in the mother liquor was significantly lower in purity (<50%) making recovery extremely challenging. Conversely, Entry 2 displayed excellent overall isolated yield (87.1%) with good purity (>90 wt% by qNMR).

This is most likely due to the repetitive nature of the optimized work-up process, i.e., co-distillation using heptane (7.5V) thrice, followed by heptane (15V) trituration. Finally, Entry 3 afforded spectacular purity (>97 wt% by qNMR), but material was lost during the trituration process due to a leak in the reactor, thus giving a decreased yield. The reaction mixture was concentrated *in vacuo* (80 Torr, 30 °C) inside the reactor until the clear-to-cloudy transition (~5V), and then heptane (20V) was slowly added using a peristaltic pump (30 mL/min). This suspension was stirred overnight at room temperature then filtered and dried in a vacuum oven at 40-50 °C to give **C5.8** as a white solid in 78.0% yield (97.4 wt% purity by qNMR). This material was used in the next step without any subsequent purification.

Table 2.3.8 Scale-up summary of LiHMDS- mediated acylation of chiral **C5.7**



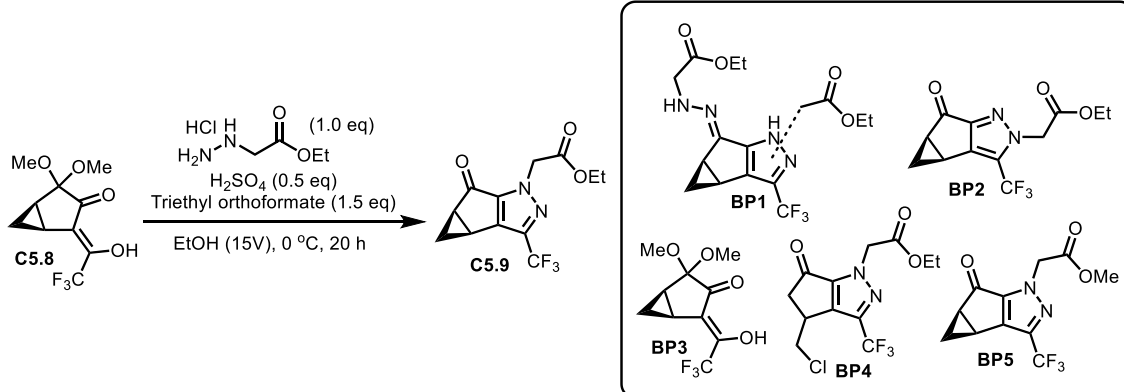
Entry	Input (Purity) ¹	Output	Purity ^{1,2}	Yield ³
1	50.0 g (97.7%)	64.8 g	89.3%	72.7%
2	70.0 g (99.5%)	109.7 g	90.5%	87.1%
3	80.0 g (97.0%)	102.7 g	97.4%	78.0% ⁴

¹Purity measured by qNMR; ²Isomer of **C5.8** (5%-12%) that converts to **C5.9** in the next step, as determined by variable temperature NMR; ³Yield calculated via qNMR; ⁴Leak in the top of the reactor led to material loss.

C5.9 initial scale-up attempts at 50-gram (Table 2.3.9, Entries 1 and 2) led to the formation of 42.0- and 36.2-grams of **C5.9** as a pale-yellow solid after precipitation from water (30V), respectively, with excellent purity (i.e., 91.8 wt% and 97.0 wt% via qNMR, respectively). This corresponds to an overall yield of 69.1% and 72.9%, respectively. Further material recovery from Entries 1 and 2 was accomplished by extracting the filtrate thrice with EtOAc (750 mL, 5V each) and passing the residual organic material through a short pad of SiO₂ with 7% EtOAc in hexanes as an eluent. This process afforded 9.30- and 9.85 grams of **C5.9** as a bright yellow solid with good purity (95.7 wt% and 96.6 wt% via qNMR, respectively), increasing the overall yield of the reactions to 91.8% and 93.0% for Entries 1 and 2, respectively. A quick check of the water content and *ee* for these reactions showed water content was 0.36% and 0.28% for Entries 1 and 2, respectively, while both reactions gave **C5.9** as the desired enantiomer (100% *ee*, the structure was

confirmed by single-crystal x-ray crystallography, see Section 4.4.1). Therefore, the material from these 50-gram reactions was used in the subsequent dithiolation step as is (see Section 2.4.2). Finally, we conducted a 150-gram scale reaction with **C5.8** (97.0% qNMR purity), which produced 112 grams of **C5.9** (water content = 0.22%, and 100% *ee*) as a yellow solid after precipitation from water (30V) corresponding to a 49.0% overall yield with excellent purity (i.e., 95.4 A% via GCMS-TIC). The lower yield is correlated to material loss in the mother liquor (25.1 A% of **C5.9** via GCMS-TIC), which wasn't extracted due to time limitations.

Table 2.3.9 Scale-up summary for Knorr pyrazole synthesis of **C5.9**



Entr y ¹	Input (Purity) ²	Output	Purity (TIC A%, GCMS) ³						Wt% (qNMR)	Yield ⁴ (%)
			C5.9	BP1	BP2	BP3	BP4	BP5		
1	50.0 g (86.2 %)	42.0 g ⁵	94.6	ND	2.2	ND	1.2	<1	91.8	69.1 ⁶
		9.3 g ⁷	96.8 ⁸	ND	ND	ND	ND	ND	95.7	91.8 ⁹
2	50.0 g (86.2 %)	36.2 g ⁵	97.4	ND	ND	ND	<1	1	97.0	72.9
		9.8 g ⁷	95.2	ND	ND	ND	<1	<1	96.6	93.0 ⁹
3	150.0 g (97.0 %)	112.0 g ⁵	95.4	1.4	1.5	ND	<1	<1	-	49.0

¹Conditions: **C5.8** (1 eq), EAG/HCl (1 eq), H₂SO₄ (0.5 eq), triethyl orthoformate (1.5 eq), 90/5/5 (v/v/v, EtOH/iPrOH/MeOH) denatured EtOH (15V), <5 °C, 20 hours; ²Purity measured by qNMR; ³Purity measured after 20 hours via GCMS; ⁴Yield calculated by qNMR; ⁵Precipitated from H₂O (30V); ⁶Loss of product during drying at 50 °C/vacuum, charred and sublimed; ⁷Filtrate was purified by a short column (SiO₂, 7% EtOAc in Hexanes); ⁸2.3 A% of an unknown impurity was observed by GCMS; ⁹Yield calculated by qNMR after combination of precipitated and column-purified material.

2.4 Milestone 4: Synthesis of **Frag C**^k

2.4.1 Optimization of the **Frag C** synthesis

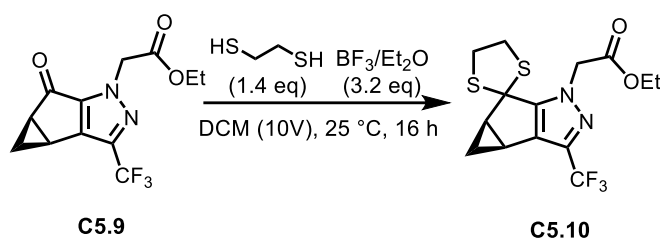
2.4.1.1 Dithiolation of **C5.9**

With **C5.9** in hand,¹ dithiolation was conducted to afford the 1,3-dithiolanes of **C5.10** (Table 2.4.1). According to the literature protocol,⁵ the dithiolation was initially performed with racemic *rac*-**C5.9** and 1,2-ethanedithiol. The reaction of *rac*-**C5.9** with 1.4 eq of ethane-1,2-dithiol in the presence of BF₃Et₂O (3.2 eq) afforded the crude *rac*-**C5.10** in 94% assay yield with 80% purity (qNMR). The major impurity was ethane-1,2-dithiol. After trituration from hexanes, *rac*-**C5.10** was obtained as a white solid in 86% isolated yield and >97% purity (qNMR) (Table 2.4.1, Entry 1). Attempts to lower the amount of ethane-1,2-dithiol (i.e., 1.1 eq, 1.2 eq, and 1.3 eq) and BF₃Et₂O (1.2 eq, 1.5 eq, 2.2 eq, 2.5 eq) gave incomplete reaction after 16 hours. Due to the limited timeline of the project, we did not further fine-tune the reaction and thus utilized the conditions (1.4 eq ethane-1,2-dithiol and 3.2 eq BF₃Et₂O) for the dithiolation of **C5.9**. The dithiolation of **C5.9** proceeded smoothly and the crude **C5.10** was obtained in 80% assay yield with 80% purity (qNMR) (Table 2.4.1, Entry 2). Surprisingly, the purification of **C5.10** by recrystallization failed. It was found that **C5.10**, unlike its racemic counterpart, does not form a crystalline solid at room temperature or -20 °C. After a column purification, **C5.10** was obtained as a yellowish oil. Differential Scanning Calorimetry (DSC) data of the purified **C5.10** affirmed its melting point of -23.6 °C. Fortunately, the major impurity in the dithiolation was 1,2-ethanedithiol and it was purged out by co-distillation with toluene.

Table 2.4.1 Optimization summary for dithiolation of chiral **C5.10**

^k The small-scale synthesis of racemic **Frag C** was complete. But due to the limited timeline of the project, process development of the LenC 5 was stopped at the penultimate step (**C5.11**).

¹ Direct fluorination of **C5.9** with deoxy fluorination reagents (i.e., PhenoFluor Mix, SO₂F₂/Me₄NF, BAST, Xtalfluor-E, DFI, and Fluolead)^{45,46,47-52} was investigated. No fluorination occurred but resulted in recovery of the starting **C5.9**.



Entry ¹	Input ²	Output (g)	Purity (%) ²	Yield (%) ³
1 ⁴	12.0 g	16.9 ⁵	79.6	94.0
		12.6 ⁶	97.2	85.8
2 ⁷	12.0 g	12.3 ⁵	79.8	79.9
		10.6 ⁸	88.2	76.5

¹Reactions were conducted with **C5.9** (1eq), ethane-1,2-dithiol (1.4 eq), BF₃Et₂O (3.2 eq), DCM (10V), 25°C, 16h, after completion of the reaction, quenched with water (5V), sat. NaHCO₃ (25V), then evaporated to dryness, unless otherwise stated. ²Purity measured by qNMR; ethane-1,2-dithiol was the major impurity. ³Corrected yield; ⁴*rac*-**C5.9** was used; ⁵Crude product after rotovap; ⁶Purified product after trituration with *n*-hexane; ⁷Enantiopure **C5.9** was used; ⁸Column purified, oil-like **C5.10** resulted in failure of purification by recrystallization.

Nonetheless, several areas are noted as worthy of further investigation in the future.

- The cycle time (16 hours) is lengthy and could be reduced by decreasing the DCM volumes (i.e. from 10V to 5V).
- While this transformation needs excess BF₃OEt₂, using a Brønsted acid (e.g., *p*-toluenesulfonic acid) might eliminate the need for super-stoichiometric quantities in thioacetal formation.
- The conditions used to fluorinate **5.10** (see Section 2.4.1.2) are susceptible to moisture. To aid in the drying of **C5.10**, solvent chasing (i.e. swapping to toluene from DCM) might streamline the workup of **C5.10** (i.e. via azeotropic distillation of toluene solution to afford dry **C5.10**).

2.4.1.2 Fluorination of **C5.10**

2.4.1.2.1 Desulfurative fluorination of **C5.10**

With **C5.10** in hand, desulfurative fluorination was carried out to install the gem-difluorinated **C.11**. Desulfurative-difluorination includes two steps: 1) activation of the dithiolated carbon center by bromination of the sulfur atom (formation of bromosulfonium); 2) a nucleophilic substitution by a fluoride ion to form C-F bond.^{17,53–55} In general, the reaction of a dithiolated

compound with 1,3-dibromo-5,5-dimethylhydantoin (DBDMH) and HF-pyridine (HF-Py) could accomplish the fluorination, yielding the gem-difluorinated product.^{56,57} This condition was used in the synthesis of racemic **Frag C**.^{5,16}

This protocol, however, is extremely challenging due to the use of the HF-Py complex (Olah's reagent) as the nucleophilic fluorine source. It is known that HF-Py is highly toxic and corrosive. It could cause acute harm to the skin, eyes, and respiratory tract tissues with minimum contact. To demonstrate this fluorination chemistry safely, we developed a SOP (Standard Operating Procedure) to ensure safety within our facility.

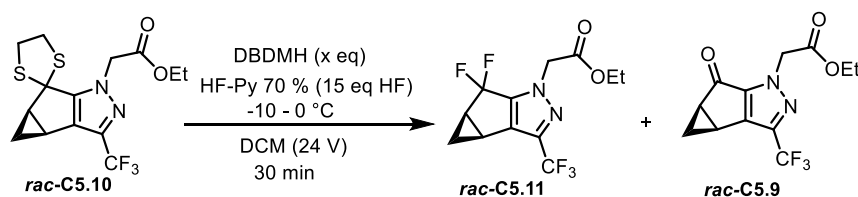
The key findings include (See Appendix 4.3 (SOP) for details):

- Having an HF-Py first-aid/spill kit (containing 2.5 % calcium gluconate gel);
- Using appropriate PPE protective equipment (e.g., acid-resistant neoprene or nitrile gloves, safety goggles, face shields, lab coats, aprons, long sleeves, and rubber boots);
- PTFE reactors are highly recommended, while polyethylene and HDP reactors can also be used;
- PTFE-coated needles for transfer of the HF-pyridine;
- PTFE-coated needle thermocouple to monitor the internal temperature;
- An inert atmosphere must be used since HF-Py and the reaction itself is moisture-sensitive;
- Bubblers containing a base solution must be placed at the end of the reaction line to quench any possible HF gas formed.

With safety protocols in place, the desulfurative fluorination with HF-Py and DBDMH was examined with racemic dithiolated compound **rac-C5.10**. The initial trial of fluorination of **rac-C5.10** under the standard condition (70% HF-Py complex (30 eq HF) and DBDMH (4 eq)) proceeded smoothly to afford the **rac-C5.11** in 87 A% (LCMS) with a trace amount of **rac-C5.9** also observed by GCMS. Encouraged by the excellent results of the fluorination, optimization was conducted to identify optimal conditions for scale-up. The eq of DBDMH, eq of HF-Py and volumes of DCM were systematically investigated. As summarized in Table 2.4.2, the equivalents of DBDMH were examined. The fluorination of **rac-C5.10** with DBDMH (2 eq) and HF-Py (30

eq) afforded **rac-C5.11** in 84 A% yield and 4 A% of **rac-C5.9** was observed (Table 2.4.2, Entry 2). Similar results were obtained when the fluorination was conducted with 15 eq HF-Py (Table 2.4.2, Entry 3). Thus, the latter screening of the equivalents of DBDMH was carried out with 15 eq HF-Py. It was found that 2.0 equivalents of DBDMH outperformed in this fluorination. Less than 2.0 equivalents of DBDMH resulted in slightly low yield of the fluorinated product (Table 2.4.2, Entry 3-6). Thus, 2.0 equivalents of DBDMH were used for further optimization.

Table 2.4.2 Screening of the equivalents of DBDMH in fluorination

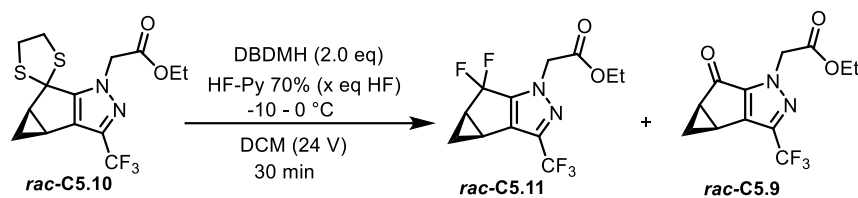


Entry ¹	DBDMH (eq)	IPC profile (A%) ³	
		rac-C5.9	rac-C5.11
1 ²	4.0	<1	87 (73 ⁴)
2 ²	2.0	4	84
3	2.0	4	88
4	1.9	3.5	86
5	1.8	7	83
6	1.7	3	82

¹All reactions were performed in PTFE reactor (100 mL) with **rac-C5.10** (500 mg, 1 eq), DBDMH as shown in the table, HF-Py (15 eq HF), DCM (24 V), -10 to 0 °C, 30 min, unless otherwise stated, after completion, quenched by a saturated NaHCO₃ solution, extracted with DCM, and washed with 1M HCl solution; ²30 eq HF (HF-Py) was used. ³A% was monitored by LCMS (254 nm). ⁴Isolated yield.

As shown in Table 2.4.3, fluorination with various equivalents of HF-Py was conducted in the presence of 2 eq DBDHM. It was found that the amount of HF could be lowered to 11 equivalents to afford **rac-C5.11** in an excellent yield (90 A%) (Table 2.4.3, Entries 1-4). Fewer equivalents of HF resulted in a low yield ((Table 2.4.3, Entries 5-6). For example, 7 eq HF produced the fluorinated product in 78 A% (Table 2.4.3, Entry 6). As a result, 11 eq HF-Py was identified as optimal for this fluorination.

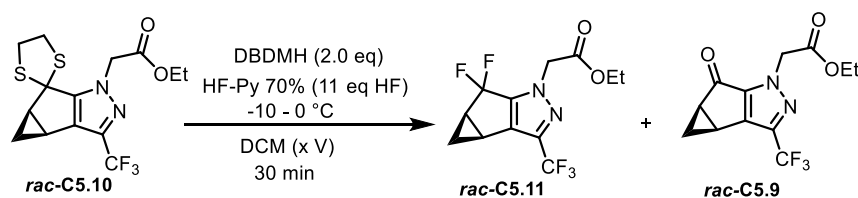
Table 2.4.3 Screening of the equivalents of HF-Py in fluorination



Entry ¹	HF-Py (eq HF)	IPC profile (A%) ²	
		<i>rac-C5.9</i>	<i>rac-C5.11</i>
1	30	4	84
2	15	4	88
3	13	3	91
4	11	4	90
5	9	4	84
6	7	5	78

¹All reactions were performed in PTFE reactor (100 mL) with *rac-C5.10* (500 mg, 1 eq), DBDMH (2.0 eq), HF-Py as shown in the table, DCM (24 V), -10 to 0 °C, 30 min, unless otherwise stated, after completion, quenched by a saturated NaHCO₃ solution, extracted with DCM, and washed with 1M HCl solution; ²A% was monitored by LCMS (254 nm).

Table 2.4.4 Screening of the solvent volumes in fluorination



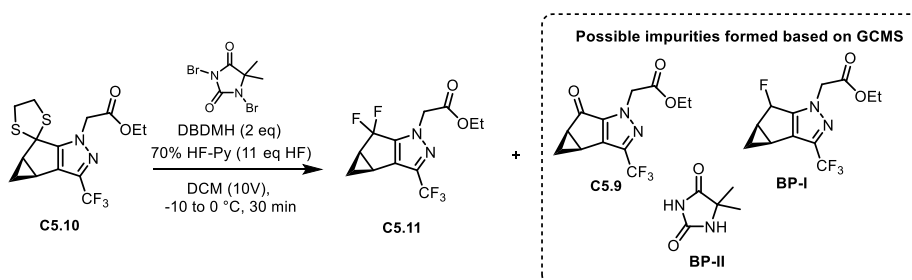
Entry ¹	DCM (V)	IPC profile (A%) ²	
		<i>rac-C5.9</i>	<i>rac-C5.11</i>
1	24	4	90
2	15	1	87
3	10	4	89
4	5	3	82

¹All reactions were performed in PTFE reactor (100 mL) with *rac-C5.10* (500 mg, 1 eq), DBDMH (2.0 eq), HF-Py (11 eq HF), DCM volumes as shown in table, -10 to 0 °C, 30 min, unless otherwise stated, after completion, quenched by a saturated NaHCO₃ solution, extracted with DCM, and washed with 1M HCl solution; ²A% was monitored by LCMS (254 nm).

The optimized condition was verified with the chiral dithiolated compound **C5.10**. As shown in Table 2.4.5, the fluorination of **C5.10** (1 g) in a 50 mL PTFE reactor showed 93 A% of **C5.11** (via GCMS-TIC) (Table 2.4., Entry 1). The fluorination condition was further evaluated in a 100 mL PTFE reactor at a 2-3 g scale. All these reactions afforded **C5.11** in 91-92 A% yield in the crude, exhibiting excellent reproducibility. In these fluorinations, several impurities were

identified by GCMS. As shown in Table 2.4.5, 2-5 A% **C5.9** was observed in all these reactions. Also, ~ 1 A% of mono-fluorinated product **BP-I** and 1-2 A% **BP-II** was detected by GCMS. All these impurities were purged out after recrystallization (see experimental part for details). From operation safety perspective, the reaction mixture (including aliquot for in-process analysis) must be fully basified before any further operations.

Table 2.4.5 Desulfurative fluorination of **C5.10**



Entry ¹	Input C5.10 (purity) ⁵	Crude (TIC A%) ⁶			
		C5.9	BP-I	BP-II	C5.11
1 ²	1 g (98 wt%)	5	-	2	93
2 ³	2 g (90 wt%)	2	1	2	92
3 ⁴	3 g (88 wt%)	3	1	1	91

¹Optimized condition: **C5.11** (1 eq), DBDMH (2 eq), 70% HF/Py (11 eq), DCM (10V), -10 to 0 °C, 30 min, after completion, quenched by a saturated NaHCO₃ solution, extracted with DCM, washed with 1M HCl solution and the DCM layer was evaporated to dryness for analysis. ²water content = 0.48 wt%, ³water content = 0.5 wt%, **C5.10** contains 3-5% unknown impurity showing the same m/z as **C5.10**. ⁴water content = 0.58 wt%, **C5.10** contains 3-5% unknown impurity showing the same m/z as **C5.10**. ⁵Purity by qNMR. ⁶A% was measured by GCMS-TIC.

NOTE – A key failure mode observed in fluorination of **C5.10** and several areas are worthy of future optimization:

- The reaction is moisture-sensitive, evident by **C5.9** formation due to water content.
- The reaction requires a PTFE reactor or HDPE plastic bottle. In a glass reactor, the fluorination will result in more impurities and even failure of the reaction.
- The reaction scale is limited due to the significant amounts of saturated NaHCO₃ required for quenching (using a NaOH solution for quench will require less volume and thus the

scale can be increased). A 13g-scale of **C5.10** was the largest operational scale in a 1L reactor for now.

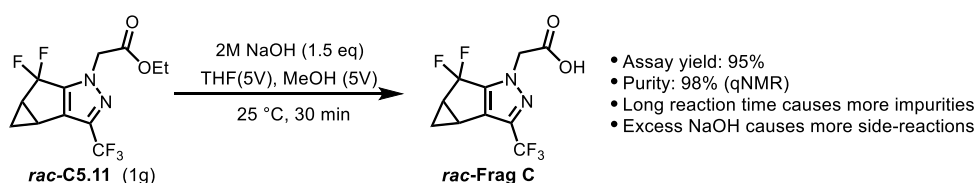
- Reaction quench must be done slowly due to rapid exotherm.
- A quench with a saturated NaHCO₃ followed by a 1M HCl wash allows for successful purging of the impurities.
- A purification process by trituration or crystallization is needed.

All the findings show that these optimized conditions are amenable to scale-up; as such, they will be tried on a 10-gram scale in a 1 L HDP plastic bottle (see Section 2.4.2).

2.4.1.3 Hydrolysis of **C5.11**

To verify the hydrolysis condition to finish up **Frag C** synthesis, we tried the reaction of *rac*-**C5.11** with NaOH. The hydrolysis of *rac*-**C5.11** with 2M NaOH (1.5 eq) in a binary solvent MeOH/THF (1/1, v/v, 10V) provided *rac*-**Frag C** with 95% isolated yield and 98% purity (by qNMR) without an extra purification. The hydrolysis process proceeded quickly and a full conversion was achieved within 30 minutes (Scheme 2.4.1). Notably, a long reaction time and excess of 2M NaOH can potentially decrease the purity profile and yield. We will evaluate the condition to produce **Frag C** on a large scale in the next phase of the project.

Scheme 2.4.1 A demonstration of hydrolysis of *rac*-**C5.11**^m



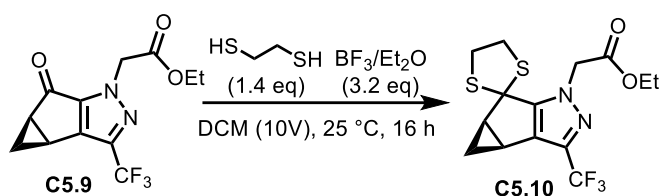
2.4.2 Scale-up of the **Frag C** synthesis

The optimized dithiolation process (see Section 2.4.1.1) for the synthesis of **C5.10** was conducted on pyrazole **C5.9** (99% qNMR purity) at a 35-gram scale producing ~47 g of **C5.10**

^mThe reaction was conducted with *rac*-**C5.11** (1 g, 1 eq), NaOH (2M, 1.2 eq), THF (5 mL) / MeOH (5 mL), 25 °C, 30 min, after completion, the mixture was quenched by HCl (3M, 1 mL), extracted with ethyl acetate (10 mL × 3), evaporated to dryness to afford *rac*-**Frag C** (760 mg).

(100% *ee*-assumed desired enantiomer based on the *x*-ray structure of **C5.9** and **C5.11**) in excellent isolated assay yield (97.5%) and good purity (i.e., 90 wt% by qNMR and 93 A% by GCMS-TIC) (Table 2.4.6) Excess ethane-1,2-dithiol, solvent, and water were removed with azeotropic distillation with toluene. Additional overnight high-vacuum drying at 40 °C afforded **C5.10** with water content of 0.5% that was used in the subsequent fluorination step as is.

Table 2.4.6 Scale-up summary for dithiolation of **C5.10**



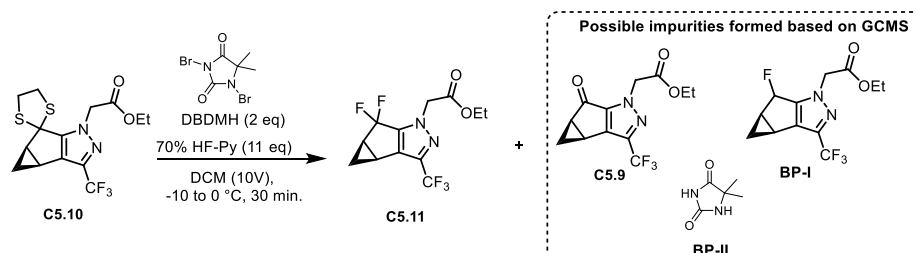
Entry	C5.9 , Input (Purity) ¹	C5.10 , Output	Purity ^{1,2}	KF ³	Yield ⁴
1	35.0 g (99.0 %)	47.4 g	90.1 %	0.5%	97.5 %

¹Purity measured by qNMR; ²ethane-1,2-dithiol and **C5.9** are major impurities (<3 A%); ³Karl-Fischer titration; ⁴Corrected yield.

The obtained **C5.10** (90 wt%) was used for the fluorination without further purification. Under the optimized fluorination condition, three 10g-scale batches were conducted in a 1 L HDPE plastic bottle (Table 2.4.7). All batches showed similar purity profiles and 86-91 A% of **C5.11** was obtained in the sticky oily crude. As expected, the main impurities were **C5.9** (2.3-3.5 A%), **BP-I** (1.3-2.6 A%), and **BP-II** (0-1.0 A%). To purge these impurities, we screened different solvents for crystallization. Heptane was initially tried. The colored oily crude was heated in heptane (5V) at 85 °C to yield a clear solution then it was cooled. Unfortunately, **C5.11** did not precipitate. Later, it was found that charcoal treatment of the colored oily crude was critical before purifying by recrystallization. Thus, the crude material was dissolved in MTBE (10V), treated with sat. Na₂CO₃ (10V × 2) and then activated charcoal (10 wt%) at 50 °C. After hot filtration, the filtrate was cooled to room temperature and a black solid was formed, which was confirmed as impurities by ¹HNMR. The solution was then concentrated and a sticky yellowish solid was obtained. This sticky solid was then taken up in hot heptane (80 °C) and filtered at the same temperature to remove insoluble impurities. This process afforded **C5.11** as a light-yellowish solid with 90 wt% purity. Recrystallization of this crude from *i*PrOH enabled purging of all the impurities, achieving a

product purity of >99 wt%. In summary, this purification process afforded **C5.11** as a light-yellow solid with >99% purity, and isolated assay yield of 81-85% (Table 2.4.7, Entries 1-3).ⁿ It is worth mentioning that a single enantiopure isomer **C5.11** was obtained (100% *ee*) and the absolute configuration of the chiral centers of **C5.11** was proven by single crystal x-ray crystallography (see 4.4).

Table 2.4.7 Fluorination of **C5.10** to prepare **C5.11**



Entry ¹	Input (g)	Crude (GCMS TIC A%) ²				Output after purification ³		
		C5.9	BP-I	BP-II	C5.11	C5.11	wt% ⁴	Yield (%) ⁵
1	10.0	3.1	1.4	1.0	90	6.4 g	99	84
2	10.9	3.5	2.6	0.4	86	7.0 g	97	81
3	13.3	2.3	1.3	0.0	91	8.7 g	99	85

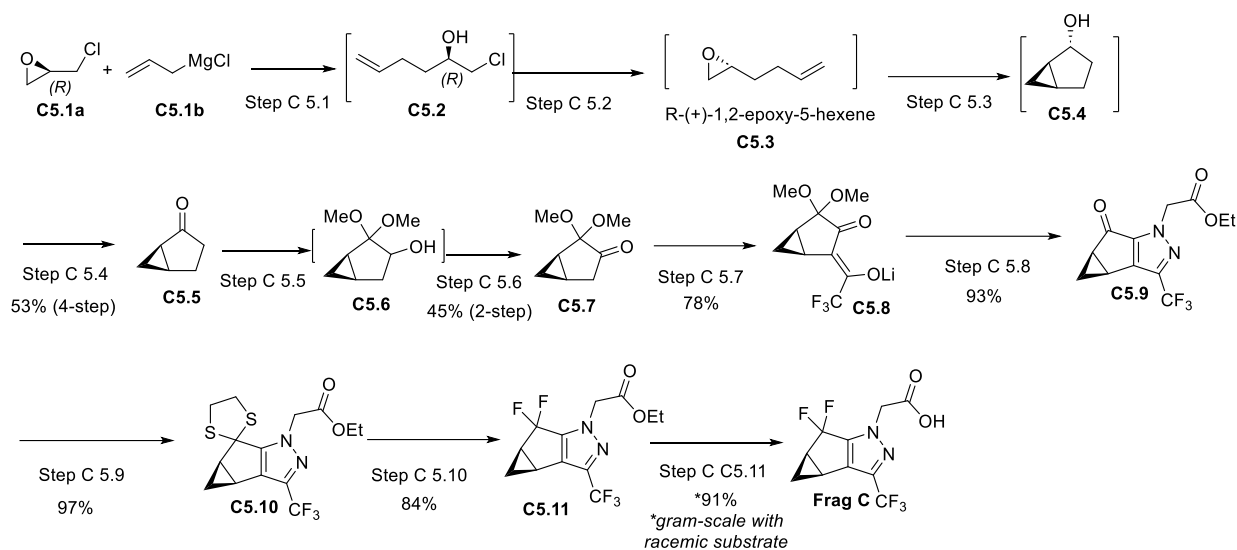
¹All reactions were carried out in 1L HDP plastic bottle following the SOP. Typical condition: **C5.10** (90.1 wt% purity, water content = 0.5 wt%, 1 eq), DBDMH (2 eq), 70 % HF-Py (11 eq HF), DCM (10V), -10 to 0 °C, 30 min. See experimental section for details. ²The crude was obtained after aqueous workup, followed by charcoal treatment and heptane trituration. A% of crude was measured by GCMS. ³The material was obtained by recrystallization from *i*-PrOH. ⁴Wt% was obtained by qNMR. ⁵Corrected yield.

3 Experimental Sections

3.1 Analytical Report for Lenacapavir **Frag C**

Based on the 11-step synthesis developed by M4All for lenacapavir **Frag C** (LenC 5), the M4All analytical team developed chiral GC-FID, chiral SFC-UV, and GC-MS detection methods for it, its intermediates, and starting materials (Scheme 3.1.1).

ⁿDuring the recrystallisation with *i*-PrOH, approximately 10 wt% of **C5.11** remained in the mother liquor. After removal of the solvent, the crude **C5.11** was collected and it showed the purity of 70-75 wt% (qNMR). Pursuit of recovery more **C5.11** from the filtrate will be pursued in our Y2 project.



Scheme 3.1.1 Synthetic route of **Frag C** (LenC5).

3.1.1 Pharmacopoeia Methods

Monographs from the United States Pharmacopoeia and the European Pharmacopoeia were not available for lenacapavir **Frag C**.

3.1.2 Method Development

3.1.2.1 Chromatographic Conditions

Due to the nature of the molecules of interest, GC-MS was chosen. The GC-MS method for the first 6 steps utilized a 30 m, 0.32 mm, 5.00 μ m Agilent J&W HP-1 GC column with a split ratio of 50:1 (70 mL/min split flow) and an injection temperature of 250 °C. The column temperature was initially held at 50 °C for 3 minutes, ramped to 225 °C at 25 °C/min, and held for 5 minutes. The chromatograms below depict the separation between the first two steps (1a, 2a, 1 and 2) of the route (Figure 3.1.1), Step 4 (Figure 3.1.2), and Step 6 (Figure 3.1.3).

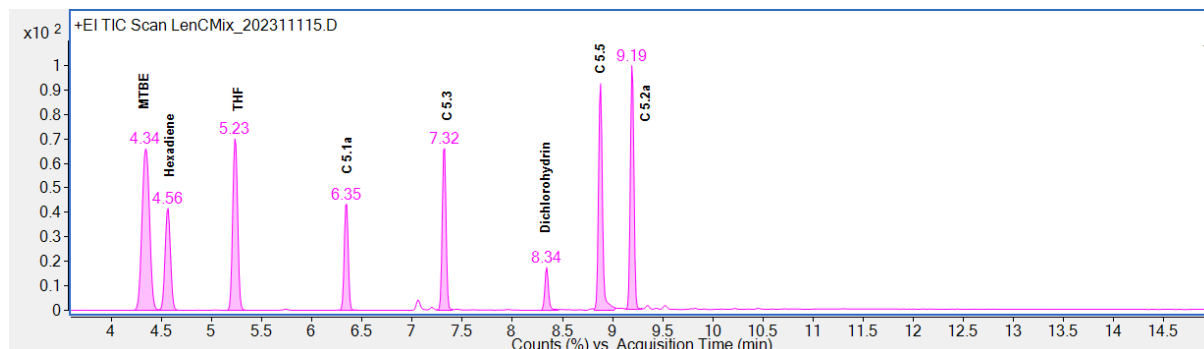


Figure 3.1.1 GC-MS chromatogram for starting materials and intermediates from the first two steps of the synthesis of **Frag C**.

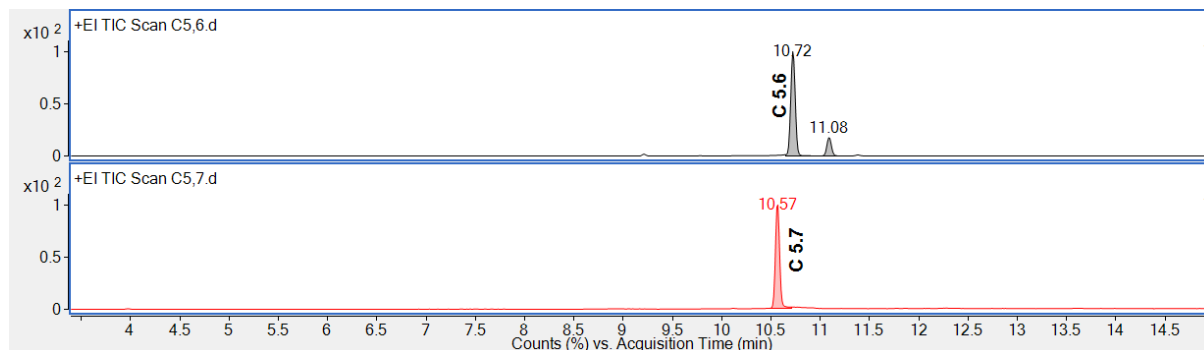


Figure 3.1.2 GC-MS chromatograms for intermediates for Step 6 of the synthesis of **Frag C**. The peak at RT 11.1 min is an unknown.

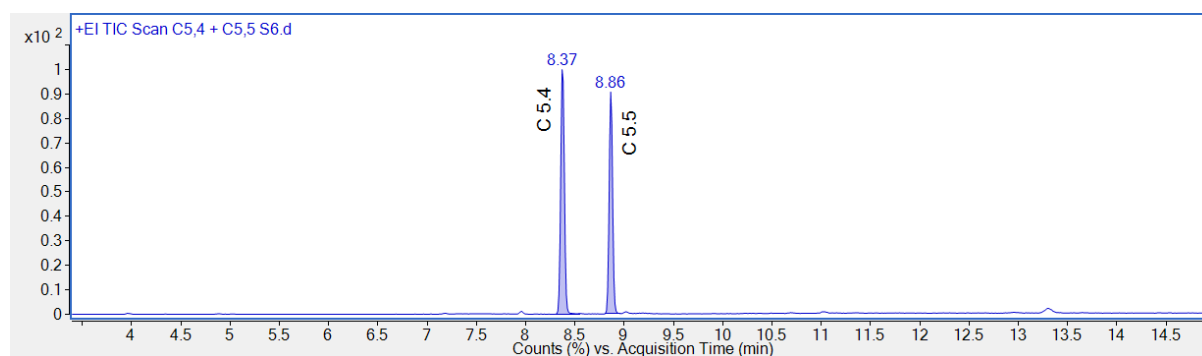


Figure 3.1.3 GC-MS chromatogram for intermediates for Step 4 of the synthesis of **Frag C**.

The final steps (8-10) utilized a GC-MS method under the following parameters: a 30 m, 0.25 mm, 0.25 μm Agilent J&W HP-5ms GC column with a split ratio of 100:1 (140 mL/min split flow) and

an injection temperature of 250 °C. The column temperature was initially held at 50 °C for 3 minutes, ramped to 250 °C at 25 °C/min, and held for 3 minutes. The chromatogram below depicts the separation between the final steps of the route, Steps 8 to 10 (Figure 3.1.4).

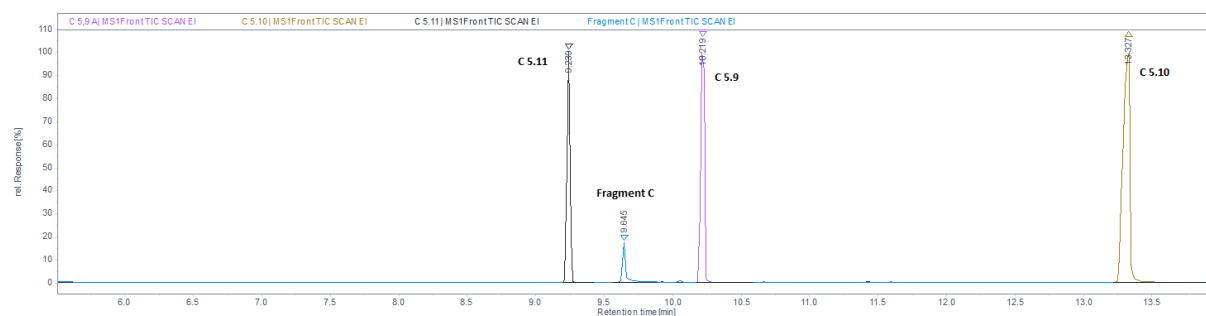


Figure 3.1.4 GC-MS chromatogram for intermediates for Steps 8 to 10 of the synthesis of **Frag C**.

Frag C contains a chiral cyclopropane fused to a five-membered ring containing a difluoromethylene group; several chiral methods were developed to monitor the state of the chiral center throughout the synthesis. Chiral intermediates of **C5.3** and **C5.6** were monitored using a GC-FID with a chiral column. The implemented GC-FID method used a 30 m, 0.25 mm, 0.25 μm Restek RT-GammaDEXsa column with a split ratio of 50:1 (71.3 mL/min split flow) and an injection temperature of 250 °C. The column temperature was isothermally held at 60 °C for 16 minutes. The chromatogram below depicts the separation between the enantiomers (Figure 3.1.5 and Figure 3.1.6).

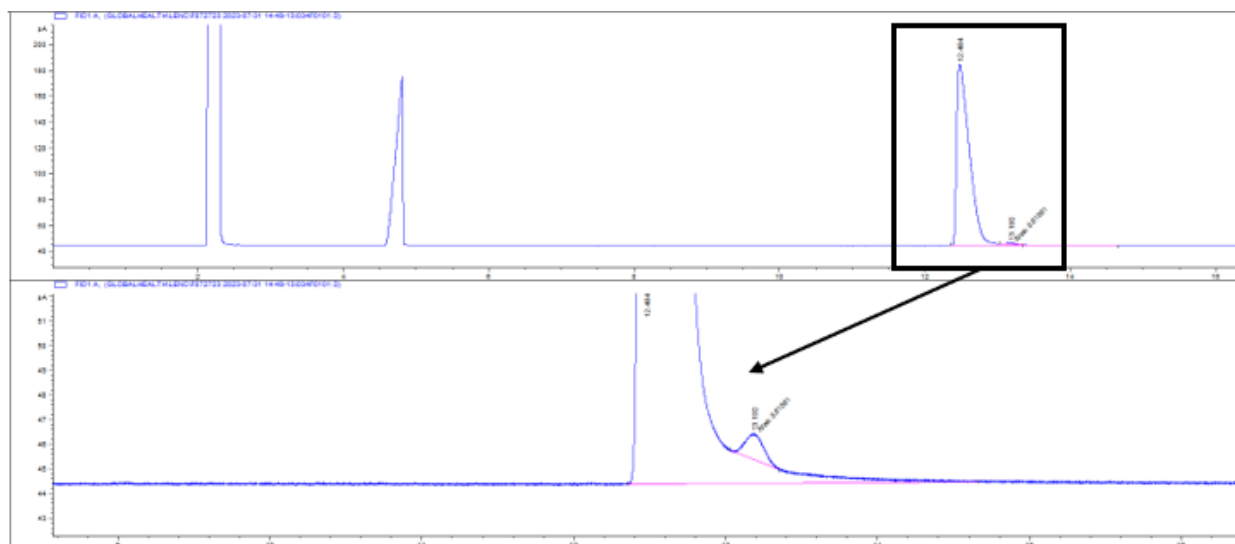


Figure 3.1.5 GC-FID chromatogram for chiral epoxide **C5.3**.

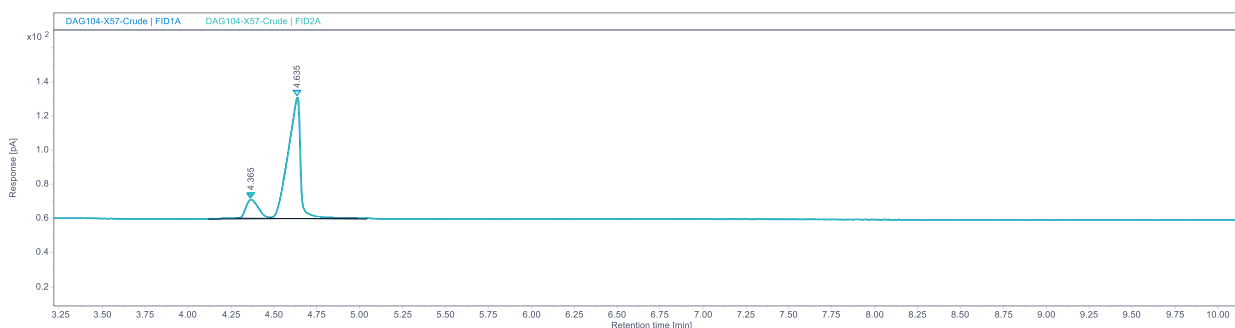


Figure 3.1.6 GC-FID chromatogram for chiral epoxide **C5.6**.

The LenC-1 GC-MS method used above for all Steps up to Step 6 was utilized for the chiral determination of the bicyclic ketone **C5.4**. The chromatogram below depicts the separation between the enantiomers (Figure 3.1.7).

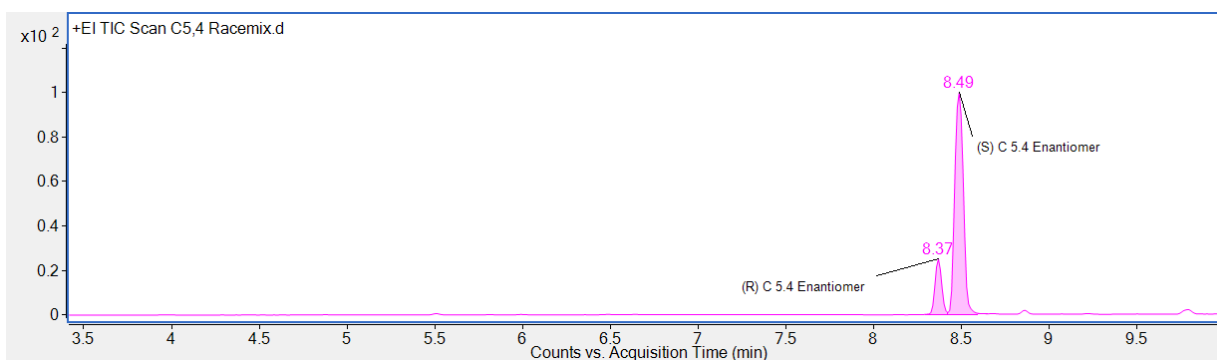


Figure 3.1.7 GC-MS chromatogram for chiral epoxide **C5.4**.

Isomers of **C5.5** were separated using a chiral GC-FID method which utilized a 30 m, 0.25 mm, 0.25 μm Restek RT-GammaDEXsa column with a split ratio of 50:1 (27.8 mL/min split flow) and an injection temperature of 200 °C. The column temperature was isothermally held at 125 °C for 45 minutes. The chromatogram below depicts the separation between the enantiomers (Figure 3.1.8).

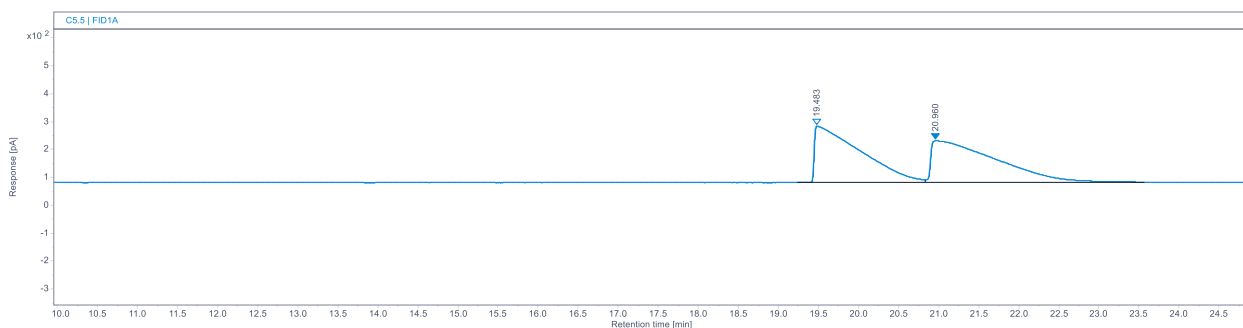


Figure 3.1.8 GC-FID chromatogram for chiral epoxide **C5.5**.

Chiral compounds **C5.7** through **C5.10** were separated by SFC-DAD. This method utilized a ChiralPak IG-3 4.6 x 250 mm; 3 μm column. Flow rate was set to 2 mL/min with an injection volume of 5 μL . Column temperature was 25 °C. Isomers were separated isocratically with 95:5 CO₂: methanol over 10 min and chromatograms were collected at 210 nm (Figure 3.1.9). Known enantiopure standards were not available for **C5.7** through **C5.10** and therefore peak assignments were not made.

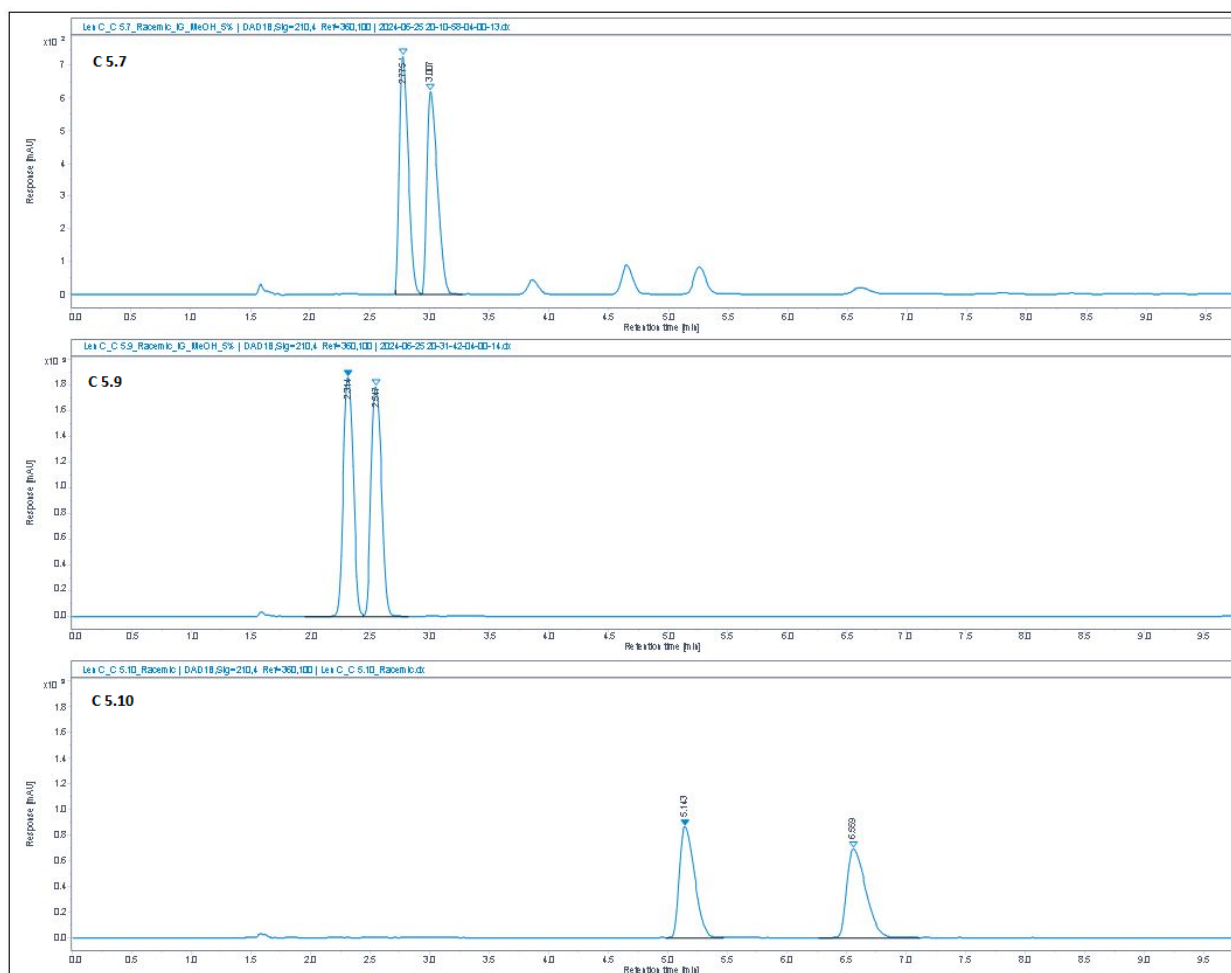


Figure 3.1.9 SFC-DAD chromatograms for chiral compounds **C 5.7** through **C 5.10**.

Isomers of **C5.11** were separated by SFC-DAD although under different conditions. This method made use of a ChiralPak IG-3 4.6 x 250 mm; 3 μ m column. Flow rate was set to 2 mL/min with an injection volume of 1 μ L. Column temperature was 25 °C. Isomers were separated isocratically with 80:20 CO₂: acetonitrile over 6 min and chromatograms were collected at 240 nm (Figure 3.1.10).

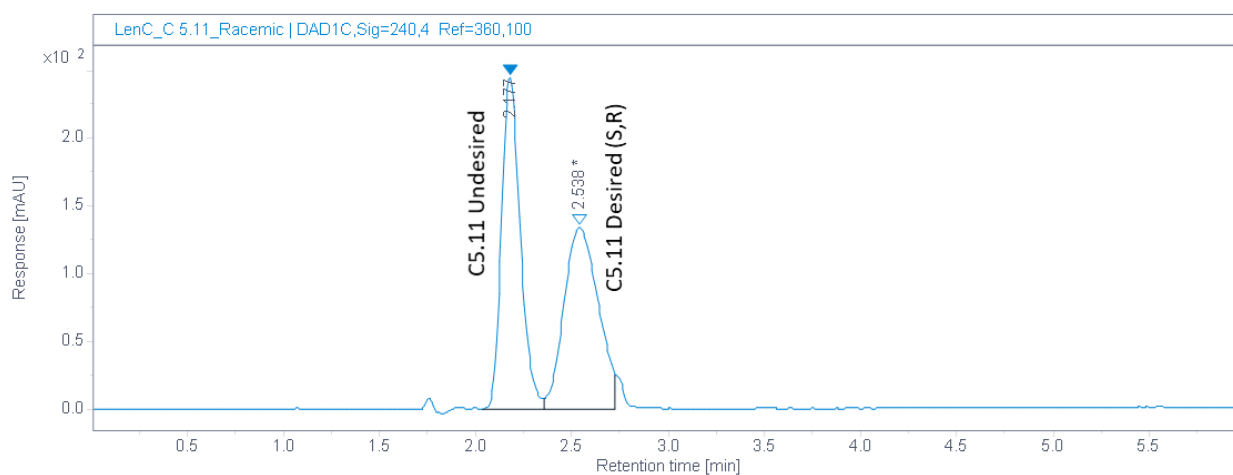


Figure 3.1.10 SFC-DAD chromatograms for chiral compound **C 5.11**.

Isomers of **Frag C** were also separated by SFC-DAD although under different conditions. This method made use of a ChiralPak IC-3 4.6 x 250 mm; 3 μ m column. Flow rate was set to 2.35 mL/min with an injection volume of 1.0 μ L. Column temperature was 25 °C. Isomers were separated isocratically with 80:20 CO₂: isopropanol (0.05% DEA) over 20 min and chromatograms were collected at 240 nm (Figure 3.1.11). A known enantiopure standard was not available for **Frag C** and therefore peak assignments were not made.

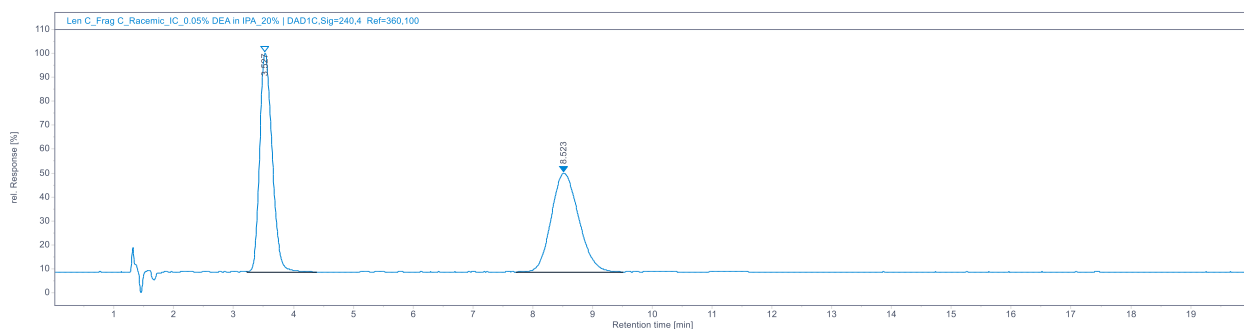


Figure 3.1.11 SFC-DAD chromatogram for chiral compound **Frag C**.

3.1.2.2 Relative Response Factors

Response factors were not determined for lenacapavir **Frag C**.

3.1.2.3 MS Spectra

MS spectra of each compound at found in Appendix 4.5.

3.1.2.4 Linearity

Linearity was checked for **C5.3** through **C5.5**, **C5.7** and **C5.9**. A minimum of 5 standard levels were used to calculate the curve with a linear fit of $R^2 > 0.99$. The chart below lists the compounds, ranges and R^2 values (Table 3.1.1). Linearity for **C5.11** and **Frag C** has not been checked at the time of this writing.

Table 3.1.1 Curve ranges for some of the compounds.

Compound	Linearity Range (mg/mL)	R ² Value
C5.3	0.005 - 1.41	0.9961
C5.4	0.048 - 1.39	0.9971
C5.5	0.189 - 1.63	0.9971
C5.7	0.016 - 2.32	0.9997
C5.9	0.056 - 1.89	0.9983

3.1.2.5 Limit of Detection (LOD) and Limit of Quantitation (LOQ)

Limits were not determined for the starting materials, intermediates, impurities or product.

3.1.3 Impurities

3.1.3.1 Starting Material Impurities

Impurities were not specified nor determined for lenacapavir **Frag C** starting materials.

3.1.3.2 Synthesis Impurities

Impurities were not isolated and characterized for lenacapavir **Frag C**.

3.1.4 Forced Degradation Studies

Forced degradation studies were not performed for lenacapavir **Frag C** nor its starting materials, intermediates and impurities.

3.1.5 Methods

Analytical methods used to support the synthesis of lenacapavir **Frag C** are appended to this report.

3.1.5.1 Key Starting Materials

C5.1a was analyzed via GC-MS using the method “LenC-1” (Section 4.5.1).

3.1.5.2 Reagent and Solvents

Residual solvents were not quantified for lenacapavir **Frag C**.

3.1.5.3 Intermediates

C5.2, C5.3, C5.4, C5.5, C5.6, C5.7, C5.8, C5.9, C5.10, and C5.11 are synthetic intermediates in this process. These intermediates, except **C5.8**, were analyzed using the “LenC-1” (Section 4.5.1) and “LenC-2” (Section 4.5.2) methods. The intermediate **C5.8** was not stable by GC-MS and thus monitored by NMR.

Chiral separation for **C5.3, C5.5 and C5.6** was monitored by GC-FID using either “LenC-3” (Section 4.5.3) or “LenC-5” (Section 4.5.5) methods. Peak assignments were not made for **C5.5** and **C5.6** due to the lack of known enantiopure standards.

Chiral separation for **C5.4** was monitored by GC-MS using “LenC-4” (Section 4.5.4).

Chiral separation for **C5.7, C5.9 and C5.10** was monitored by SFC-DAD using “LenC-6” (Section 4.5.6). Peak assignments were not made due to the lack of known enantiopure standards.

Chiral separation work for **C5.11** was monitored by SFC-DAD using “LenC-7” (Section 4.5.7).

3.1.5.4 In-Process Controls (IPC)

Requirements for IPCs were not set on this process. However, when IPCs were collected, they were analyzed via GC-MS using the “LenC-1” (Section 4.5.1) and “LenC-2” (Section 4.5.2) methods.

3.1.5.5 Final Product Analysis

Synthesized racemic **Frag C** material was assayed using the “LenC-2” (Section 4.5.2) method. Isolated known enantiomeric pure **Frag C** was not available for peak assignments. However, isomers of fragment C were separated using SFC method “LenC-8” (Section 4.5.8).

3.1.5.6 Method Appropriateness

During the development of these methods, certain performance characteristics were evaluated to select analytical conditions. These results are described above and include linearity. These methods were not tested for specificity. Method validation was not performed.

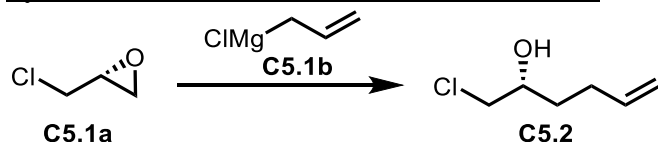
3.2 Detailed Experimental Procedures

3.2.1 General Methods

Reagents and solvents were obtained from commercial suppliers and used as received unless otherwise indicated. Where applicable, reactions were conducted in oven-dried (120 °C) glassware, which was assembled while hot, and cooled to ambient temperature under an inert atmosphere. Reactors were pre-rinsed with reaction solvent and subjected to evacuation/back-fill cycles (3x) as necessary. All reactions were conducted under an inert atmosphere (Nitrogen) unless otherwise noted. Reactions were monitored by TLC (precoated silica gel 60 F254 plates, EMD Chemicals), Agilent GCMS, or chiral Agilent GC-FID using various methods. TLC was visualized with UV light or by treatment with phosphomolybdic acid (PMA), ninhydrin, and/or KMnO₄. ¹H NMR and ¹³C NMR spectra were routinely recorded on Bruker Avance III HD Ascend 600 MHz spectrometer. All chemical shifts are reported in parts per million (ppm) relative to residual CHCl₃ (7.26 ppm for ¹H, 77.16 ppm for ¹³C) or tetramethylsilane (0.0 ppm for ¹H and ¹³C). Coupling constants J are reported in hertz (Hz). The following abbreviations were used to designate signal multiplicity: s, singlet; d, doublet; t, triplet; q, quartet, p, pentet; dd, doublet of doublets; ddd, doublet of doublet of doublets; dt, double of triplets; ddt, doublet of doublet of triplets; m, multiplet; br, broad.

3.2.2 Experimental Procedure

Synthesis of (*R*)-1-chlorohex-5-en-2-ol (**C5.2**)



THF (150 mL, 1V) and (*R*)-epichlorohydrin **C5.1a** (148 g, 1.6 mol, 1 eq) were charged to a 5 L ChemRxnHub reactor under a nitrogen atmosphere. This mixture was cooled at -25 °C (internal temperature was -14.5 °C) using a Huber circulating chiller. When the internal temperature

achieved $-14.5\text{ }^{\circ}\text{C}$, allyl magnesium chloride **C5.1b** (800 mL, 1.6 mol, 1 eq, 2M in THF) was added using a peristaltic pump at a flow rate of 5 mL/min, maintaining the internal temperature below $-5.0\text{ }^{\circ}\text{C}$. After addition, this mixture was stirred at the same temperature for an additional 1h. After reaction completion (monitored by GCMS), MeOH (162 mL, 4.0 mol, 2.5 eq) was added dropwise, keeping the internal temperature below $0\text{ }^{\circ}\text{C}$, followed by the addition of 2M HCl (1.6 L, 2.0 eq) at $0\text{ }^{\circ}\text{C}$. The circulating cooling system was turned off, and MTBE (740 mL) was added. The organic layer was collected and washed with 2M HCl (300 mL) and then water (300 mL). This resulting organic layer (1360 mL corresponding to 1150 g) gave an in-solution yield of 99 % (corrected weight 215.3 g) for **C5.2** assayed by GCMS (19 wt%), with 95% GCMS TIC A% purity, *ee*: 99.9 % and containing 0.7% GCMS TIC A% of dichlorohydrin and 1.8% GCMS TIC A% of epoxide **C5.3**. The crude compound **C5.2** was used for the next step without further purification.



Grignard addition

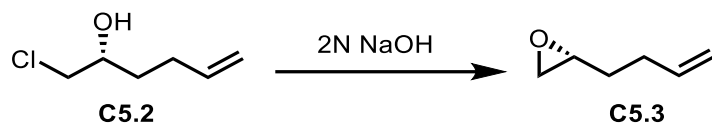


MeOH and HCl quench

$^1\text{H NMR}$ (600 MHz, CDCl_3-d) δ 5.78 (ddt, $J = 17.0, 10.2, 6.7\text{ Hz}$, 1H), 5.01 (ddd, $J = 17.1, 3.4, 1.7\text{ Hz}$, 1H), 4.94 (ddd, $J = 10.2, 3.0, 1.3\text{ Hz}$, 1H), 3.55 (dd, $J = 11.1, 3.9\text{ Hz}$, 1H), 3.44 (dd, $J = 11.1, 6.7\text{ Hz}$, 1H), 3.05 (d, $J = 5.7\text{ Hz}$, 1H), 2.31 (s, 2H), 2.20 – 2.12 (m, 2H), 1.61 – 1.57 (m, 2H).

MS-EI (m/z) (M^+): 134.1.

Synthesis of *R*-(+)-1,2-epoxy-5-hexene (**C5.3**)



A solution of chlorohydrin **C5.2** in MTBE (1126 g) was charged to a 5 L ChemRxnHub reactor, then an aqueous solution of NaOH (960 mL, 1.2 eq, 2M) was added. The mixture was heated to 50 °C and stirred for 2 h. After the reaction was completed, the organic layer was collected and washed with water (250 mL × 4) until a pH of 7 was determined in the aqueous layer. The organic layer was then used for drying process development, as described below.



Reflux



Extraction



Concentration

¹H NMR (600 MHz, CDCl₃-*d*) δ 5.81 – 5.72 (m, 1H), 5.02 – 4.87 (m, 2H), 2.88 – 2.81 (m, 1H), 2.67 (t, *J* = 4.5 Hz, 1H), 2.40 (dd, *J* = 5.0, 2.7 Hz, 1H), 2.20 – 2.07 (m, 2H), 1.61 – 1.48 (m, 2H).

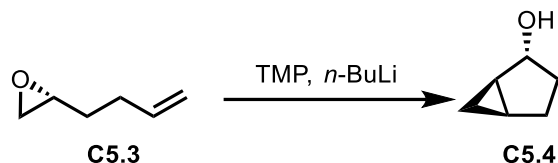
MS-EI (*m/z*) (*M*⁺): 98.1

Drying crude solution of **C5.3** by azeotropic distillation with Dean-Stark trap

The MTBE solution (reaction from 148 g of **C5.1a** according to the procedure as shown above, KF: 1.5 %) was charged to a 2 L RBF with a Dean-Stark trap. The solution was refluxed at 70 °C for 16 h to remove about 10 g of water. The KF of the resulting MTBE solution was decreased to 0.13 %. This resulting organic layer (617.75 g) gave an in-solution yield of 98 % (corrected weight 136 g, over two steps from **C5.1a**) for epoxide **C5.3** assayed by GCMS (22% purity by qNMR and 17.2% by GCMS wt%), with 98.7% GCMS TIC A% (excluding solvents) and containing

epichlorohydrin of 1.3% GCMS TIC A%. The crude compound **C5.3** was used for the next step without further purification.

Synthesis of (*1R,2R,5S*)-bicyclo[3.1.0]hexan-2-ol (**C5.4**)



A 5 L ChemRxnHub reactor was charged with a solution of epoxide **C5.3** in MTBE (617.15 g), and then TMP (117 mL, 0.5 eq) was added to the reactor under a nitrogen atmosphere. This mixture was cooled at -10 °C (internal temperature was -9.9 °C) using a Huber circulating chiller. When the internal temperature achieved -9.9 °C, *n*-butyllithium (610 mL, 1.5 mol, 1.1 eq, 2.5M in hexane) was added using a peristaltic pump with a flow rate of 4.0 mL/min, maintaining the internal temperature below -5.0 °C. After the addition, this mixture was stirred at the same temperature for an additional 1 h. After completion of the reaction, 3M HCl (740 mL, 1.6 eq) was added dropwise, keeping the internal temperature below 25 °C. The circulating cooling system was turned off, and the aqueous layer was drained (pH = 10). Then, more 3M HCl (230 mL, 0.5 eq) was added to wash the organic layer (pH = 1). The combined aqueous layer was charged back to the reactor and extracted twice with 5V and 2.5V MTBE (635 mL and 340 mL, respectively). This combined organic layer (2220 mL) was concentrated at 40 °C under vacuum (150–255 Torr) to about 5V. This resulting organic layer (630.06 g, 810 mL) afforded bicyclo alcohol **C5.4** with an in-solution yield of 70 % (corrected weight 95.14 g) by GCMS (15.1% wt%, 91.2% GCMS TIC A% excluding solvents or 14.7 % purity by qNMR). The crude compound **C5.4** was used for the next step without further purification.

Note: **C5.4** can also be purified by distillation at this stage. Crude **C5.4** was distilled under vacuum (233-341 Torr) at 70 °C to remove MTBE and further distilled at 45 °C (1-7 Torr) to afford the desired compound **C5.4** with 65-70 % isolated yield.

¹H NMR (600 MHz, CDCl₃-*d*) δ 4.21 (d, J = 4.7 Hz, 1H), 1.97 – 1.72 (m, 2H), 1.65 (dd, J = 12.3, 8.3 Hz, 1H), 1.53 (dd, J = 14.5, 8.3 Hz, 1H), 1.44 – 1.37 (m, 1H), 1.31 (ddd, J = 12.4, 8.2, 4.8 Hz, 2H), 0.41 (dd, J = 7.7, 5.7 Hz, 1H), 0.00 (dd, J = 7.9, 4.2 Hz, 1H).

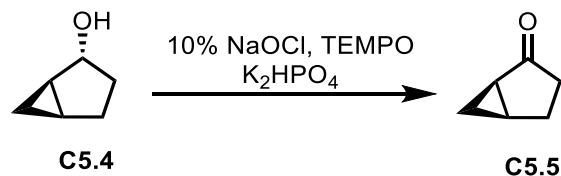
¹³C NMR (151 MHz, CDCl₃-*d*) δ 74.5, 30.4, 26.9, 24.5, 16.1, 6.9.

IR (ATR) ν_{max} = 3328.5, 2935.3, 2870.1, 1328.8, 1177.8, 1101.4, 1043.7, 984.0, 870.3, 808.8, 717.5.

MS-EI (*m/z*) (M⁺): 98.1

[α]_D²⁰ (deg·mL·g⁻¹·dm⁻¹) (MeOH (10mg/mL) at 20 °C under 589nm): +23.96

Synthesis of (*1R,5S*)-bicyclo[3.1.0]hexan-2-one (**C5.5**)



A 5 L ChemRxnHub reactor was charged with a solution of **C5.4** in MTBE (630.06 g). To the reactor was added a solution of potassium phosphate dibasic (366.3 g, 2.1 mol, 1.5 eq) in water (555 mL, 22 eq) followed by TEMPO (5.44 g, 34.6 mmol, 0.025 eq). This mixture was cooled at -5 °C (internal temperature was -3.8 °C) using a Huber circulating chiller. When the internal temperature achieved -3.8 °C, 10 % sodium hypochlorite solution (1.3 L, 2.1 mol, 1.5 eq) was added using a peristaltic pump with a 12 mL/min flow rate, maintaining the internal temperature below 5.0 °C. After the addition, the circulating cooling system was turned off, and when the internal temperature achieved 20 °C, the reaction was stirred for an additional 3 h. After completion of the reaction, sodium sulfite solution (61.1 g, 0.35 eq in 280 mL of water) was added, keeping the internal temperature below 30 °C. The organic layer was separated, and the aqueous layer was extracted twice using 5V and 2.5V MTBE (685 mL and 340 mL). This combined organic layer (1780 mL) was concentrated at 40 °C under vacuum (150–255 Torr) to remove MTBE. This

resulting oil 221.5 g (255.5 mL) gave an in-solution yield of 98.4% (91.7 g) for bicyclo ketone **C5.5** (41 wt% by qNMR).



Reaction setup



During 10 % NaOCl addition



After 10 % NaOCl addition

Note: **C5.5** can also be purified by distillation at this stage. The resulting crude material was distilled at 25–40°C under vacuum (4–1.8 Torr) with a vapor temperature between 30–40°C to afford **C5.5** (75.8 g, yield: 80.2 % based purity, purity: 97% TIC A% by GCMS and 98.6 wt% by qNMR, *ee*: 100 % - assumed desired).

$^1\text{H NMR}$ (600 MHz, CDCl_3-d) δ 2.19–1.94 (m, 5H), 1.78–1.70 (m, 1H), 1.22–1.14 (m, 1H), 0.96–0.88 (m, 1H).

$^{13}\text{C NMR}$ (151 MHz, CDCl_3-d) δ 215.2, 31.4, 27.4, 22.6, 21.6, 13.5.

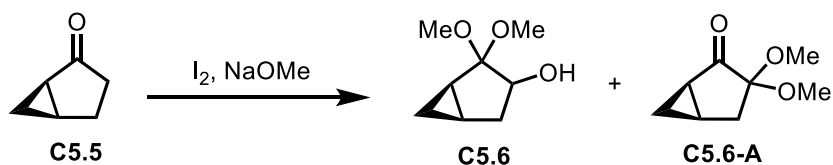
MS-DART(m/z) (MH^+): 97.1.

IR (ATR) ν_{max} = 3328.5, 2935.3, 2870.1, 1328.8, 1177.8, 1101.4, 1043.7, 984.0, 870.3, 808.8, 717.5.

ee: 100 %-assumed desired

$[\alpha]_D^{20}$ (deg · mL · g⁻¹ · dm⁻¹) (MeOH (10mg/mL) at 20 °C under 589nm): +20.79

Synthesis of (1*R*,5*R*)-2,2-dimethoxybicyclo[3.1.0]hexan-3-ol (**C5.6**)



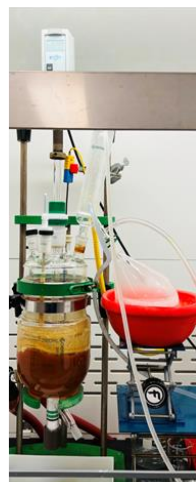
A 2 L ChemRxnHub reactor was charged with NaOMe/MeOH (563.3 g, 596 mL, 25 wt%, 2.52 eq, 2.607 mol) and cooled to -10 °C (T_J) under a nitrogen atmosphere. Iodine (315.0 g, 1.2 eq, 1.241 mol) was added to the reactor once the internal temperature reached -5 °C. A slight exotherm was noticed (2-10 °C) during this operation. The resulting solution was allowed to stir for 15-20 min at -5 °C to -10 °C. Then, **C5.5** (105.80 g, 94 wt%, 1 eq, 978 mmol) was added dropwise using a peristaltic pump (2 mL/min) maintaining NMT 0 °C internal temperature. The reaction mixture was stirred at 0 °C for 4 h, then warmed to 25 °C, and allowed to stir overnight. After completion of the reaction (monitored by GCMS and ^1H NMR), the reaction mixture was concentrated under vacuum (45 °C) to remove the MeOH. The resulting residue was dissolved in DCM (1000 mL, 10V) and stirred for 10 min. Water (200 mL, 2V) was added, and the mixture was stirred for another 10 min. The DCM layer was separated, and the aqueous layer was extracted with DCM (300 mL, 3V). The combined DCM solution was charged to the reactor and washed with saturated Na_2SO_3 solution (200 mL x 2, 2V) and brine (200 mL, 2V). The DCM layer was collected and concentrated *in vacuo* to afford the crude product **C5.6** (160.35 g, 82 wt% by qNMR, 80% corrected assay yield; 6%-7% byproduct **C5.6-A**) as a pale-yellow oil. The crude product was used for the next step out with further purification.



Initial Reaction



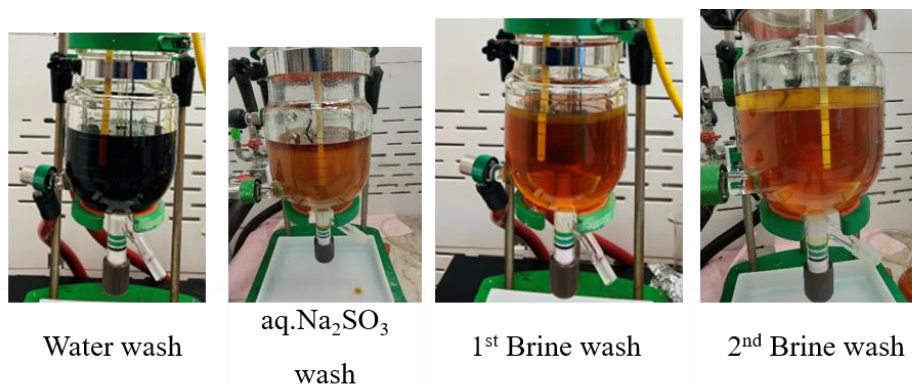
Color
change
during
reaction



Distillation



After DCM
Charge



Note: **C5.6** can also be purified by distillation at this stage. Crude **C5.6** was distilled at 40°C (1 Torr) to afford the desired compound **C5.6** in 70-75% isolated yield.

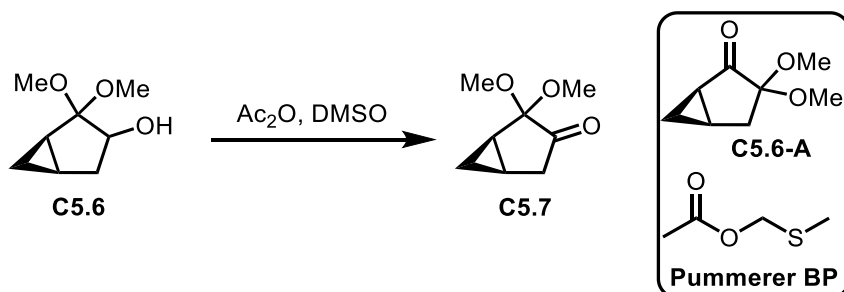
¹H NMR (600 MHz, CDCl₃-d) δ 3.97 (d, *J* = 7.1 Hz, 1H), 3.44 (s, 3H), 3.25 (s, 3H), 2.37 (s, 1H), 2.24 – 2.15 (m, 1H), 1.78 (dd, *J* = 14.1, 0.8 Hz, 1H), 1.53 – 1.44 (m, 1H), 1.38 (dd, *J* = 8.8, 5.0 Hz, 1H), 0.82 (dd, *J* = 9.0, 4.2 Hz, 1H), 0.58 (ddt, *J* = 8.5, 5.0, 1.2 Hz, 1H).

¹³C NMR (151 MHz, CDCl₃-d) δ 110.3, 72.3, 51.3, 49.2, 34.1, 21.8, 14.9, 8.5.

IR: 3475.7, 2942.7, 2834.6, 1448.1, 1366.1, 1341.8, 1142.4, 1049.2, 1030.6, 978.4, 911.3, 814.4.

HRMS (ESI) *m/z*: calcd for C₈H₁₄O₃·Na⁺ = [M+Na]⁺ 181.0841, found 181.0844

Synthesis of (*1R,5R*)-2,2-dimethoxybicyclo[3.1.0]hexan-3-one (**C5.7**)

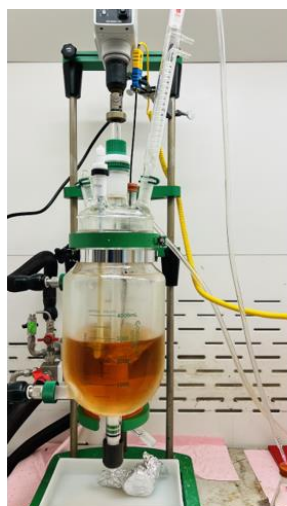


A 5 L ChemRxnHub reactor was equipped with a thermocouple, baffle, nitrogen flow, and a bleach trap. DMSO (1.08 kg, 979 mL, 19 eq, 15.813 mol) and **C5.6** (143.94 g, 725.8 mmol, 80 % purity)

were charged to the reactor at 25 °C. Then, acetic anhydride (1.04 kg, 959 mL, 14 eq, 10.16 mol) was added at the same temperature. The reaction mixture was heated to 50 °C and stirred for 1.5 h under a nitrogen atmosphere. After completion of the reaction (once **C5.6** was <5 A% by GCMS TIC A% and ¹H NMR), the reaction mixture was cooled to 0 °C and diluted with water (1600 mL, 10V) and EtOAc (1600 mL, 10V). The mixture was stirred at 0 °C for 30 min. The water layer was then separated and extracted with EtOAc (800 mL × 2). The combined EtOAc layer was washed with sat. NaHCO₃ (1000 mL × 3) to pH = 6-7 and then brine (1 L). The resulting EtOAc layer was concentrated under 300 Torr at 50 °C to afford the crude **C5.7** as a pale-yellow liquid (683.10 g, 13.95 % qNMR purity, 84 % yield). The ratio of **C5.7** and the Pummerer **BP** was 2.4:1, along with **C5.6-A** at 4% TIC A% (GCMS).

Purification by distillation and recrystallization

The crude product was purified by vacuum distillation using a 12" Vigreux column and a J-KEM vacuum controller. The first fraction was collected at 50 °C (T_J) under 7-35 Torr to purge a mixture of EtOAc, acetic anhydride, and Pummerer **BP** (441 g). The resulting residue was further distilled at 60 °C under 1-2 Torr to afford **C5.7** (92 g, 95 A% by GCMS-TIC, 77 % corrected assay yield, containing <1 A% the Pummerer **BP** and 3-4 A% **C5.6-A**). The obtained **C5.7** was dissolved in hexanes (500 mL, 5V) and cooled to T_J = -40 to -45 °C with overhead stirring to produce **C5.7** as an amorphous solid. Once precipitation of **C5.7** was completed, the supernatant was suctioned through a 20 µm glass inlet filter via a peristaltic pump at 20 mL/min until dry. The residue was quantitatively collected with MTBE and concentrated *in vacuo* to yield **C5.7** as a pale-yellow oil at 25 °C (84.5 g, 97 wt% by qNMR, 72% corrected assay yield; containing 3 % **C5.6-A**).



Reaction mixture



Work-up



Work-up

^1H NMR (600 MHz, CDCl_3-d) δ 3.19 (s, 3H), 3.01 (s, 3H), 2.54 (ddd, $J = 18.8, 5.5, 2.2$ Hz, 1H), 2.04 (d, $J = 18.7$ Hz, 1H), 1.49 (td, $J = 7.9, 4.2$ Hz, 1H), 1.42 – 1.34 (m, 1H), 0.71 (dq, $J = 8.2, 2.1$ Hz, 1H), -0.01 (dt, $J = 6.3, 4.3$ Hz, 1H).

^{13}C NMR (151 MHz, CDCl_3-d) δ 207.7, 102.9, 50.9, 50.5, 38.9, 19.2, 9.3, 8.9.

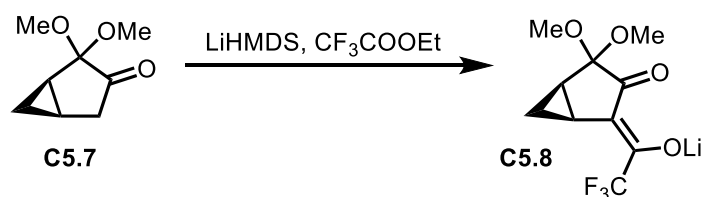
IR: 2994.9, 2946.5, 2909.2, 1755.6, 1092.1, 1067.9, 1043.7, 1017.6, 997.1, 915.1, 810.7.

ee: 100 %

$[\alpha]_D^{20}$ ($\text{deg}\cdot\text{mL}\cdot\text{g}^{-1}\cdot\text{dm}^{-1}$) (MeOH (10mg/mL) at 20 °C under 589nm): +57.13

HRMS (ESI) m/z : calcd for $\text{C}_8\text{H}_{12}\text{O}_3\cdot\text{Na}^+ = [\text{M}+\text{Na}]^+$ 179.0684, found 179.0680.

Synthesis of lithium (Z)-1-((1S,5R)-4,4-dimethoxy-3-oxobicyclo[3.1.0]hexan-2-ylidene)-2,2,2-trifluoroethan-1-olate (C5.8)



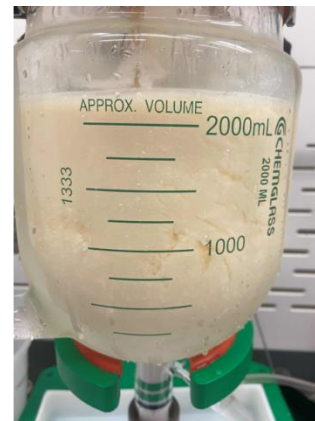
To a 2 L ChemRxnHub reactor equipped with a J-KEM thermocouple and baffle was added **C5.7** (80.0 g, 97 wt%, 1 eq, 496.9 mmol) and THF (800 mL, Sigma-Aldrich, anhydrous) under a nitrogen atmosphere. The mixture was stirred at 250 rpm via an overhead stirrer and then was cooled to -15 °C with a Huber circulating chiller. Upon reaching the temperature, LiHMDS (91.4 g, 546.55 mL, 1.0 molar, 1.1 eq, 546.55 mmol) was added dropwise over 2.5 h via a peristaltic pump while maintaining the internal temperature below -5 °C. The reaction mixture was stirred at -15 °C for 1 h. Then ethyl 2,2,2-trifluoroacetate (108.0 g, 90.8 mL, 98 wt%, 1.5 eq, 745.3 mmol) was added dropwise over 1 h via a peristaltic pump while keeping the internal temperature below -5 °C. The mixture was stirred at -15 °C for 1 h and the chiller was turned off. The reaction was allowed to warm to room temperature overnight under nitrogen. After this, the mixture was concentrated to 5V under reduced pressure (80 Torr, 30 °C), and heptane (1600mL, 20V) was slowly added via peristaltic pump (30 mL/min) and stirred at room temperature overnight. Finally, the solid was filtered and dried in a vacuum oven at 40 °C overnight to give **C5.8** as an off-white solid (102.7 g, 387 mmol, 97.4 wt% by qNMR, 78.0 % corrected assay yield).



After addition



Distillation



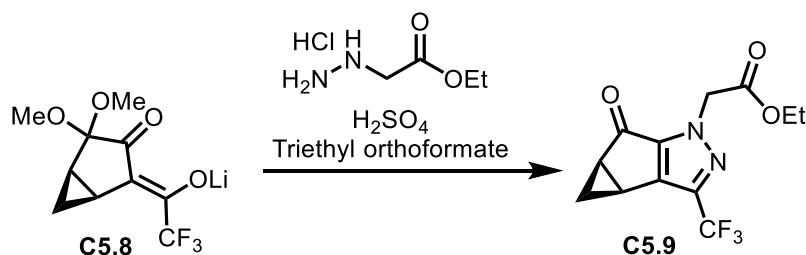
Precipitation

¹H NMR (600 MHz, DMSO-*d*₆) δ 3.31 (s, 3H), 3.27 (s, 3H), 2.02 (tt, *J* = 3.48, 6.60 Hz, 1H), 1.42 (dt, *J* = 4.40, 7.98 Hz, 1H), 0.96 (dt, *J* = 4.49, 7.47 Hz, 1H), 0.08 (q, *J* = 4.22 Hz, 1H)

¹³C NMR (150 MHz, DMSO-*d*₆) δ 192.7, 120.4, 118.5, 105.1, 103.6, 50.3, 49.5, 16.9, 15.8, 13.4

¹⁹F NMR (565 MHz, DMSO-*d*₆) δ -73.51, -71.79, -70.57

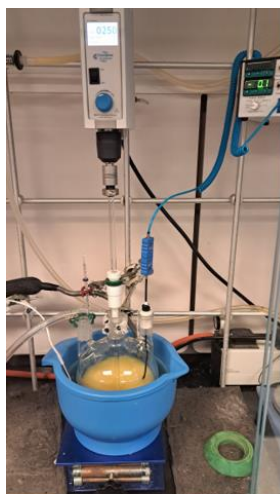
Synthesis of ethyl 2-((3*bS*,4*aR*)-5-oxo-3-(trifluoromethyl)-3*b*,4,4*a*,5-tetrahydro-1*H*-cyclopropa[3,4]cyclopenta[1,2-*c*]pyrazol-1-yl)acetate (**C5.9**)



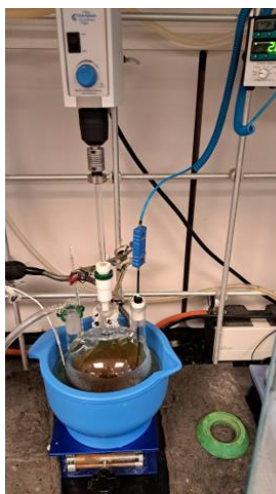
To a 2 L three-necked round bottom flask, equipped with a thermocouple and over-head stirrer, was added **C5.8** (50.0 g, 86.2 wt%, 1 eq, 166.9 mmol), ethyl amino glycinate hydrochloride (26.6 g, 97 wt%, 1 eq, 166.9 mmol), and denatured ethanol^o (750 mL, 15V). The mixture was stirred at 250 rpm via an overhead stirrer and cooled to <5 °C using a Thermo Scientific™ Neslab CC65 Immersion Cooler under a nitrogen atmosphere. When the internal temperature was below <5 °C, sulfuric acid (8.2 g, 4.6 mL, 18.0 M, 0.5 eq, 83.5 mmol) via a syringe pump, keeping the internal temperature below 5.0 °C. Then, triethyl orthoformate (37.9 g, 42.5 mL, 98 wt%, 1.5 eq, 250.3 mmol) was added by an additional funnel, keeping the internal temperature below 5.0 °C. After addition, the mixture was stirred at the same temperature for 20h. Once the reaction was complete (monitored by GCMS and ¹H NMR), the reaction mixture was concentrated to 5V. Water (500mL, 10V) was charged dropwise using an additional funnel at room temperature. The mixture was then cooled to 0 °C and stirred for 3 h. The precipitate was filtered and washed with 350 mL (7V) water. The wet solid was dried by azeotropic distillation with toluene (50 mL, 1V each) thrice (5 Torr, 30 °C). The obtained solid was further dried overnight under high-vacuum (1-3 Torr) at room temperature to afford 36.2 g of **C5.9** as a pale-yellow solid (36.2 g, 73.2% corrected assay yield, 97 wt% by qNMR and 97.4 A% by GCMS-TIC). The mother liquor was extracted thrice with EtOAc (750 mL, 5V) and concentrated (5 Torr, 30 °C) onto SiO₂. This material was subject to purification over a short pad of SiO₂ with 7 % EtOAc in *n*-hexanes as an eluent, affording 9.52

^oDenatured EtOH with alcohols (90/5/5, v/v/v, EtOH/*i*PrOH/MeOH) was purchased from LabChem™.

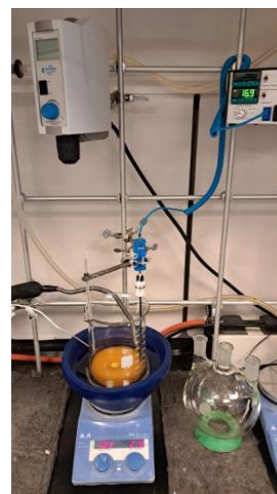
g of **C5.9** as a bright yellow solid (96.6 wt% by qNMR and 95.2 A% by GCMS-TIC) bringing the overall isolated yield to 93.0%.



After addition



After 20 hours



Precipitation

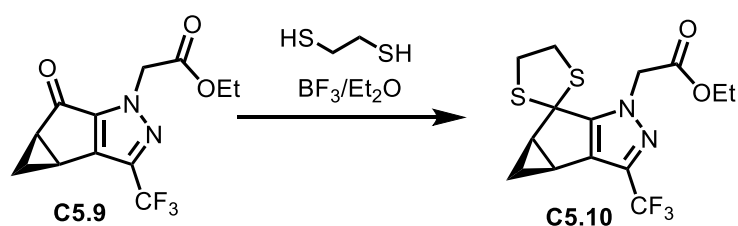
^1H NMR (600 MHz, $\text{DMSO-}d_6$) δ 5.17 (q, $J = 17.6$ Hz, 1H), 4.16 (q, $J = 7.0$ Hz, 1H), 2.92 (d, $J = 3.7$ Hz, 1H), 2.82 – 2.61 (m, 1H), 1.72 (dt, $J = 7.2, 6.1$ Hz, 1H), 1.64 (d, $J = 2.1$ Hz, 1H), 1.19 (t, $J = 7.0$ Hz, 1H)

^{13}C NMR (150 MHz, $\text{DMSO-}d_6$) δ 187.0, 166.6, 143.5, 142.6, 134.4, 120.8, 61.8, 52.0, 35.3, 31.6, 13.9, 13.4

^{19}F NMR (565 MHz, $\text{DMSO-}d_6$) δ -60.3

ee: 100 % - assumed desired

Synthesis of ethyl 2-((3*bS*,4*aR*)-3-(trifluoromethyl)-4,4a-dihydrospiro[cyclopropa[3,4]cyclopenta[1,2-*c*]pyrazole-5,2'-[1,3]dithiolane]-1(3*bH*)-yl)acetate (**C5.10**)



To a 2 L round-bottom flask equipped with a J-KEM thermocouple probe and overhead stirrer was added **C5.9** (35.0 g, 99 wt%, 1 eq, 120.2 mmol) and DCM (350.0 mL, Sigma-Aldrich, anhydrous) under a nitrogen atmosphere. The mixture was stirred at 250 rpm and then ethane-1,2-dithiol (16.2 g, 14.4 mL, 98 wt%, 1.4 eq, 168.3 mmol) was added dropwise via syringe, followed by boron trifluoride diethyl etherate (117.4 g, 102 mL, 46.5 wt%, 3.2 eq, 384.7 mmol) via additional funnel. The reaction mixture was stirred at 25 °C for 16 h under a nitrogen atmosphere. After the allotted time, water (175 mL, 5V) was added. Then, saturated aqueous NaHCO₃ was added until the reaction mixture was neutral (900 mL, 25V). The mixture was extracted thrice with DCM (175 mL, 5V each). The combined organic layer was washed with H₂O (175 mL, 5V) and then brine (175 mL, 5V) before being passed through a column loaded with activated charcoal (20 g, top), SiO₂ gel (20 g, middle), and Celite (20 g, bottom). The column was washed thrice with DCM (175 mL, 5V each). The organic solution was concentrated under reduced pressure (80 Torr, 30 °C) to afford a residue. This material was dried by azeotropic distillation with toluene (35 mL, 1V each) thrice (5 Torr, 30 °C) to give the crude product. The crude material was further dried under a high vacuum (1-3 Torr) at 40 °C overnight to give **C5.10** as a deep red oil (47.4 g, 117 mmol, 90.1 wt% by qNMR, 93.2 A% by GCMS-TIC, 97.5% corrected assay yield).

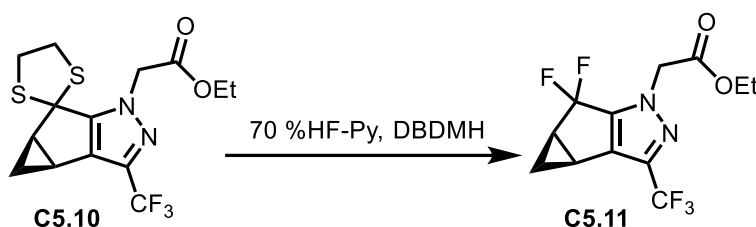
¹H NMR (600 MHz, CDCl₃-*d*) δ 4.93 (dd, *J* = 17.42, 40.35 Hz, 2H), 4.16 - 4.26 (m, 2H), 3.43 - 3.53 (m, 4H), 2.62 (ddd, *J* = 4.22, 5.59, 8.16 Hz, 1H), 2.41 (ddd, *J* = 3.67, 5.69, 7.15 Hz, 1H), 1.25 (t, *J* = 7.15 Hz, 3H), 0.88 (t, *J* = 7.15 Hz, 1H), 0.64 (td, *J* = 4.01, 5.73 Hz, 1H)

¹³C NMR (150 MHz, CDCl₃-*d*) δ 166.9, 147.3, 135.5, 129.0, 120.1, 65.5, 61.9, 51.1, 40.9, 40.5, 23.3, 22.3, 15.9, 14.0

¹⁹F NMR (565 MHz, CDCl₃-*d*) δ -61.70

ee: 100 % - assumed to be the desired enantiomer

Synthesis of ethyl 2-((3*bS*,4*aR*)-5,5-difluoro-3-(trifluoromethyl)-3*b*,4,4*a*,5-tetrahydro-1*H*-cyclopropa[3,4]cyclopenta[1,2-*c*]pyrazol-1-yl)acetate (**C5.11**)



To a plastic bottle (1 L HDP) equipped with a magnetic stirring bar, DBDMH (14.1 g, 49.5 mmol, 2 eq) was added. Under a nitrogen atmosphere, anhydrous DCM (50 mL) was added. The mixture was cooled to -10.0 °C (internal temperature was -15 °C) using an ice/salt bath.^P Then, 70 % HF-Py complex (7.1 mL, 272.0 mmol, 11 eq) was added while the internal temperature was kept below 0 °C. The mixture was stirred for 10 minutes at the same temperature. After that, **C5.10** (10.0 g, 90.1 wt%, 24.7 mmol, 1 eq) in DCM (50 mL) was slowly added while the internal temperature was kept below 0 °C. The reaction was stirred for 30 minutes. After completion of the reaction (monitored by GCMS and ¹H NMR), a saturated aqueous NaHCO₃ solution (37.4 g, 18 eq in 400 mL of water) was added slowly, keeping the internal temperature below 0 °C. The mixture was extracted with DCM (100 mL × 3). The organic layer was washed with 1 M HCl (100 mL × 2) and brine (100 mL × 2), dried over anhydrous sodium sulfate, filtered, and concentrated under reduced pressure to give **C5.11** as a brown solid (10.7 g, 23.1 mmol, 93.5% assay yield, 67.2 wt% purity by qNMR).

Purification: The resulting crude material was dissolved in MTBE (10V) and washed with a saturated aqueous Na₂CO₃ (10V × 2) solution and brine (10V × 2). To this organic layer, 10 % (1.0 g) of activated charcoal was added. The mixture was heated (50 °C) and stirred for 30 minutes. It was then cooled to room temperature and stirred for an additional 1 h. This suspension was filtered and washed with MTBE (5V). The combined organic layer was concentrated to give a

^P A plastic thermocouple was used to monitor the internal temperature. For small scale (1- 3 g), a PTFE coated-needle thermocouple was used to monitor the internal temperature.

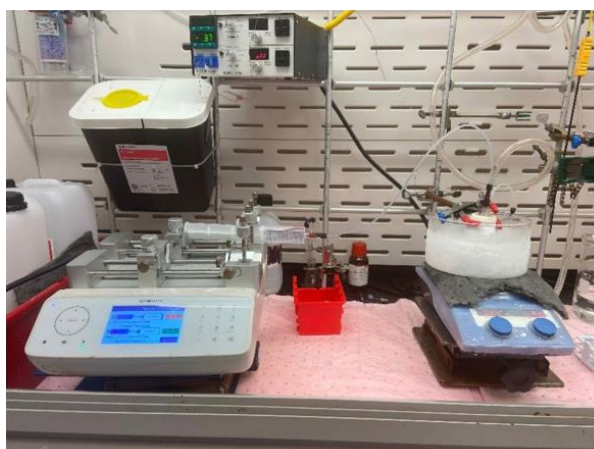
yellow sticky solid. The resulting crude material was dissolved in heptane (10V), heated to 80 °C, stirred for 30 minutes, and filtered (hot-filtration). The remaining black sticky solid was extracted with hot heptane (50 mL × 2, 80 °C) to separate **C5.11** from this sticky solid. The combined organic layer was concentrated to give crude **C5.11** as a light-yellow solid (7.85 g, 22.82 mmol, 92.3% yield, 90.2 wt% purity by qNMR). The resulting compound was dissolved in isopropanol (1V, 8 mL, denatured w/ alcohols), heated to 50 °C until dissolved, cooled to 25 °C, stirred for 1 h, cooled to 0 °C, and stirred for 1h. The resulting solid was filtered and washed with cold isopropanol/water (2 mL / 2 mL) to afford **C5.11** as a light-yellow solid (6.42 g, 20.7 mmol, 83.7% yield, 99.9 wt% purity by qNMR, *ee*: 100 % desired).



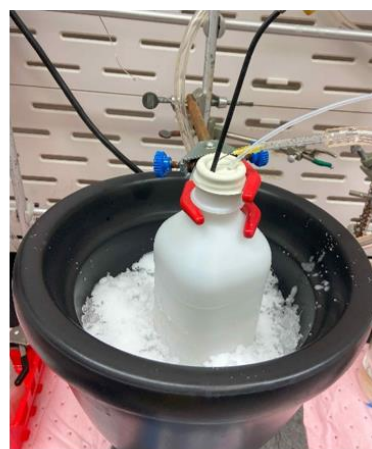
Reaction setup



NaOH bubble



NaHCO₃ quench



Scale-up (1 L HDP bottle)

¹H NMR (600 MHz, CDCl₃-*d*) δ 5.85 (brs, 2H), 4.23 (q, J = 7.2 Hz, 2H), 2.50 – 2.43 (m, 2H), 1.42 – 1.38 (m, 1H), 1.26 (t, J = 7.2 Hz, 3H), 1.16 – 1.13 (m, 1H).

¹³C NMR (151 MHz, CDCl₃-*d*) δ 166.0, 143.4 (t, J = 29.3 Hz), 136.6 (q, J = 39.8 Hz), 132.8 (m), 121.6 (q, J = 268.8 Hz), 120.2 (t, J = 244.3 Hz), 62.5, 52.2, 28.1 (dd, J = 29.3, 5.4 Hz), 23.4 (d, J = 2.0 Hz), 14.1, 12.4 (t, J = 3.6 Hz).

¹⁹F NMR (565 MHz, CDCl₃-*d*) δ -61.8, -81.5 (d, J = 254.7 Hz), -104.23 (d, J = 254.9 Hz).

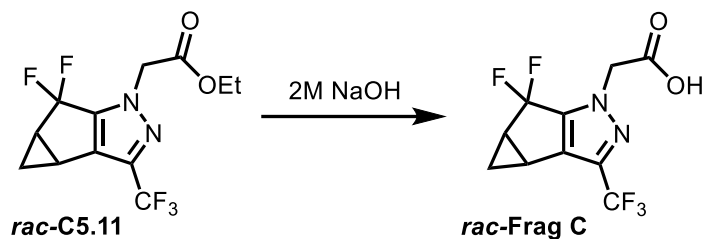
HRMS (ESI) *m/z*: calcd for C₁₂H₁₁F₅N₂O₂·H⁺ = [M+H]⁺ 311.0819, found 311.0813

IR (ATR) ν_{\max} = 1750.0, 1720.2, 1537.5, 1395.9, 1377.3, 1356.8, 1340.0, 1317.6, 1271.0, 1135.0, 1094.0, 1041.8, 829.3, 808.8.

ee: 100 % - desired

$[\alpha]_D^{20}$ (deg · mL · g⁻¹ · dm⁻¹) (MeOH (10mg/mL) at 20 °C under 589nm): -30.17

Synthesis of 2-(5,5-difluoro-3-(trifluoromethyl)-3b,4,4a,5-tetrahydro-1H-cyclopropano[3,4]cyclopenta[1,2-c]pyrazol-1-yl)acetic acid (*rac*-Frag C)



To a vial (40 mL) equipped with a magnetic stirring bar were added *rac*-C5.11 (1 g, 2.9 mmol, 1.04 eq), THF (5 mL), and MeOH (5 mL). Then, an aqueous 2M NaOH solution (1.69 mL, 1.2 eq) was added. The reaction mixture was stirred at 25 °C for 30 min. After completion of the reaction, the pH of the mixture was adjusted to pH = 1-2 with aqueous HCl (3M, 1 mL). The mixture was extracted with EtOAc (10 mL × 3). The combined organic layer was washed with brine (10 mL), dried over anhydrous sodium sulfate, filtered, and concentrated under reduced pressure to afford

rac-Frag C (760 mg, yield: 95 % based on the purity, purity: 96 A% by LCMS (254 nm) and 98.3 wt% by qNMR).

¹H NMR (600 MHz, DMSO-*d*₆) δ 5.01 (q, J = 17.7 Hz, 2H), 2.68 – 2.57 (m, 2H), 1.46 (q, J = 7.5 Hz, 1H), 1.04 – 1.02 (m, 1H).

¹³C NMR (151 MHz, DMSO-*d*₆) δ 167.9, 142.8 (t, J = 29.3 Hz), 134.3 (q, J = 39.0 Hz), 132.5 (m), 121.7 (q, J = 268.5 Hz), 120.3 (t, J = 243.3 Hz), 52.3, 27.7 (dd, J = 28.9, 5.7 Hz), 23.5, 11.8.

¹⁹F NMR (565 MHz, DMSO-*d*₆) δ -60.4, -80.0 (d, J = 253.3 Hz), -103.2 (d, J = 253.3 Hz).

3.3 NMR & GCMS Spectra

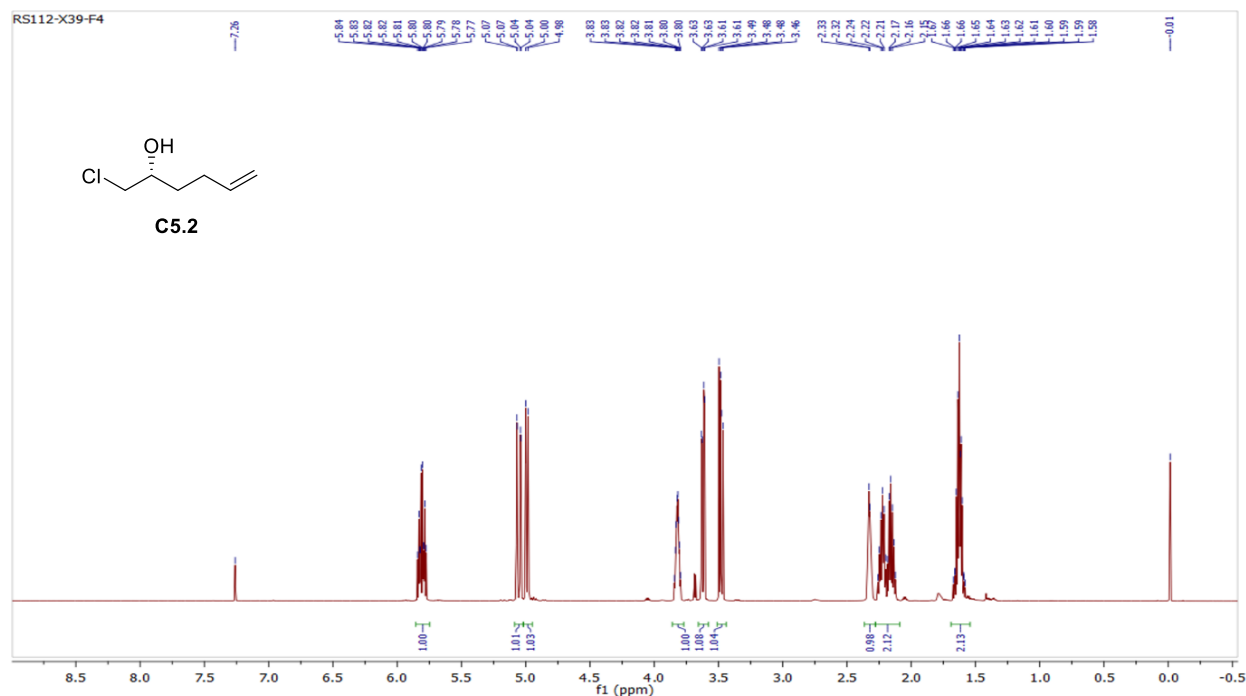


Figure 3.3.1 ¹H NMR (600 MHz, CDCl₃-*d*) of C5.2

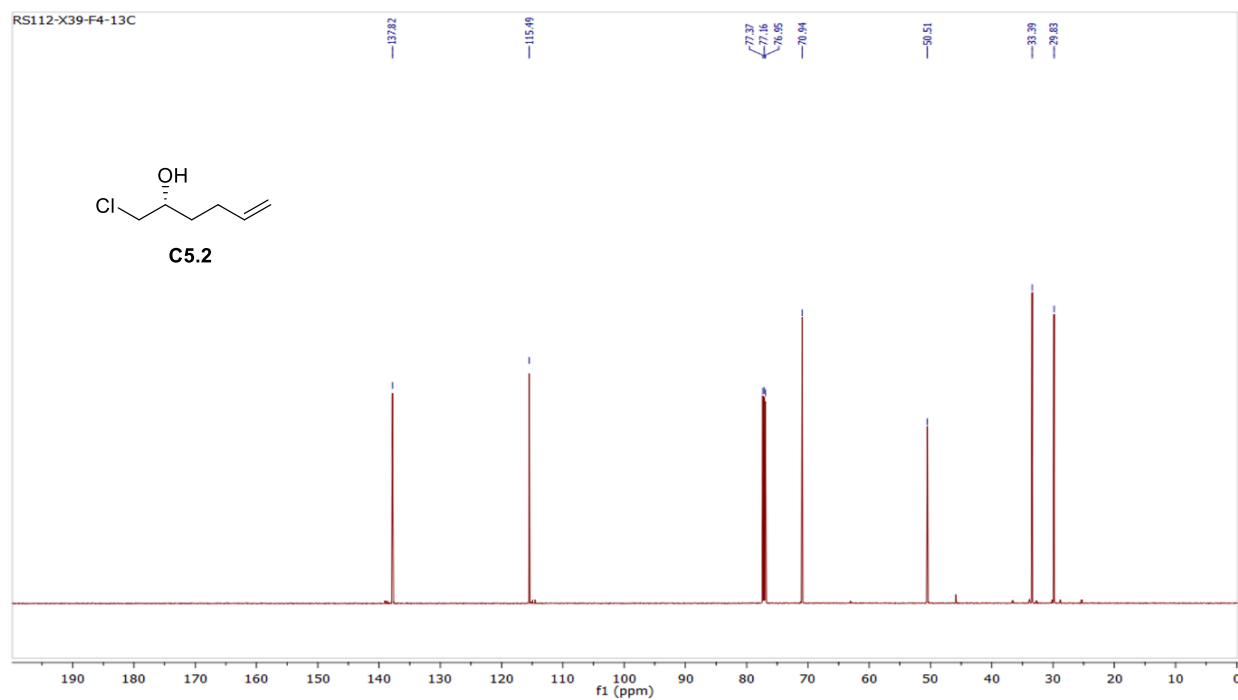


Figure 3.3.2 ^{13}C NMR (150 MHz, CDCl_3-d) of **C5.2**

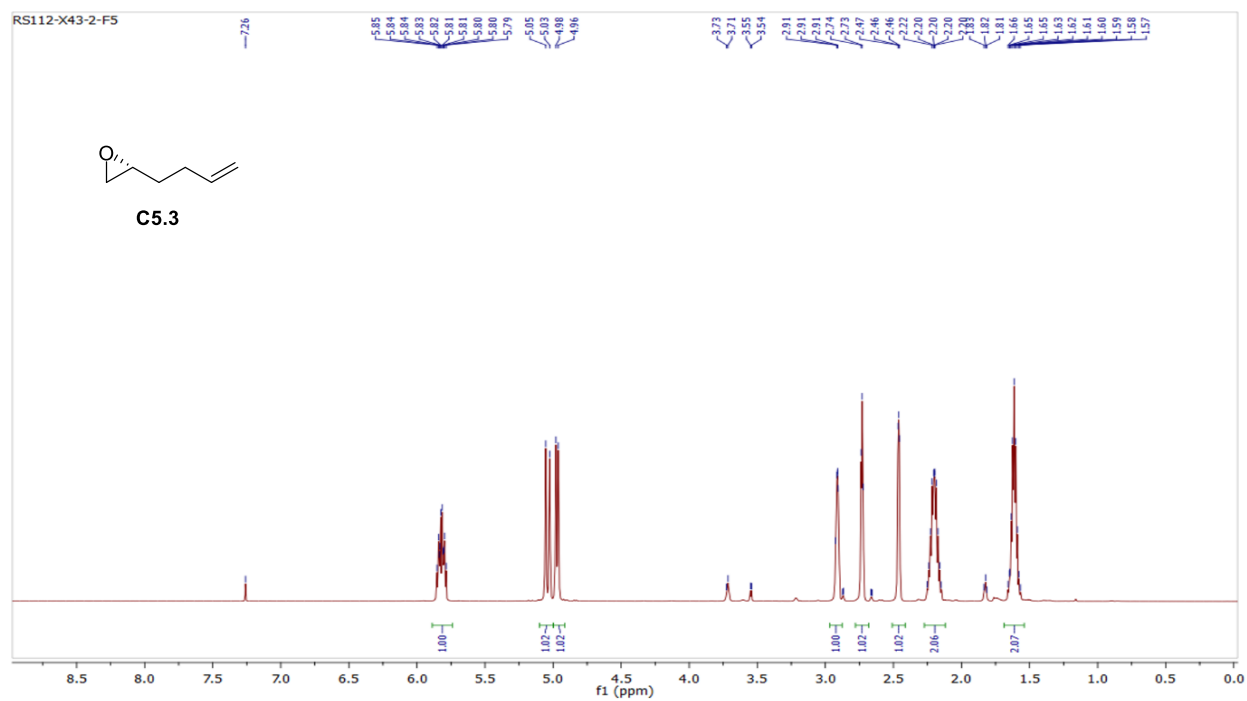


Figure 3.3.3 ^1H NMR (600 MHz, CDCl_3-d) of **C5.3**

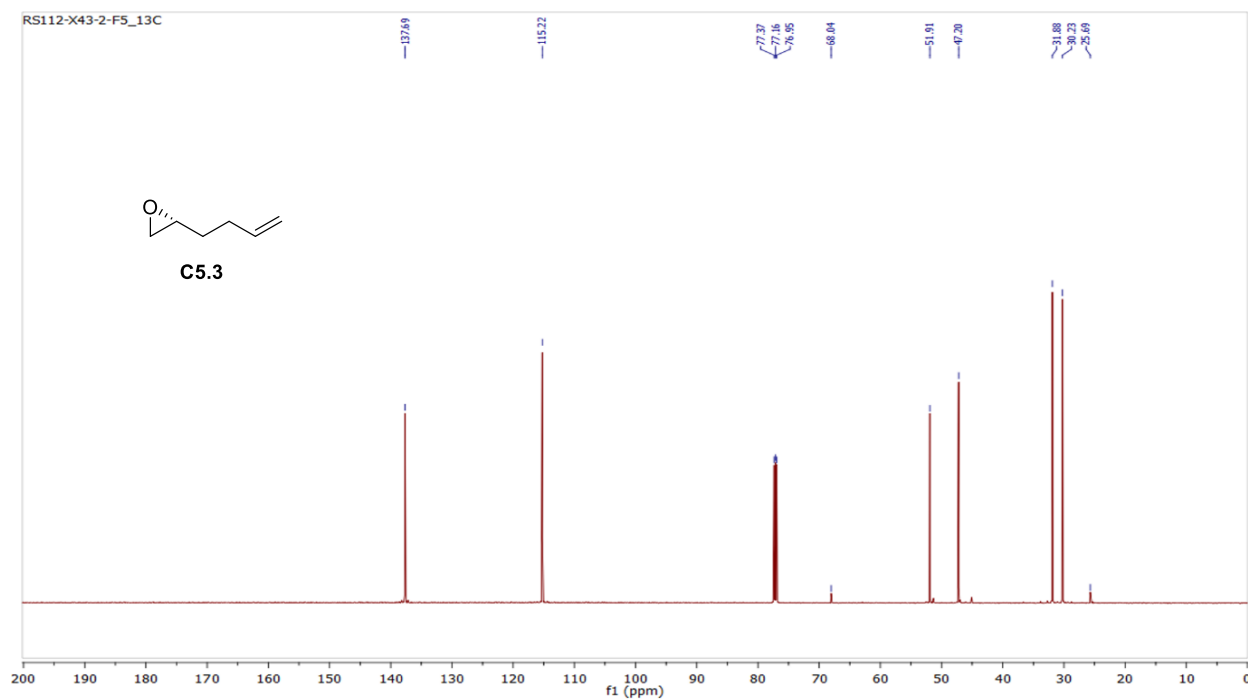


Figure 3.3.4 ^{13}C NMR (150 MHz, CDCl_3-d) of **C5.3**

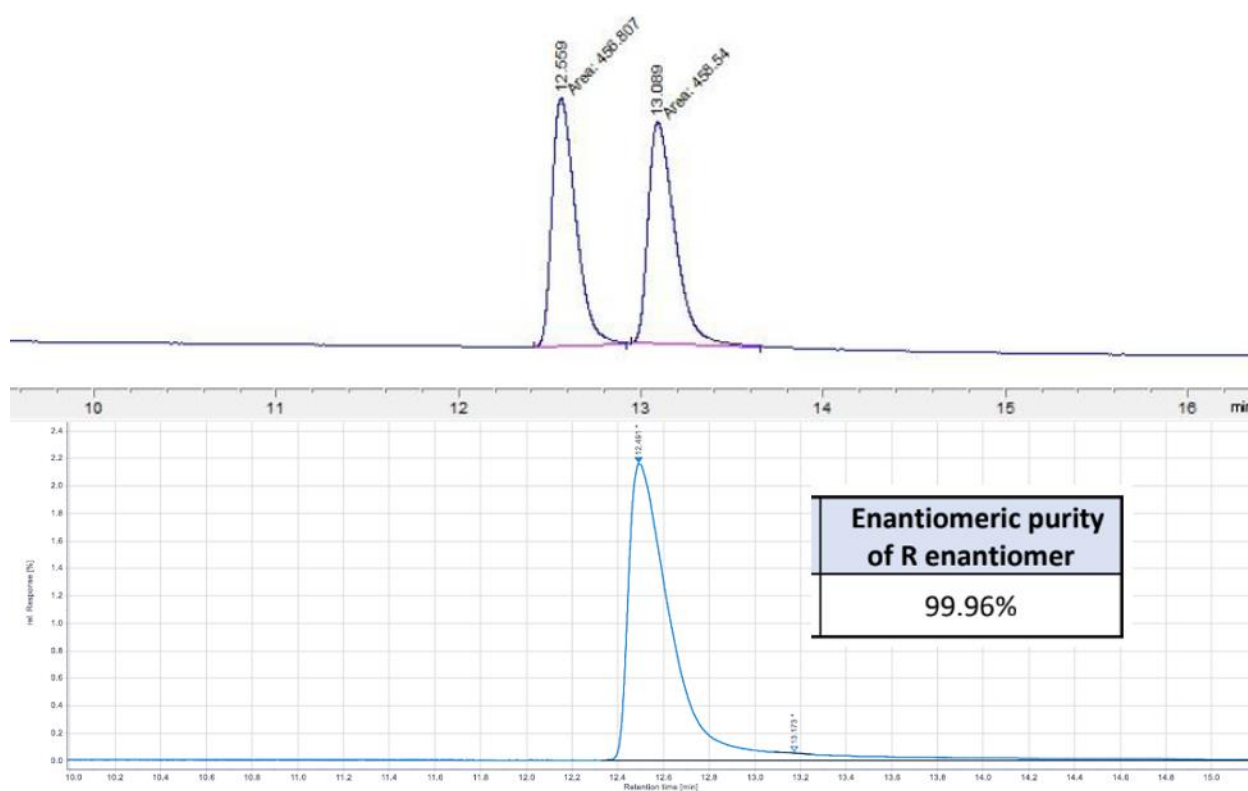


Figure 3.3.5 Chiral GC (GC-FID) spectrum of *rac*-C5.3-*rac* and C5.3 (from epichlorohydrin route)

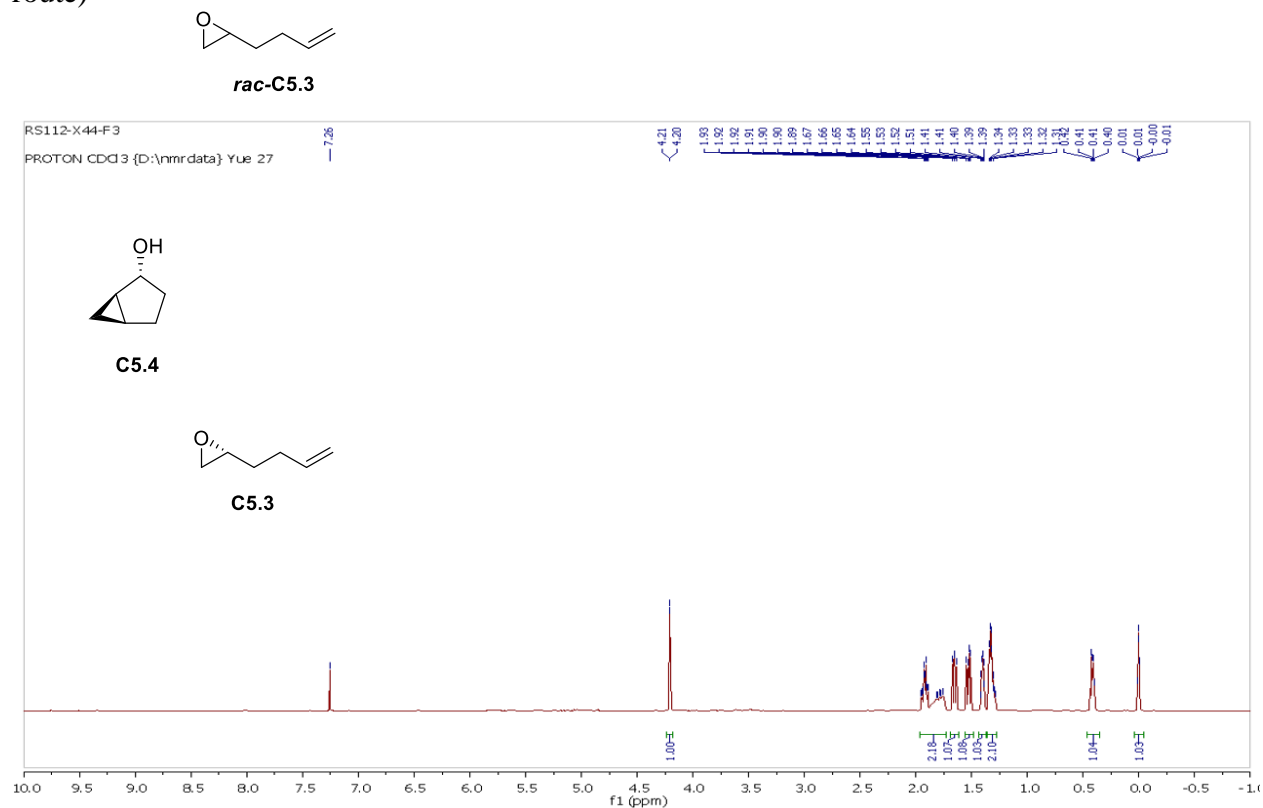


Figure 3.3.6 ^1H NMR (600 MHz, CDCl_3-d) of C5.4

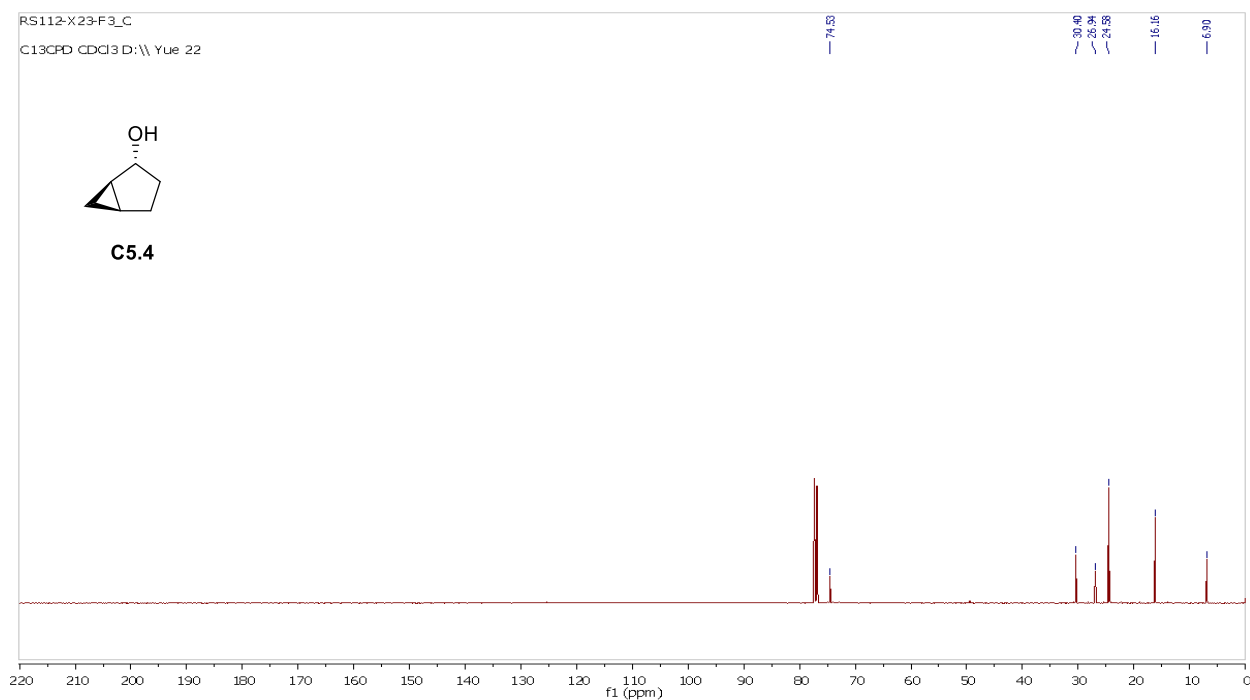


Figure 3.3.7 ¹³C NMR (150 MHz, CDCl₃-d) of **C5.4**

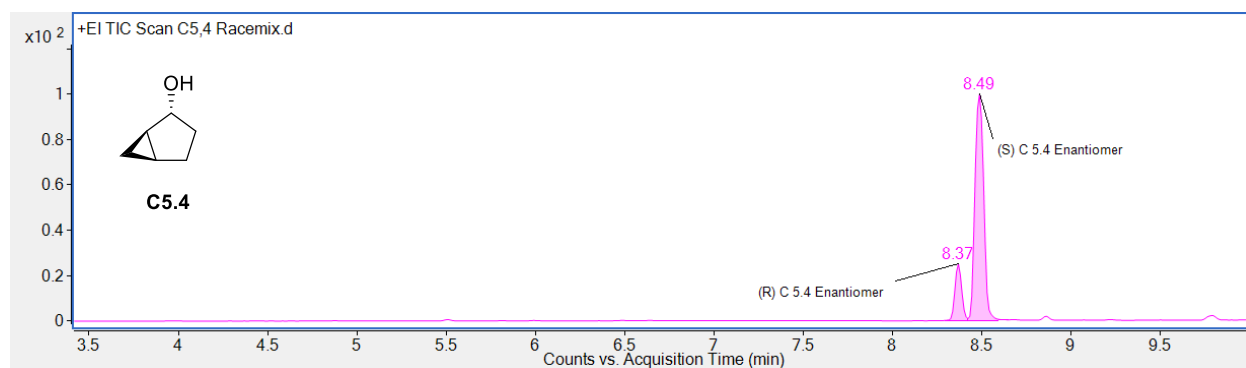


Figure 3.3.8 Chiral GC (GC-FID) spectrum of **C5.4**

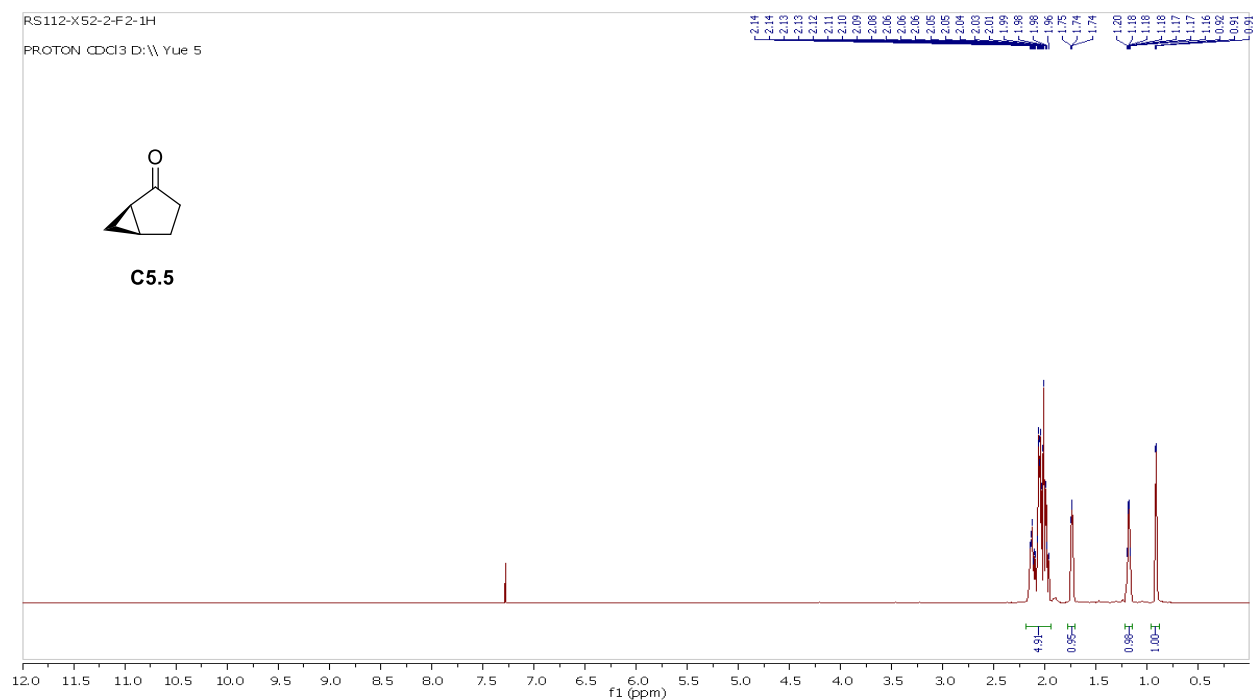


Figure 3.3.9 ^1H NMR (600 MHz, CDCl_3-d) of **C5.5**

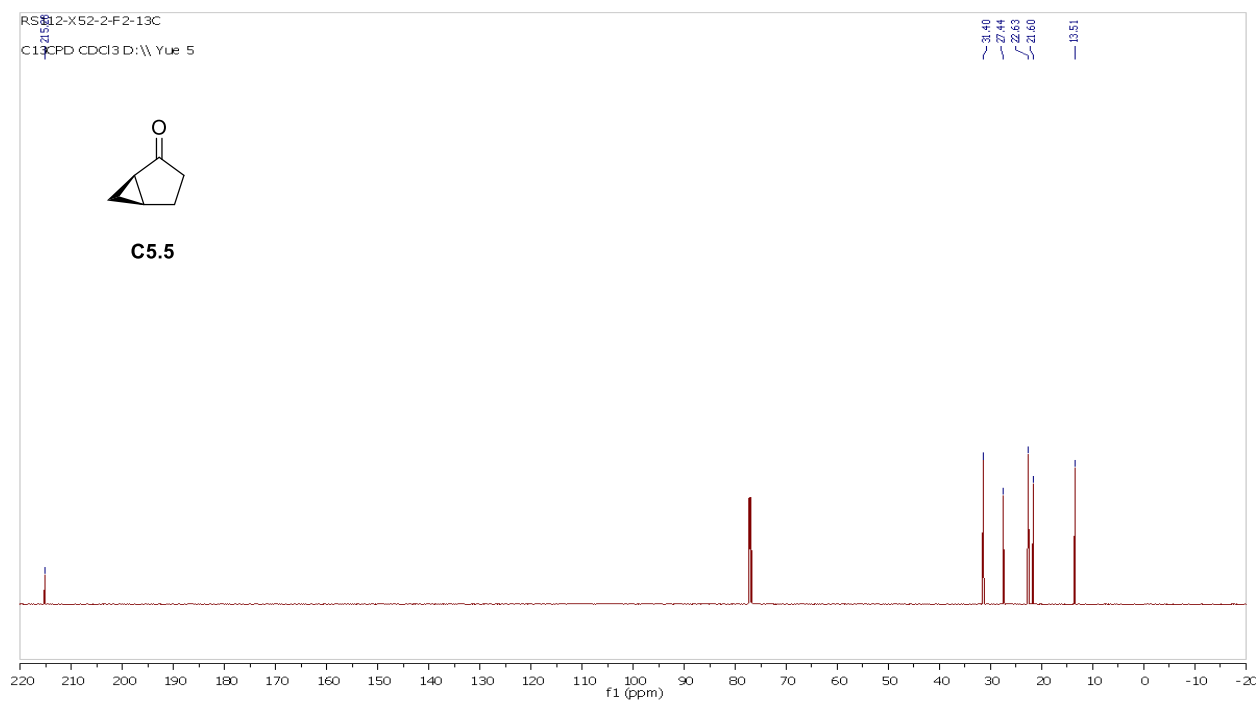


Figure 3.3.10 ^{13}C NMR (150 MHz, CDCl_3-d) of **C5.5**

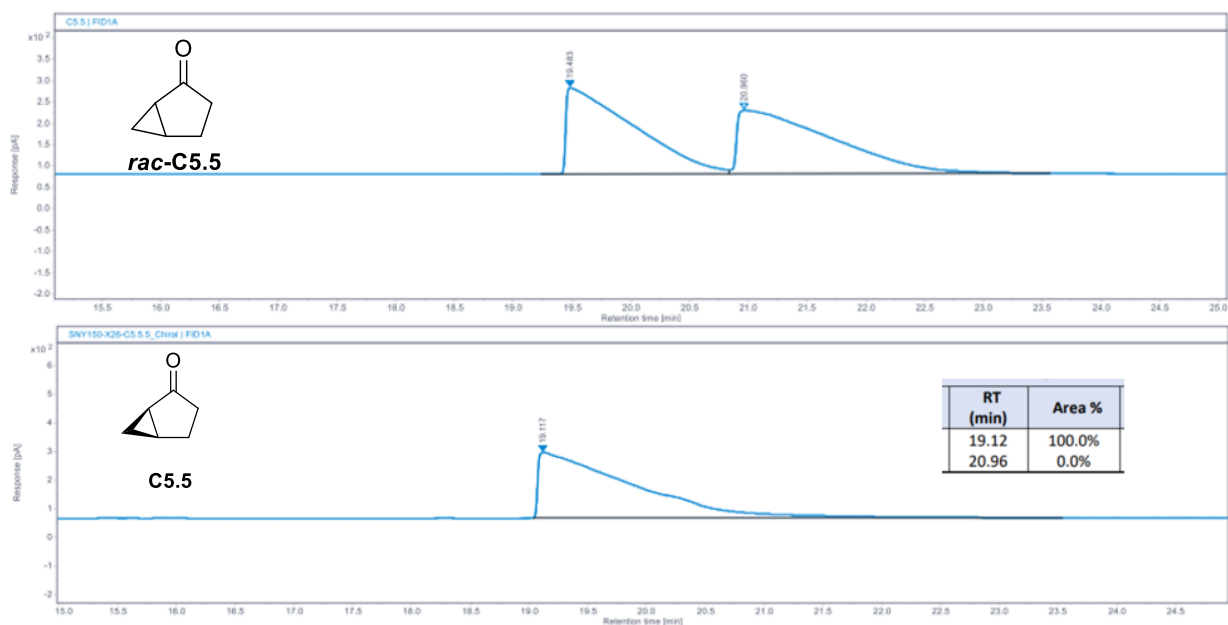


Figure 3.3.11 Chiral GC (GC-FID) spectrum of *rac*-C5.5 and C5.5

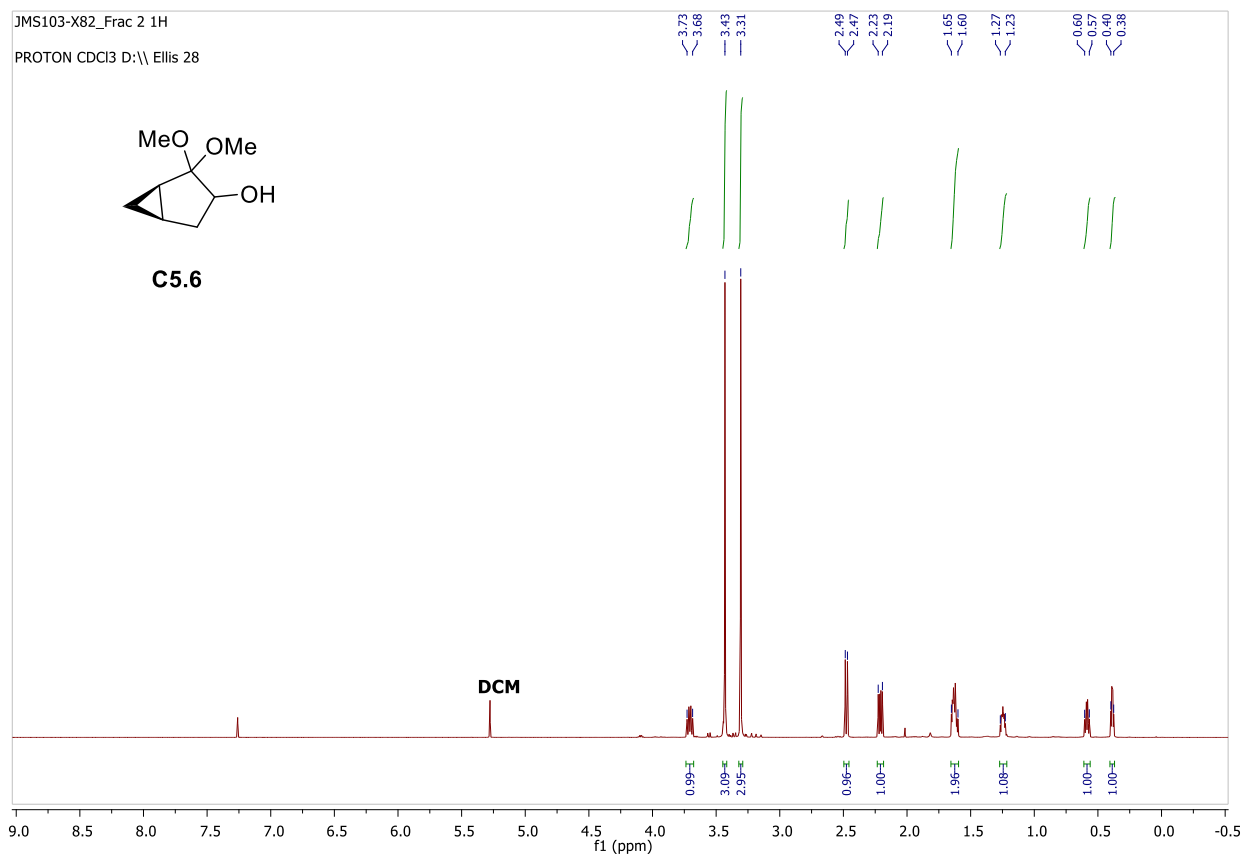


Figure 3.3.12 ^1H NMR (600 MHz, CDCl_3-d) of **C5.6**

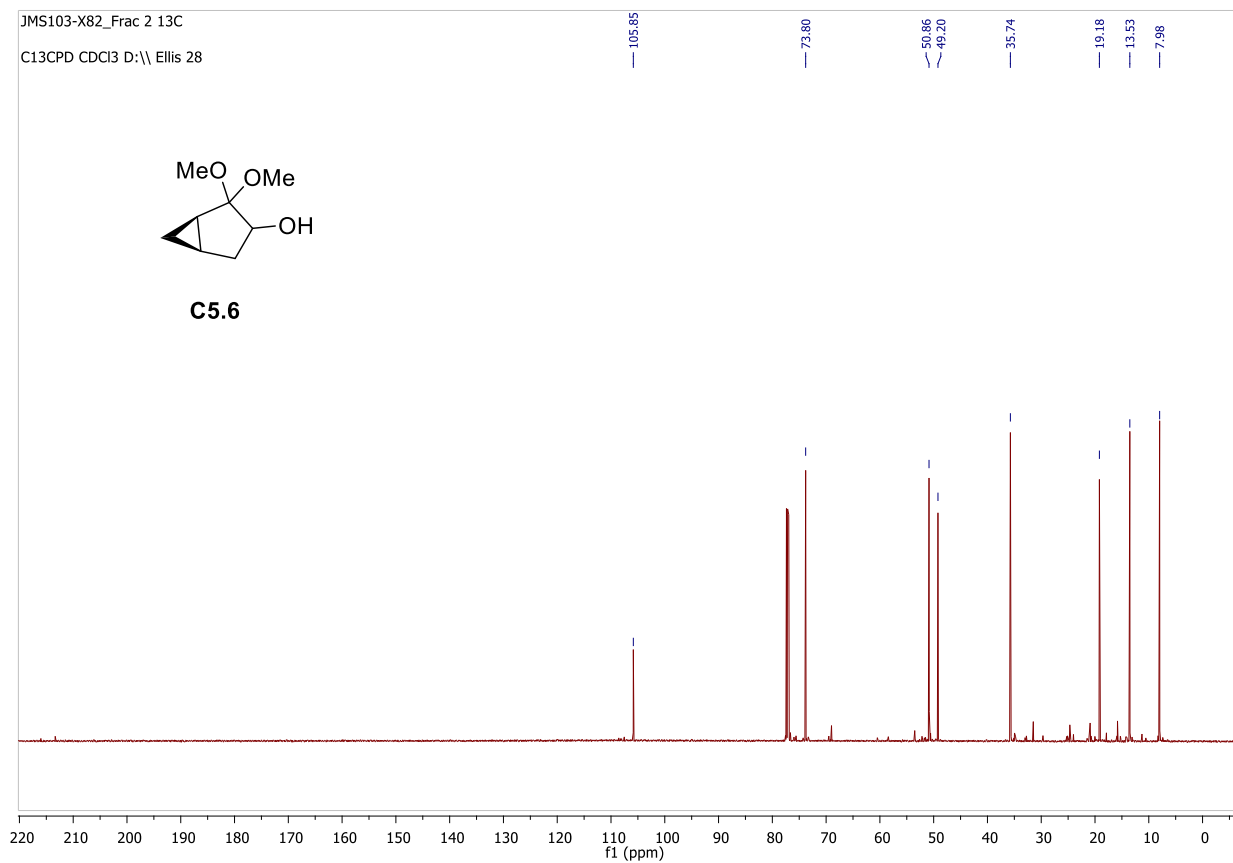


Figure 3.3.13 ^{13}C NMR (150 MHz, CDCl_3-d) of **C5.6**

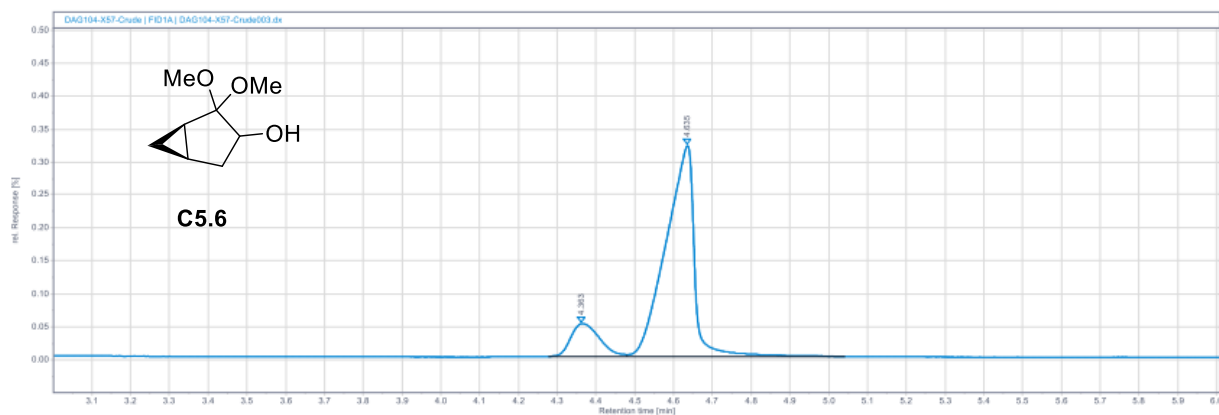


Figure 3.3.14 Chiral GC (GC-FID) spectrum of **C5.6**

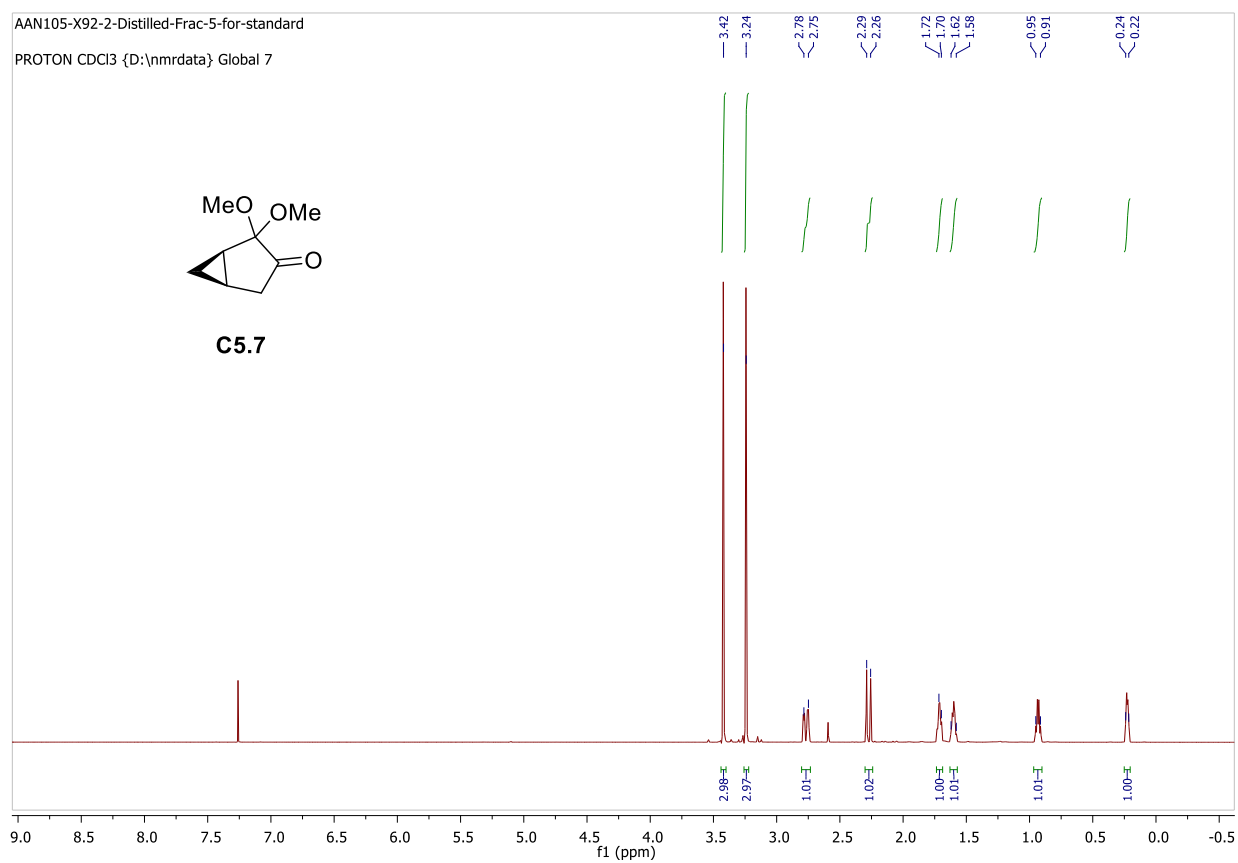


Figure 3.3.15 ¹H NMR (600 MHz, CDCl₃-d) of **C5.7**

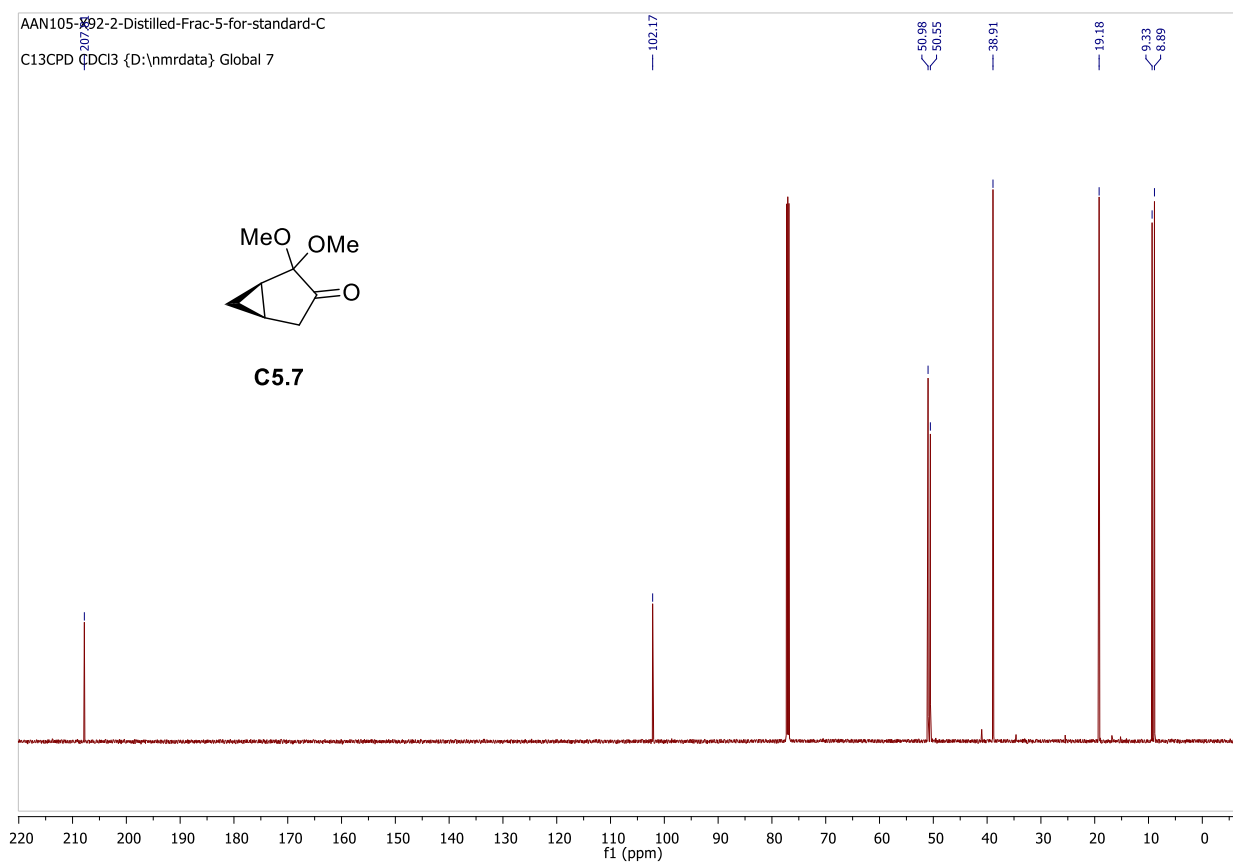


Figure 3.3.16 ^{13}C NMR (150 MHz, CDCl_3-d) of **C5.7**

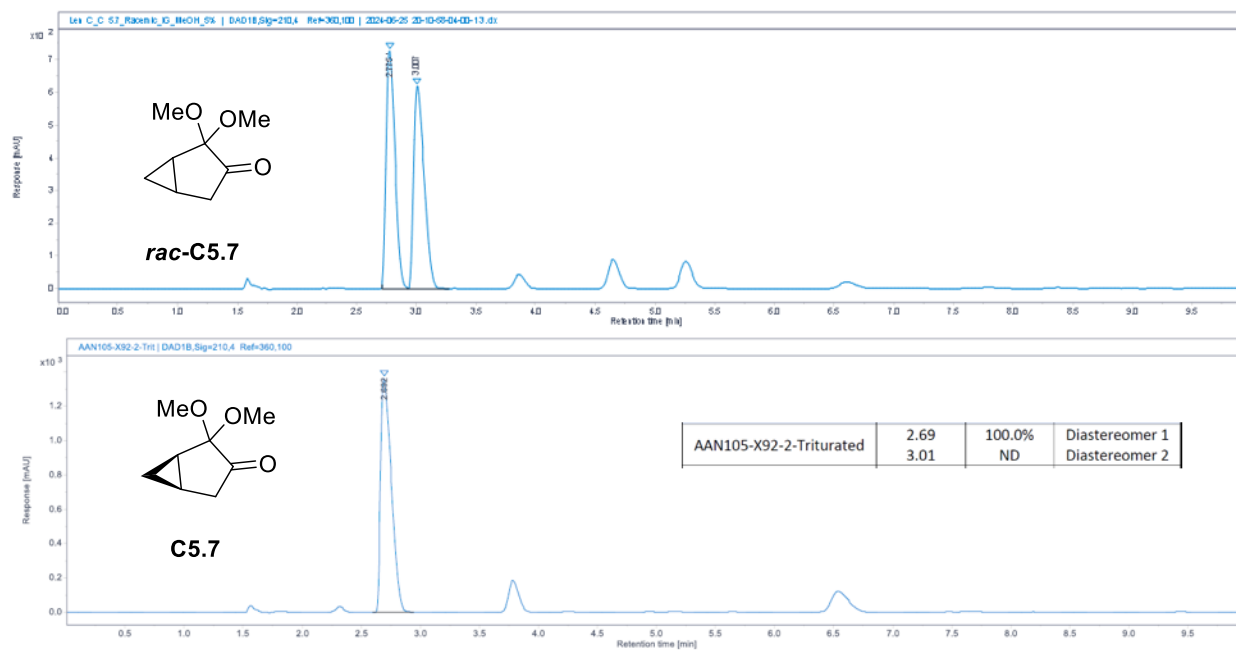


Figure 3.3.17 Chiral GC (GC-FID) spectrum of *rac-C5.7* and *C5.7*

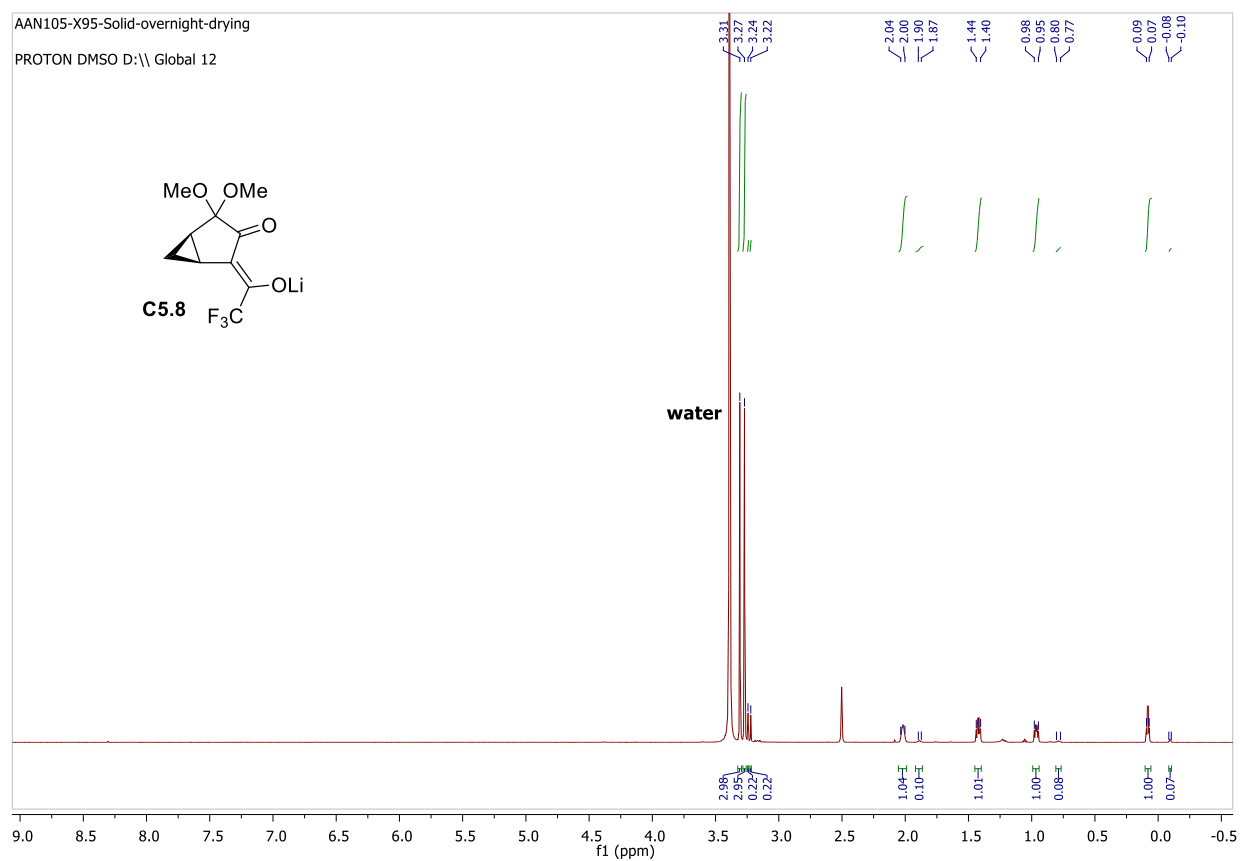


Figure 3.3.18 ¹H NMR (600 MHz, DMSO-*d*₆) of **C5.8**

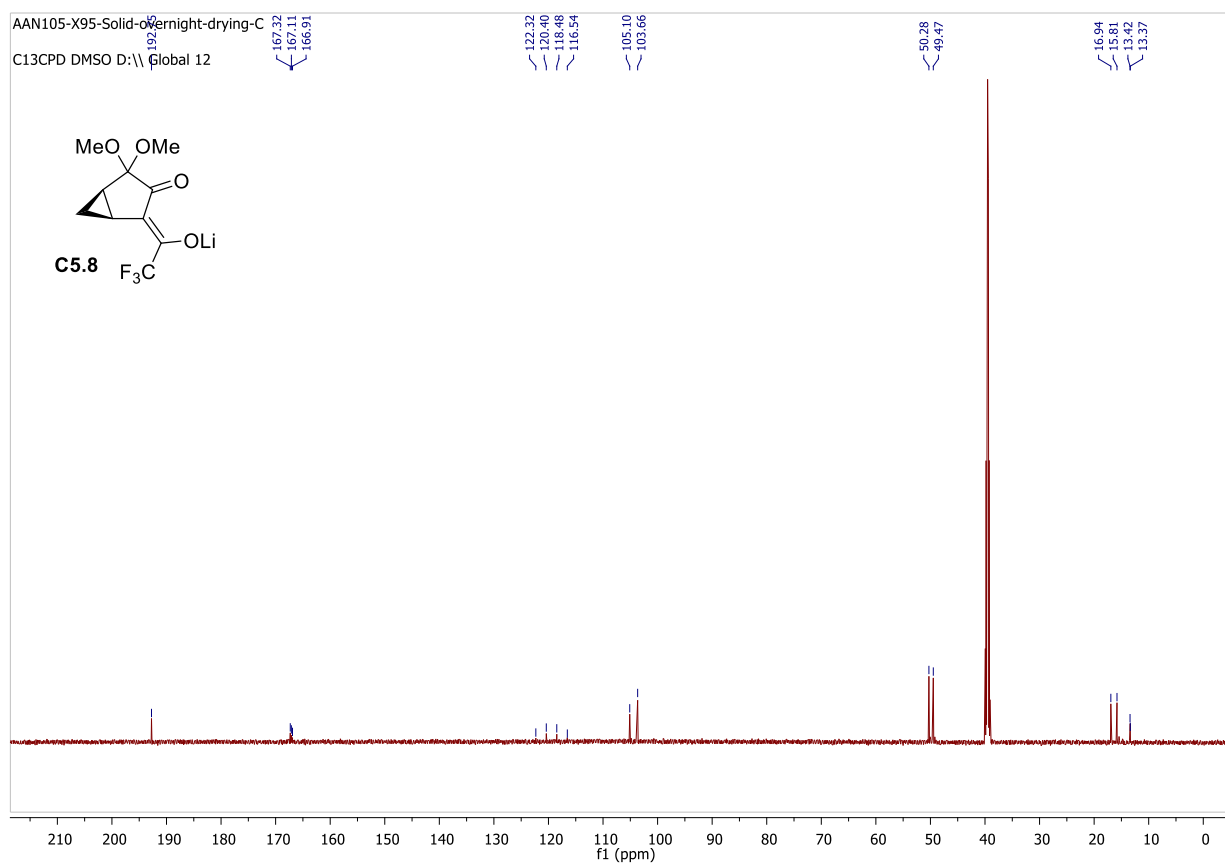


Figure 3.3.19 ^{13}C NMR (150 MHz, $\text{DMSO-}d_6$) of **C5.8**

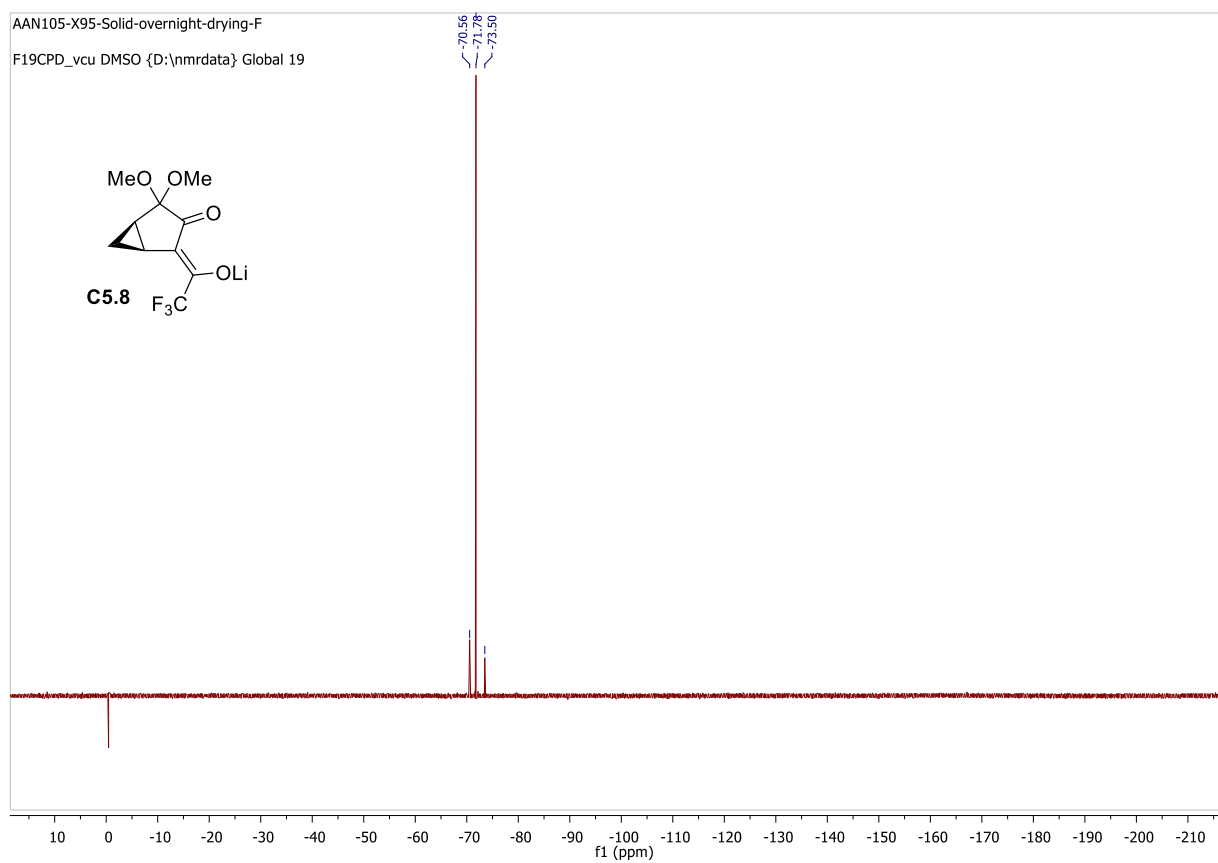


Figure 3.3.20 ^{19}F NMR (565 MHz, $\text{DMSO-}d_6$) of **C5.8**

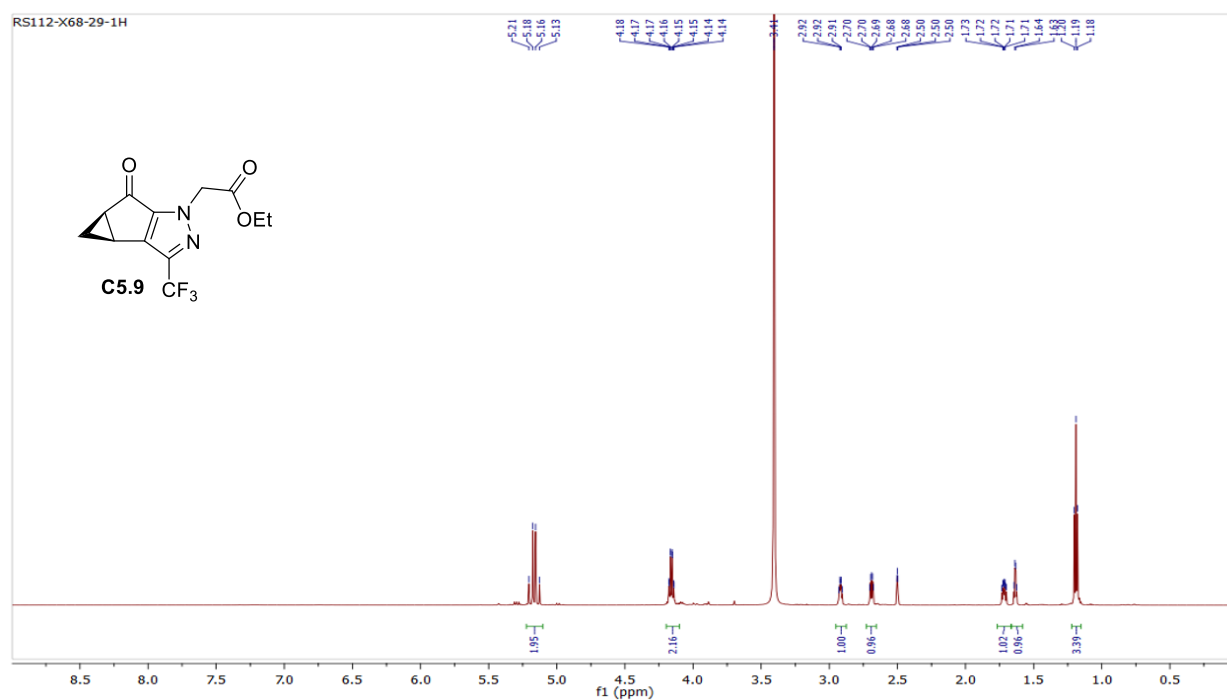


Figure 3.3.21 ^1H NMR (600 MHz, $\text{DMSO-}d_6$) of **C5.9**

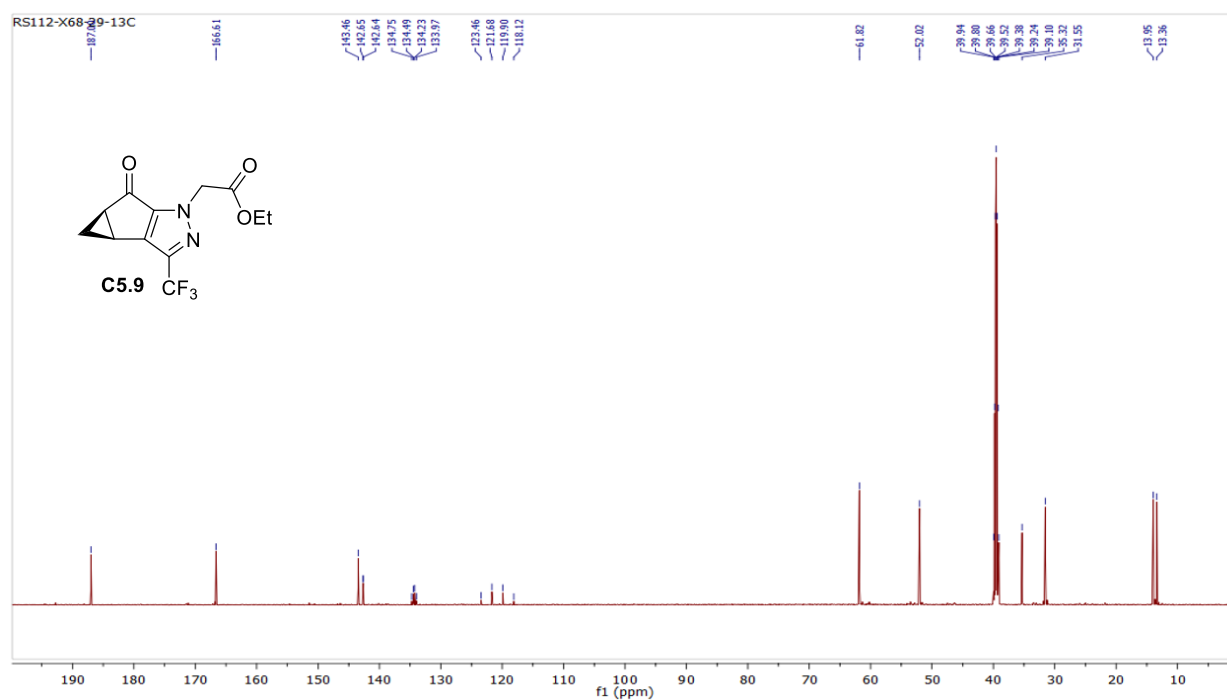


Figure 3.3.22 ^{13}C NMR (150 MHz, $\text{DMSO-}d_6$) of **C5.9**